THE CONTRIBUTION OF MOLECULAR INTERACTION POTENTIALS TO PROPERTIES AND ACTIVITIES OF IONIC LIQUID IONS IN SOLUTION

Vom Fachbereich Produktionstechnik

der

UNIVERSITÄT BREMEN

zur Erlangung des Grades
Doktor – Ingenieur
genehmigte

Dissertation

von

M.Sc. Chul-Woong Cho

Gutachter:
Prof. Dr. -Ing. Jorg Thöming
Prof. Dr. rer. nat. Ingo Krossing, Universität Freiburg

Tag der mündlichen Prüfung: 23. April 2012

Diese Arbeit wurde in der Zeit von August 2008 bis August 2011 im Fachbereich Produktionstechnik) der Universität Bremen angefertigt.

Eingereicht am: 16. November 2011

Verteidigt am: 23. April 2012

Prüfungskommission:

Gutachter:	Prof. Dr. –Ing. Jorg Thöming Prof. Dr. rer. nat. Ingo Krossing, Universität Freiburg
Prüfer:	Prof. Dr. –Ing. Lucio Colombi Ciacchi Dr. rer. nat. Stefan Stolte
Mitarbeiter:	Dr. rer. nat. Jürgen Arning
Student:	Philipp Ciaciuch

“In the beginning God created the heavens and earth”

- Genesis 1 Vers 1-

Only for the Glory of Jesus Christ.

Abstract

Ionic liquids (ILs) have attracted significant interest due to their beneficial and tuneable physicochemical properties, *e.g.* excellent thermal and electrochemical stability, low vapour pressure and favourable solvation properties. The most striking advantage is their structural variability which allows for the potential to design chemicals with optimised physicochemical properties. To experimentally identify the IL structure(s) most suited for a certain technical purpose with no adverse effects to man and the environment, it would result in a nearly insurmountable number of "trial and error" experiments. Therefore, it is essential to understand the molecular interaction potentials (later on referred to as solute descriptors or LFER descriptors in this thesis) of ions *i.e.* excess molar refraction (E), dipolarity/polarizability (S), hydrogen-bonding acidity (A), hydrogen-bonding basicity (B), and McGowan volume (V). Using these descriptors will then allow predicting the physicochemical and biological property of ILs in various environments before their first synthesis. Thus, experiments were carried out with high performance liquids chromatography (HPLC) to estimate the molecular interaction potentials of 30 cations and 20 anions. An *in silico* method, *i.e.* COSMO-calculation, was employed to calculate the descriptors for more conventional and easily accessible approaches. With the experimental and computational methods, the molecular interaction potentials of ions were successfully quantified. Using the measured and the calculated solute descriptors, we could thereby predict the physicochemical properties of technical importance such as octanol-water partitioning coefficient, water solubility, critical micelle concentration, anionic activity coefficient in water and hydrophobicity in octanol-water; and biological properties such as cytotoxicity [EC_{50}] towards rat leukaemia cell line IPC-81, *Vibrio fischeri* (marine bacterium), and *Secendesmus vacuolatus* (limnic green alga). The main conclusions of each Chapter 3 ~ 6 can be summarized as follows:

- In Chapter 3 the molecular interaction potentials of 30 cations were successfully estimated using five reverse stationary phases in HPLC, and it could be verified that the type of head group, alkyl chain length and further substituent of the 30 cations of ILs have significant influence on the dipolarity/polarizability and the hydrogen bonding acidity, and functionalized groups (hydroxyl, ether, and dimethylamino) lead to hydrogen bonding basicity of the cation.
- Chapter 4 is mainly focused on how to determine the solute descriptors of 20 anions using multi-stationary phases in the HPLC, and whether the suitability of the linear model is available to evaluate the solute descriptors of the anions. The obtained results show that the applied multi-stationary phase systems were suitable to determine the solute descriptors, and Z term (stands for

ionic interaction) of the conceptual model should be modified to address both the cations (z_cZ_c) and the anions (z_aZ_a). At last, based on the extended model, we could estimate the solute descriptors of 20 anions.

- In Chapter 5, it is reported that the calculated or the measured solute descriptors of IL ions can be used to predict with error of 0.182 to 0.217 log units for the octanol-water partitioning coefficient and 0.131 to 0.166 log units for the water solubility. The CMC, anionic activity coefficient at the IL saturated condition in water, and anionic hydrophobicity at IL-equilibrated condition in octanol-water system can be predicted with COSMO-calculation alone with an R^2 of at least 0.99 as well as an error below 0.168 log units. The regression coefficients (system parameters) for the predictions using measured descriptors (exp. Ds) and calculated descriptors (calc. Ds) of ions are given below:

– For the activity coefficient [C_a] of anion in water [dimensionless]

(using the calc. Ds) = $- 3.103 + 4.110E_a - 7.084S_a – 7.543A_a + 4.783B_a + 0.670V_a – 0.715 (-1/V_a)$

– For the water solubility of ionic liquids [g/mol]

(using the calc. Ds) = $+ 4.586 + 0.340E_c – 1.661S_c + 1.166A_c + 4.552B_c – 2.099V_c – 0.996C_a$

(using the exp. Ds) = $–1.395 – 0.429E_c + 0.431S_c + 0.280A_c – 1.769V_c + 1.038C_a$

– For the hydrophobicity of anion [H_a] in octanol-water [dimensionless]

(using the calc. Ds) = $0.298 – 0.841E_a + 0.263S_a + 1.691A_a – 0.571B_a + 1.319V_a$

– For the partitioning coefficient of ILs in octanol-water [dimensionless]

(using the calc. Ds) = $– 6.239 – 0.603E_c – 0.794S_c – 0.901A_c – 6.765B_c + 2.976V_c + 1.007H_a$

(using the exp. Ds) = $– 4.678 + 0.118E_c – 0.710S_c – 0.529A_c – 3.310B_c + 2.985V_c + 0.983H_a$

– For the critical micelle concentration [$mmol/L^{-1}$] of ILs in water

(using the calc. Ds) = $16.721 + 3.058E_c – 7.647S_c – 2.601A_c + 1.696B_c – 1.648V_c – 0.411(1/V_c) + 0.796E_a – 2.024S_a – 2.731A_a + 1.452B_a – 2.099V_a + 0.623(-1/V_a)$

- Chapter 6 shows that the calculated descriptors allow for modeling cationic hydrophobicity and IL cytotoxicity towards the rat leukaemia cell line IPC-81, *Vibrio fischeri*, and *Scenedesmus vacuolatus successfully as well as providing* an understanding of the contributions of the molecular interaction potentials to these properties. It was observed that the volume of the cation strongly contri-

butes to the hydrophobicity of cation, while hydrogen bonding ability (B and A), as opposite effect to V, reduces the hydrophobic effect of cation. The cytotoxicity prediction study showed that V terms are most important descriptors to predict toxicity followed by hydrogen bonding basicity terms for *Leukaemia rat cell line* and *Vibrio fischeri* and by charge density terms for *Scenedesmus vacuolatus*.

In case of rat leukaemia cell line IPC-81, by adding additional terms (E and charge density terms) the predictivity can be reached at SD of 0.500 log units:

Log [$1/EC_{50}$], *Leukaemia rat cell line* = $-9.423 + 0.514E_c - 1.822B_c + 2.653V_c + 1.738(1/V_c) - 0.528E_a - 0.049B_a + 0.555V_a - 0.184(-1/V_a)$

One additional term i.e. charge density to model (V + B) for *Vibrio fischeri* allowed us to predict the toxicity values in SD of 0.530. The model is:

Log [$1/EC_{50}$], *Vibrio fischeri* = $-9.918 - 2.227B_c + 3.822V_c + 1.084(1/V_c) + 0.116B_a + 0.778\ V_a - 0.005(-1/V_a)$

The model comprising of V, charge density, B and S terms can be used to predict the toxicity for *Scenedesmus vacuolatus* in SD of 0.643:

Log [$1/EC_{50}$], *Scenedesmus vacuolatus* = $-34.787 - 0.382S_c - 2.702B_c + 13.714V_c + 16.101(1/V_c) + 0.892S_a - 0.600B_a + 1.768V_a - 0.766\ (-1/V_a)$

ZUSAMMENFASSUNG

Ionische Flüssigkeiten (ILs) haben in den vergangenen Jahren große Aufmerksamkeit erfahren. Grund dafür sind ihre vorteilhaften und leicht steuerbaren physiko-chemischen Eigenschaften wie beispielsweise eine hohe thermische und elektrochemische Stabilität, ein sehr niedriger Dampfdruck und gute Lösungseigenschaften für zahlreiche organische Substanzen. Das Besondere dieser oft schon bei Raumtemperatur flüssigen Salze ist ihre enorme Strukturvielfalt, welche das gezielte Design von optimal an ihren technologischen Einsatz angepassten ILs erlaubt. Um aus dieser riesigen Strukturvielfalt experimentell diejenige IL zu identifizieren, die einerseits optimal an ihren technologischen Einsatz angepasst ist und gleichzeitig ein möglichst geringes Gefahrenpotenzial für Mensch und Umwelt aufweist, müsste man quasi unendlich viele „trial and error“ Experimente durchführen. Um dies zu umgehen ist es essentiell, das molekulare Wechselwirkungspotenzial (später in der Arbeit auch als „solute descriptors“ oder „LFER descriptors“ bezeichnet) der IL-Ionen zu verstehen. Dieses molekulare Wechselwirkungspotenzial kann über folgende Deskriptoren beschrieben werden: excess molar refraction (E), Dipolarität/Polarisierbarkeit (S), Wasserstoffbrücken-Donorpotenzial (A), Wasserstoffbrücken-Akzeptorpotenzial (B) und McGowan Volumen (V). In dieser Arbeit wird gezeigt, dass mit Hilfe einer Linearkombination dieser Deskriptoren die physiko-chemischen Eigenschaften und die möglichen biologischen Effekte von ILs theoretisch vorhergesagt werden können, ohne jede IL einzeln synthetisieren zu müssen. Exemplarisch wurden von 30 IL-Kationen und 20 IL-Anionen deren molekulare Wechselwirkungspotenziale mittels High Performance Liquid Chromatography (HPLC) ermittelt. Zusätzlich wurden COSMO-Berechnungen als *in silico* Methode verwendet, um die genannten molekularen Deskriptoren auf einem schneller zugänglichen Weg zu erhalten. Mit diesem Ansatz aus experimentellen und theoretisch berechneten Daten konnten die molekularen Wechselwirkungspotenziale der Ionen erfolgreich quantifiziert werden. Unter Verwendung der so bestimmten Deskriptoren war es dann möglich, folgende technologisch relevanten physiko-chemsiche Eigenschaften der Ionen vorherzusagen: Oktanol-Wasser Verteilungskoeffizient, Wasserlöslichkeit, kritische Mizellbildungskonzentration, Aktivitätskoeffizient sowie die Hydrophobie der Anionen in Wasser. Außerdem konnten folgende biologische Eigenschaften vorhergesagt werden: Zytotoxizität [EC_{50}] gegenüber der Rattenleukämie-Zelllinie IPC-81, des marinen Bakteriums *Vibrio fischeri* und der limnischen Grünalge *Scenedesmus vacuolatus*. Die wesentlichen Ergebnisse aus den Kapiteln 3-6 lassen sich wie folgt zusammenfassen:

- In Kapitel 3 ist dargestellt, dass die Bestimmung der molekularen Wechselwirkungspotenziale von 30 Kationen erfolgreich gelungen ist. Dafür wurden fünf unterschiedliche stationäre Phasen in der HPLC eingesetzt, und es konnte gezeigt werden, dass die Kopfgruppe sowie Art und Länge der Alkylseitenkette an dieser Kopfgruppe einen entscheidenden Einfluss auf die Dipolarität/Polarisierbarkeit und das Wasserstoffbrücken-Donorpotenzial haben. Zusätzlich konnte gezeigt werden, dass durch die Einführung von funktionellen Gruppen (Hydroxyl-, Ether- und Dimethylamino-Gruppen) in die IL auch ein Wasserstoffbrücken-Akzeptorpotenzial in die Kationen eingebracht werden kann.
- In Kapitel 4 liegt der Fokus auf der Bestimmung der Deskriptoren für 20 Anionen mit Hilfe der multi-stationären Phasen HPLC. Außerdem wurde untersucht, ob sich das verwendete lineare Modell zur Bewertung der Deskriptoren eignet. Die erhaltenen Resultate zeigen, dass das verwendete HPLC-System geeignet ist, um die Deskriptoren, sowie den Z Term (Term, der die ionische Wechselwirkung beschreibt) zu bestimmen. Es zeigte sich, dass der Z Term in dem Modell-Ansatz modifiziert werden sollte, um sowohl die Interaktion der Kationen (z_cZ_c) als auch der Anionen (z_aZ_a) zu berücksichtigen. Mit diesem so erweiterten Modell konnten dann die Deskriptoren der 20 Anionen bestimmt werden.
- In Kapitel 5 werden die berechneten oder gemessenen Deskriptoren verwendet, um folgende physiko-chemische Eigenschaften der IL Ionen vorherzusagen: den Oktanol-Wasser Verteilungskoeffizient mit einem Fehler von 0,182 bis 0,217 log Einheiten und die Wasserlöslichkeit mit einem Fehler von 0,131 bis 0,166 log Einheiten. Die CMC, der anionische Aktivitätskoeffizient unter IL Sättigungsbedingungen in Wasser und die anionische Hydrophobie unter IL-Gleichgewichtsbedingungen in einem Oktanol-Wasser System konnten ebenfalls, allein basierend auf COSMO-Berechnungen, mit einem Fehler von unter 0,168 log Einheiten und einem R^2 von mindestens 0,99 vorhergesagt werden. Die Regressionskoeffizienten (Systemparameter) für die Vorhersagen basierend auf den gemessenen Deskriptoren (exp. Ds) und den berechneten Deskriptoren (calc. Ds) lauten wie folgt:

- Für den Aktivitätskoeffizient der Anionen [C_a] in Wasser [dimensionslos]

(auf Basis der calc. Ds) = $- 3.103 + 4.110E_a - 7.084S_a - 7.543A_a + 4.783B_a + 0.670V_a - 0.715 (-1/V_a)$

- Für die Wasserlöslichkeit der ILs [g/mol]

(auf Basis der calc. Ds) = $+ 4.586 + 0.340E_c - 1.661S_c + 1.166A_c + 4.552B_c - 2.099V_c - 0.996C_a$

(auf Basis der exp. Ds) = $-1.395 - 0.429E_c + 0.431S_c + 0.280A_c - 1.769V_c + 1.038C_a$

- Für die Hydrophobie der Anionen [H_a] in OKtanol-Wasser [dimensionslos]

(auf Basis der calc. Ds) = $0.298 - 0.841E_a + 0.263S_a + 1.691A_a - 0.571B_a + 1.319V_a$

- Für den Oktanol-Wasser Verteilungskoeffizienten der ILs [dimensionslos]

(auf Basis der calc. Ds) = $-6.239 - 0.603E_c - 0.794S_c - 0.901A_c - 6.765B_c + 2.976V_c + 1.007H_a$

(auf Basis der exp. Ds) = $-4.678 + 0.118E_c - 0.710S_c - 0.529A_c - 3.310B_c + 2.985V_c + 0.983H_a$

- Für die kritische Mizellbildungskonzentration [mmol/L^{-1}] der ILS in Wasser

(auf Basis der calc. Ds) = $16.721 + 3.058E_c - 7.647S_c - 2.601A_c + 1.696B_c - 1.648V_c - 0.411(1/V_c) + 0.796E_a - 2.024S_a - 2.731A_a + 1.452B_a - 2.099V_a + 0.623(-1/V_a)$

o Kapitel 6 zeigt, dass die berechneten Deskriptoren auch die Bildung von Vorhersage-Modellen für der Kationen Hydrophobie und der Zytotoxizität gegenüber der IPC-81 Zelllinie, *Vibrio fischeri* und *Scenedesmus vacuolatus* erlauben und so zu einem tieferen Verständnis des Beitrags der molekularen Wechselwirkungen zu diesen Eigenschaften führen. Es konnte gezeigt werden, dass das molekulare Volumen (V) des Kations einen starken Beitrag zur Hydrophobie liefert, während das Wasserstoffbrücken-Bindungspotenzial (A und B) die Hydrophibie des Kations senkt. Die Studie zur Vorhersage der Zytotoxizität zeigte, dass der V Term der wichtigste Deskriptor zur Vorhersage der Effekte ist, gefolgt von dem Wasserstoffbrücken-Akzeptorpotenzial für die IPC-81 Zelllinie und dem Leuchtbakterium *Vibrio fischeri.* Für die Grünalge *Scenedesmus vacuolatus* ist der zweitwichtigste Deskriptor die Ladungsdichte. Für die IPC-81 Zellinie konnte die Vorhersage der Zytotoxizität auf eine SD von 0,500 log Einheiten verbessert werden, in dem zusätzliche Terme (E und Ladungsdichte) in das Modell eingefügt wurden:

Log [$1/EC_{50}$], *IPC-81 Zelllinie* = $-9.423 + 0.514E_c - 1.822B_c + 2.653V_c + 1.738(1/V_c) - 0.528E_a - 0.049B_a + 0.555V_a - 0.184(-1/V_a)$

Ein zusätzlicher Term (Ladungsdichte) in dem Modell für V und B erlaubte eine Verbesserung der Vorhersage der Zytotoxizität für *Vibrio fischeri* auf eine SD von 0,530:

Log [$1/EC_{50}$], *Vibrio fischeri* = $-9.918 - 2.227B_c + 3.822V_c + 1.084(1/V_c) + 0.116B_a + 0.788V_a - 0.005(-1/V_a)$

Ein Modell mit den Termen V, Ladungsdichte, B und S erlaubt die Vorhersage der Zytotoxizität der ILs gegenüber *Scenedesmus vacuolatus* mit einer SD von 0,643:

Log [$1/EC_{50}$], *Scenedesmus vacuolatus* = $-34.787 - 2.702B_c - 0.382S_c + 13.714V_c + 16.101(1/V_c) + 0.892S_a - 0.600B_a + 1.768V_a - 0.766(-1/V_a)$

ACKNOWLEDGEMENTS

This project was mainly funded by German research foundation DFG - SPP 1191, but in parts by University of Bremen, University of Freiburg, and Deutsche Bundesstiftung Umwelt DBU.

I am very fortune to be surrounded by many good people to give willingly their time, effort and several supports in order to complete this thesis.

I would like to express my sincere gratitude to Prof. Jorg Thöming for giving me an opportunity to study in Bremen and for having supervised my PhD. Your guidance and support from initial to the final stage enabled me to develop understanding of the subject. Especially your valuable comments about family made me - as a father - happy and comfort.

I am heartily thankful to Prof. Ingo Krossing for having supervised my PhD. Your support and encouragement helped me maintain confidence and motivation. Especially computational skill from your group inspired me to extend my research area. To be honest I would like to learn your passion for research.

I would like to thank to Prof. Yun, Yeoung-Sang for always cheering me from Korea. Since I have started the research under your supervision, I am not able to quit the research.

I would like to thank (in Bremen)

- Stefan Stolte for arranging almost official stuffs from initial to now, and for technical and experimental advices and discussion, and for your warm mind.
- Jürgen Arning for correcting the toxicity paper with many good discussions, and for helping me write this thesis, and for always warming your e-mails.
- Johannes Ranke for helping me that I could come to Bremen for PhD study, for providing theoretical idea and its explanation, for discussion on the experimental results and improvement of scientific paper, and for your frank and friendly talks with me.
- Jenny Neumann for your successful cooperation about biodegradation test, your technical and analytical advices for HPLC-MS measurement, supporting advanced information and life in Germany and for beautiful hand-made baby shoes for my second daughter.
- Christian Jungnickel for your cooperation for this project, submission of paper, English correction, presentations at the DFG meeting, and your discussion for the paper and poster.
- Jan Köser for your good information on life in Bremen, nice and frank talks face to face, and interest in Korean foods.
- Jóse Fernández for your guidance how to write this thesis and how to study in Bremen.
- Ha Bui Thi Thu for speaking in Korean and talking about Korea life together with me. It is

helpful for me to overcome my homesick.

- Magdalena for your cooperation about biodegradation test, analytic performance and taking sample I was out of office when my daughter was born.
- Ioana Stan for your picking me up when I was here in Bremen for the first time, and helping me to rent flat, explaining information on Bremen, University, and lab.
- Ulrike Bottin-Weber, Andrea Böschen, Antje Mathews, Antje Siol, Ruth Krumrey-Rosch, and Ruth Beckermann for supporting to my research and official stuffs and your contributions to our lab. Because of you, our lab looks very beautiful and healthy. So I am happy.
- Michael Baune, Detlef Bobenhausen, Dietmar Grotheer, Mirko Weinhold, George Okoth, Waldemar Retkowski, Stephanie Steudte, Barbara Stoess, Jürgen Ulpts, Thomas Veltzke, Wiebke Velztze, Ralf Sievering, Ahmed Ibrahim Salem Yussef, and Fei Du for your nice friendship. I hope we can have more time in private and cooperation in near future.

I would like to thank (in Freiburg)

- Ulrich Preiss for your teaching for computational way, discussing about prediction modeling and providing information for life in Freiburg.
- Philipp Eiden, Lucia Alvarez, Mara Bürchner, and Witali Beichel for helping me learn COSMO calculation, and for your kind friendship.
- Vera Brucksch and Brigitte Jörger for arranging all official stuff and beautiful smile.
- Werner Deck, Maribel Sierra, Alexander Higelin, Julia Schaefer, Mathias Hill, Fadime Bitgül, Harald Scherer, Anna Maria Erle, Daniel Himmel, Nils Trapp, Sascha Goll, Christoph Schulz and others for your great friendship.

I explicitly would like to thank to my wife Shin, Eun-kyoung. Without your dedication and pray with tear, I could not succeed to complete my PhD study.
Yoon-Seo and Yoon-Ha!! You let me realize again the love of God.
I would like to thank to my parents and parents in law for financial support and praying for us at every dawn or staying all night.
Thanks my other family for financial support and your pray.

Thanks to EBTL members for keeping your nice contact and cheering me.
I would like to thank members of church for your prying for me and my family. Especially I would like to thank to Pastor Han, Min-Soo; Pastor Hwang, Hun-Sik; Pastor Rhee Sang-Ho.

TABLE OF CONTENTS

List of Tables

List of Figures

The list of symbol and abbreviations

A	Hydrogen bonding acidity
ACN	Acetonitrile
B	Hydrogen bonding basicity
C_a	Activity coefficient of anion at the ionic-liquids saturated condition in water
Calc.	Predicted or calculated
CMC	Critical micelle concentration
COSMO	COnductor–like Screening Model
COSMO-RS	COSMO for Real Solvents
C^i_o	Concentration of ILs in octanol phase
C^i_w	Concentration of ILs in water phase
d	System parameter of activity coefficient of anion in water
E	Excess molar refraction
EC_{50}	Effective Concentration for which half of the maximal effect is observable
Exp.	Measured
F	Fisher statics
f_a	System parameter of charge density of anion
H_a	Hydrophobicity of anion
HBA3	Hydrogen bonding acidity 3
HBD3	Hydrogen bonding donor 3
HPLC	High performance liquids chromatography
LFER	Linear free energy relationship
Log *k*	Capacity factor of molecule
Log k_o	Cationic hydrophobicity
Log $P_{o/w}$	Octanol-water partitioning coefficient
MeOH	Methanol
MLR	Multiple linear regression
MR	Molar refractivity
MS	Mass spectrometer
PLS-DA	Partial Least Squeres–Discriminant Analysis
QSAR	Quantitative Structure Activity Relationship
R^2	Statistical coefficient
S	Dipolarity/polarizability
SD	Standard deviation
sig 2(σ^2)	Sigma moment 2
sig 3 (σ^3)	Sigma moment 3
TATB	Tetraphenyl Arsenate – Tetraphenyl Borate

V	McGowan volume
Z	Ionic descriptors
$[Choline]^+$	Choline
$[Gu01111O2]^+$	Tetramethylguanidinium
$[IM]^+$	Imidazolium
$[IM01]^+$	1-Methylimidazolium
$[IM04]^+$	1-Butylimidazolium
$[IM1\text{-}10]^+$	1-Decyl-3-methylimidazolium
$[IM1\text{-}14]^+$	1-Methyl-3-tetradecylimidazolium
$[IM1\text{-}16]^+$	1-Hexadecyl-3-methylimidazolium
$[IM1\text{-}18]^+$	1-Methyl-3-octadecylimidazolium
$[IM11CN]^+$	1-(Cyanomethyl)-3-methylimidazolium
$[IM11O2]^+$	1-(Ethoxymethyl)-3-methylimidazolium
$[IM1\text{-}1Ph]^+$	1-Benzyl-3-methylimidazolium
$[IM12]^+$	1-Ethyl-3-methylimidazolium
$[IM1\text{-}2C6F13]^+$	1-Methyl-3-(3,3,4,4,5,5,6,6,7,7,8,8,8-tridecafluorooctyl)imidazolium
$[IM12O1]^+$	1-(2-Methoxyethyl)-3-methylimidazolium
$[IM12O2]^+$	1-(2-Ethoxyethyl)-3-methylimidazolium
$[IM12OH]^+$	1-(2-Hydroxyethyl)-3-methylimidazolium
$[IM13]^+$	1-Methyl-3-propylimidazolium
$[IM13O1]^+$	1-(3-Methoxypropyl)-3-methylimidazolium
$[IM13OH]^+$	1-(3-Hydroxypropyl)-3-methylimidazolium
$[IM14]^+$	1-Butyl-3-methylimidazolium
$[IM14\text{-}2Me]^+$	1-Butyl-2,3-dimethylimidazolium
$[IM15]^+$	1-Methyl-3-pentylimidazolium
$[IM16]^+$	1-Hexyl-3-methylimidazolium
$[IM16\text{-}2Me]^+$	1-Hexyl-2,3-dimethylimidazolium
$[IM17]^+$	1-Heptyl-3-methylimidazolium
$[IM18]^+$	1-Methyl-3-octylimidazolium
$[IM19]^+$	1-Methyl-3-nonylimidazolium
$[IM24]^+]$	1-Butyl-3-ethylimidazolium
$[IM26]^+$	1-Ethyl-3-hexylimidazolium
$[Melamine]^+$	1,3,5,-Trazine-2,4,6,-triamine
$[Mor11CN]^+$	4-(Cyanomethyl)-4-methylmorpholinium
$[Mor11O2]^+$	4-(Ethoxymethyl)-4-methylmorpholinium
$[Mor12]^+$	4-Ethyl-4-methylmorpholinium
$[Mor12O1]^+$	4-(2-Methoxyethyl)-4-methylmorpholinium
$[Mor12O2]^+$	4-(2-Ethoxyethyl)-4-methylmorpholinium
$[Mor12OH]^+$	4-(2-Hydroxyethyl)-4-methylmorpholinium
$[Mor13O1]^+$	4-(3-Methoxypropyl)-4-methylmorpholinium

$[Mor13OH]^+$	4-(3-Hydroxypropyl)-4-methylmorpholinium
$[Mor14]^+$	4-Butyl-4-methylmorpholinium
$[N0,1,1,2OH]^+$	(2-Hydroxyethyl)dimethylammonium
$[N1,1,1,1]^+$	Tetramethylammonium
$[N1,1,1,16]^+$	Trimethylhexadecylammonium
$[N1,1,1,4]^+$	Butyltrimethylammonium
$[N1,1,14,1Ph]^+$	Benzyldimethyltetradecylammonium
$[N1,1,2,1CN]^+$	(Cyanomethyl)ethyldimethylammonium
$[N1,1,2,1COO2]^+$	(Ethoxycarbonylmethyl)ethyldimethylammonium
$[N1,1,2,1O2]^+$	(Ethoxymethyl)ethyldimethylammonium
$[N1,1,2,2O1]^+$	Ethyl(2-methoxyethyl)dimethylammonium
$[N1,1,2,2O2]^+$	(2-Ethoxyethyl)ethyldimethylammonium
$[N1,1,2,3O1]^+$	Ethyl(3-methoxypropyl)dimethylammonium
$[N1,1,2,3OH]^+$	Ethyl(3-hydroxypropyl)dimethylammonium
$[N1,1,2,4]^+$	Butylethyldimethylammonium
$[N1,1,Bz,10]^+$	Benzyldecyldimethylammonium
$[N1,1,Bz,12]^+$	Benzyldodecyldimethylammonium
$[N1,8,8,8]^+$	Methyltrioctylammonium
$[N2,2,2,6]^+$	Triethylhexylammonium
$[N4,4,4,4]^+$	Tetrabutylammonium
$[P1i4i4i4]^+$	Methyltris(2-methylpropyl)phosphonium
$[P4,4,4,2]^+$	Tributylethylphosphanium
$[P4,4,4,4]^+$	Tetrabutylphosphanium
$[P6,6,6,14]^+$	Trihexyltetradecylphosphanium
$[Pip11CN]^+$	1-(Cyanomethyl)-1-methylpiperidinium
$[Pip11O2]^+$	1-(Ethoxymethyl)-1-methylpiperidinium
$[Pip12O1]^+$	1-(2-Methoxyethyl)-1-methylpiperidinium
$[Pip12O2]^+$	1-(2-Ethoxyethyl)-1-methylpiperidinium
$[Pip12OH]^+$	1-(2-Hydroxyethyl)-1-methylpiperidinium
$[Pip13O1]^+$	1-(3-Methoxypropyl)-1-methylpiperidinium
$[Pip13OH]^+$	1-(3-Hydroxypropyl)-1-methylpiperidinium
$[Pip14]^+$	1-Butyl-1-methylpiperidinium
$[Py0]^+$	Pyridinium
$[Py1\text{-}4NMe2]^+$	4-(Dimethylamino)-1-methylpyridinium
$[Py1CN]^+$	1-(Cyanomethyl)pyridinium
$[Py1O2]^+$	1-(Ethoxymethyl)pyridinium
$[Py2]^+$	1-Ethylpyridinium
$[Py2\text{-}4NMe2]^+$	4-(Dimethylamino)-1-ethylpyridinium
$[Py2O1]^+$	1-(2-Methoxyethyl)pyridinium
$[Py2O2]^+$	1-(2-Ethoxyethyl)pyridinium
$[Py2OH]^+$	1-(2-Hydroxyethyl)pyridinium

$[Py3]^+$	1-Propylpyridinium
$[Py3O1]^+$	1-(3-Methoxypropyl)pyridinium
$[Py3OH]^+$	1-(3-Hydroxypropyl)pyridinium
$[Py3SO3H]^+$	1-(3-Sulfopropyl)pyridinium
$[Py4]^+$	1-Butylpyridinium
$[Py4–2Me]^+$	1-Butyl-2-methylpyridinium
$[Py4\text{-}3Me]^+$	1-Butyl-3-methylpyridinium
$[Py4\text{-}3Me\text{-}4Me]^+$	1-Butyl-3,4-dimethylpyridinium
$[Py4\text{-}3Me\text{-}5Me]^+$	1-Butyl-3,5-dimethylpyridinium
$[Py4\text{-}4Me]^+$	1-Butyl-4-methylpyridinium
$[Py4\text{-}4NMe2]^+$	1-Butyl-4-(dimethylamino)pyridinium
$[Py5]^+$	1-Pentylpyridinium
$[Py6]^+$	1-Hexylpyridinium
$[Py6\text{-}3Me]^+$	1-Hexyl-3-methylpyridinium
$[Py6\text{-}4Me]^+$	1-Hexyl-4-methylpyridinium
$[Py6\text{-}4NMe2]^+$	4-(Dimethylamino)-1-hexylpyridinium
$[Py8]^+$	1-Octylpyridinium
$[Py8\text{-}3Me]^+$	3-Methyl-1-octylpyridinium
$[Py8\text{-}4Me]^+$	4-Methyl-1-octylpyridinium
$[Pyr11COO2]^+$	1-(Ethoxycarbonylmethyl)-1-methylpyrrolidinium
$[Pyr11O2]^+$	1-(Ethoxymethyl)-1-methylpyrrolidinium
$[Pyr12O1]^+$	1-(2-Methoxyethyl)-1-methylpyrrolidinium
$[Pyr12O2]^+$	1-(2-Ethoxyethyl)-1-methylpyrrolidinium
$[Pyr12OH]^+$	1-(2-Hydroxyethyl)-1-methylpyrrolidinium
$[Pyr13O1]^+$	1-(3-Methoxypropyl)-1-methylpyrrolidinium
$[Pyr13OH]^+$	1-(3-Hydroxypropyl)-1-methylpyrrolidinium
$[Pyr14]^+$	1-Butyl-1-methylpyrrolidinium
$[Pyr16]^+$	1-hexyl-1-methylpyrrolidinium
$[Pyr18]^+$	1-Methyl-1-octylpyrrolidinium
$[Pyr66]^+$	1,1-Dihexylpyrrolidinium
$[Quin4]^+$	1-Butylquinolinium
$[Quin6]^+$	1-Hexylquinolinium
$[Quin8]^+$	1-Octylquinolinium
$[S122]^+$	Diethylmethylsulfanium
$[S222]^+$	Triethylsulfanium
$[TMG]^+$	1,1,3,3,-Tetramethylguanidine
$[Xn1111]^+$	2,3,6,7-Tetrahydro-1,3,7,9-tetramethyl-2,6-dioxo-purinium
Cl^-	Chloride
I^-	Iodide
$[(2\text{-}OPhO)2B]^-$	Bis[1,2-benzenediolato(2-)]borate(1-)

$[(2\text{-}SO_2PhCO)N]^-$	1,1-Dioxo-1,2-dihydrobenzo[d]isothiazol-3-onate(1-)
$[(C_2F_5)_2PO_2]^-$	Bis(pentafluoroethyl)phosphinate
$[(C_2F_5)_3PF_3]^-$	Trifluoridotris(pentafluoroethyl)phosphate(1-)
$[(CF_3)_2N]^-$	Bis(trifluoromethyl)amide(1-)
$[(CF_3SO_2)_2N]^-$	Bis(trifluoromethylsulfonyl)amide(1-)
$[(CF_3SO_2)_3C]^-$	Tris(trifluoromethylsulfonyl)methanide(1-)
$[1COO]^-$	Acetate
$[1O2O2OSO3]^-$	*O*-2-(2-methoxyethoxy)ethyl sulfate
$[1OSO3]^-$	*O*-Methyl sulfate
$[1SO3]^-$	Methanesulfonate
$[2OSO3]^-$	*O*-Ethyl sulfate
$[4MePhSO3]^-$	4-Methylbenzenesulfonate
$[8OSO3]^-$	*O*-Octyl sulfate
$[Al_2Cl_7]^-$	μ-Chlorohexachloridodialuminate(1-)
$[B(CN)_4]^-$	Tetracyanidoboranuide(1-)
$[BF_4]^-$	Tetrafluoridoboranuide(1-)
$[Cap]^-$	Caprylate
$[CF_3COO]^-$	Trifluoroacetate
$[CF_3SO_3]^-$	Trifluoromethanesulfonate
$[Cl4SO_3]^-$	4-Chloro-1-butanesulfonate
$[F4SO_3]^-$	4-Fluoro-1-butanesulfonate
$[FeCl_4]^-$	Tetrachloridoferrate(1-)
$[HCOO]^-$	Formate
$[HSO_4]^-$	Hydrogen sulfate
$[N(CN)_2]^-$	Dicyanidoamide(1-)
$[PF_6]^-$	Hexafluoridophosphate(1-)
$[SbF_6]^-$	Hexafluoridoantimonate(1-)
$[SCN]^-$	Thiocyanate
Br^-	Bromide

1. Motivation

Since industrial revolution, quantitative and qualitative expansion of chemical industries with advancement in science and technology have been beneficial to human life, as well as improved the quality of life. For example, chemical developments after the 19th century helped to increase the average life–expectancy of human beings through the development of medicines and have also remarkably enhanced agriculture productivity by using fertilizer and pesticides.

However in the industrial processes, major interest always focused on economically important products. To achieve this, many chemicals have been imprudently synthesized. As illustrated by the Chemical Abstract Service (CAS; an agency providing database of resisted chemical substance information worldwide),[1] until now (27–July–2011) approximately 61 million organic and inorganic substances are registered, whereof around 54 million chemicals are commercially available from around 900 chemical companies. Every day approximately 12,000 additional substance are newly created. The synthesized chemicals, at least purchasable substances, can be potentially released to the environment through direct or indirect way in various products or from their production processes.

The chemicals, if released into the environment, are likely to accumulate in microorganisms and human body, therefore induce harmful effects to environments and human e.g. carcinogenicity, deformed children delivery. In fact many chemicals have been released and caused problems. In 1961 the intake of thalidomide, developed for reducing vomiting of pregnancy, during pregnancy leads to fatal deformities. CFC (chlorofluorocarbon) as a coolant in heat exchange system destroyed ozone. By release of waste water with cadmium and mercury in Japan in 1950's, many people were poisoned with the heavy metals. In Italy in 1976, released dioxin led to 100 cases of chloracne and an evacuation of people lasting for months. And in Bhopal (India), around 20 thousand people were killed by leakage of methyl isocyanate gas from a Union Carbide plant.[2]

These accidents were due to release of high concentration of harmful substances which were beyond the self–purification ability of the ecosystem. Consequently each country has established various techniques and policies to properly treat harmful materials and manage safe environment[3] *e.g.* the safe treatment techniques, emission reduction techniques in final outlet of industrials, and emission levy. The techniques and policies have achieved some visible results up-to-date, however the policies regarding 'treatment after usage' can be limited to manage continuously synthesized

various chemicals because newly designed chemicals might have unforeseeable toxic effect in nature. Therefore, a new paradigm for environmental management to prevent the chemical risks is required. Such a paradigm was established – namely the policy of 'Green Chemistry' –also called 'Sustainable Chemistry' in the EU – was established at the beginning of 1991 in EPA (USA).[3] 'Green Chemistry' is not a collection of specific techniques, but it is a paradigm of science to promote the research, development and implementation of innovative chemical technologies in a scientifically sound and cost effective manner.[3] The Green Chemistry program supports chemical technologies to minimize or eliminate contaminant emission and usage of harmful chemical from the beginning to ending of chemical and industrial processes.

To achieve the aim of Green Chemistry, Anastas and Warner (1998)[4] proposed the 12 principles of green chemistry (Table 1.1). Furthermore to recognize the importance of green engineering, they also proposed the 12 principles of green engineering.[5] Afterwards, based on the principles from Anastas and Warner, Tang[6] reinforced the green principles and green engineering.

Table 1.1. The 12 principles of green chemistry (Anastas and Warner, 1998)[5]

1	It is better to prevent waste than to treat or clean up waste after it is formed.
2	Synthetic methods should be designed to maximize the incorporation of all materials used in the process into the final product.
3	Wherever practicable, synthetic methodologies should be designed to use and generate substances that possess little or no toxicity to human health and the environment.
4	Chemical products should be designed to preserve efficacy of function while reducing toxicity.
5	The use of auxiliary substances (e.g. solvents, separation agents, etc.) should be made unnecessary wherever possible and, innocuous when used.
6	Energy requirements should be recognized for their environmental and economic impacts and should be minimized. Synthetic methods should be conducted at ambient temperature and pressure.
7	A raw material or feedstock should be renewable rather than depleting wherever technically and economically practicable.
8	Reduce derivatives – Unnecessary derivatization (blocking group, protection/ deprotection, temporary modification) should be avoided whenever possible.
9	Catalytic reagents (as selective as possible) are superior to stoichiometric reagents.
10	Chemical products should be designed so that at the end of their function they do not persist in the environment and break down into innocuous degradation products.
11	Analytical methodologies need to be further developed to allow for real–time, in–process monitoring and control prior to the formation of hazardous substances.
12	Substances and the form of a substance used in a chemical process should be chosen to minimize potential for chemical accidents, including releases, explosions, and fires.

In such a pursue of these 12 principles of green chemistry and green engineering, many researchers and engineers have developed an interest in ionic liquids (ILs) because the ILs are a class of solvents which have the potential to adhere to the principles of Green chemistry and provide solutions to many applications due to their unique physicochemical properties:

- non–flammable
- non–explosive
- non–volatile
- high thermal stability
- high reuse potentials
- high conductivity
- tunable solvation ability:

The properties of the solvent can be significantly designed ("tailor-made") by changing the nature of the ions

Due to ILs' negligible volatility, excellent thermal stability, and good solvation properties for both organic and non–organic materials, they can replace traditional organic solvents –which are one of the problems in environment.[7] Their miscibility with water can be adjusted for separation processes where they can be recovered after usage.[8] Moreover, since they can be designed by the modification of ionic structures and the selective combination of cations and anions, they might be infinitely applied in the industrial processes.[9] On the other hand, this implied that, in the viewpoint of the environment, their numerous possibilities might evoke many unforeseen toxic effects in the aquatic environment, if they are to be accidentally released. Therefore it is essential to understand the physical and chemical, as well as biological properties of IL ions on a molecular level to successfully designing ILs with technical relevance and environmental benign properties. This is especially relevant for the environmental behavior i.e. toxicity is extremely crucial for the chemicals to avoid the hazardous materials before synthesis, as suggested by the 12 principles of green chemistry.

When the molecular interactions of the ILs come into play, two common situations can be differentiated: Their roles as solvent and as solutes. For an understanding of the first situation, systematic roles of ILs as stationary phases were investigated by inverse gas chromatography facilitated by their low vapor pressures.[10-12] And also by measuring absorbance change according to impurity compounds in UV–spectrometer, their molecular interaction potentials were evaluated.[13-17] However, the second situation (as a role of solute) involves the possibility of separately investigating

the two IL components, namely cations and anions. This presents both a challenge and a chance. It is a challenge because they will be isolated or more or less associated in the form of ion pairs, clusters or aggregates depending on IL concentrations, their chemical environment and their own interactions.[18] For a simple example, the conductivity of aqueous IL solutions indicates the presence of free ions in solution.[19] The opportunity associated with the characterization of ILs as solutes stems from the possibility to characterize the molecular interaction potentials of the individual ions in a largely isolated manner. It can be expected that various properties such as liquid–liquid partitioning, liquid–surface partitioning, solubility and activity coefficient of ILs in various environments can be better understood and even predicted if the molecular interaction potentials of their ions can be successfully characterized. However, until now little is known about molecular interaction potential of ILs.

Thus, in this thesis, the key aims are:

- To estimate the molecular interaction potentials of individual ions *i.e.* 30 cations and 20 anions, using high performance liquid chromatography (HPLC) as ion–isolator, and COSMO calculation.
- To predict the physical, chemical and biological properties of ILs in aqueous solution *i.e.* activity coefficient, water–solubility, octanol–water partitioning coefficient, hydrophobicity, critical micelle concentration (CMC), cationic lipophilicity and cytotoxicity towards *Leukaemia rat cell line*, *Vibrio fishceri*, and *Scenedesmus vacuolatus* based on the calculated and measured descriptors of ions.
- To investigate how the calculated and measured descriptors contribute to the properties of ionic liquids.

The study is divided into seven chapters. They can be outlined as shown below:

Chapter 2 will introduce the conceptual backgrounds on the linear model based on linear free energy relationship (LFER), and explains the experimental and the computation methods for the determination of the LFER descriptors.

Chapter 3 will show the determination of MIPs of 30 cations – based on theoretical background and computational methods as shown in Chapter 2 and explain their MIPs according to the structures.

Chapter 4 will demonstrate the determination of the LFER descriptors of 20 anions based on theoretical and computational methodology (Chapter 2) and measured MIPs of cations (Chapter 3). And we clarified whether our conceptual model suggested in Chapter 2 is available for both ions *i.e.* cation and anion and estimated the LFER descriptors of anions.

Chapter 5 will establish the prediction models of the physical chemical properties of ILs using the calculated (Chapter 2) and measured (Chapter 3) LFER descriptors. Here we address how MIPs of ions contributes to the physical chemical properties *i.e.* water solubility, octanol–water partitioning, activity coefficient of anion at the IL saturated condition in water, and hydrophobicity of anion at the IL Equilibrated condition in water–octanol.

Chapter 6 will set out the prediction models on cytotoxicity decadic logarithm of $[1/EC_{50}]$ of ILs toward rat leukaemia cell line IPC-81, *Vibrio fischeri*, and *Scenedesmus vacuolatus* using only the calculated LFER descriptors based on the COSMO calculation explained in the chapter 2 and present how the molecular interaction potentials of IL ions affect the cytotoxicity.

Finally Chapter 7 will summarize the main conclusion of this study and suggest further studies.

2. Methodology

2.1. Conceptual approach for determination of molecular interaction potentials

Significant types of theoretical approaches for investigation of molecular interaction of ILs are group contribution methods, thermodynamically refined group contribution methods like the UNIFAC method,[20] poly–parameter Linear Free Energy Relationships (pp–LFER) like the Abraham equations[21] and methods based on quantum chemical calculations like continuum solvation models.[22] All of these methods have their strengths and weaknesses. Here, the versatility of the pp–LFER methods (Abraham equation) was stressed, which is based on the possibility to estimate partitioning of solutes between two arbitrary phases, if solute descriptors as well as system parameters of the phases are known. Out of the pp–LFERs, the Abraham equation [23-28] Eq. (2.1) is the most commonly used one:

$$SP = c + e\,E + s\,S + a\,A + b\,B + v\,V \qquad \text{Eq. (2.1)}$$

In Eq. (2.1), the dependent variable SP refers to some property of a series of solutes in a fixed phase. These solute descriptors are based on the physically meaningful cavity model of solute–system interactions. Here, E represents the excess molar refraction in units of $(cm^3\ mol^{-1})/10$, which models dispersive interactions arising from the greater polarizability of π and n– electrons. S represents the solute dipolarity and polarizability due to solute–solvent interaction between bond dipoles and induced dipoles. The A and B indicate the hydrogen bonding acidity and hydrogen bonding basicity of the solute. *V* is the McGowan characteristic molar volume in units of $(cm^3\ mol^{-1})/100$. The coefficient *e* is a measure of the propensity of the phase to interact with solute π– and n–electron pairs; coefficient *s* is a measure of the system dipolarity/polarizability; coefficient *a* is a measure of the hydrogen bond basicity, which interacts with an acidic solute; and *b* is a measure of the hydrogen bond acidity, which interacts with a basic solute. The system parameter *v* describes cavity formation in the case of bulk media. Finally, the parameter c is the property dependent offset of the LFER and obtained as regression constant.

However the Eq. (2.1) is of limited use for studying ion and ion species. Here, the term 'ion' refers to permanent ions such as Na^+ and Cl^-, and the term 'ion species' refers to ions derived by addition of subtraction of a proton from a neutral molecule. Thus Abraham and Zhao [29] constructed several system parameters for water–solvent partitions and for the first time determined ionic solute

descriptors using Gibbs energies of transfer of single ions based on the tetraphenyl arsenate – tetraphenyl borate (TATB) assumption[30] by adding the ionic terms j^+J^+ for cations, and j^-J^- for anions Eq. (2-2) to the Abraham equation Eq. (2-1)[29] which was originally developed for neutral compounds. Recently, using their newly determined solute descriptors, Abraham and Acree[31-33] have extended this work to study system parameters from water to several organic phases and characterized the solute descriptors for more ion species.

$$SP = c + e\,E + s\,S + a\,A + b\,B + v\,V + j^+J^+ + j^-J^- \qquad \text{Eq. (2.2)}$$

In an independent approach to address the special case of charged molecules in multiparameter linear free enthalpy relationships (mLFER) is proposed to add the solute descriptor Z and the system descriptor *z* to Eq. (2.1) as below

$$SP = c + e\,E + s\,S + a\,A + b\,B + v\,V + z\,Z \qquad \text{Eq. (2.3)}$$

Here, I assumed that the ionic interaction potential Z of any monovalent cation is 1, that of any monovalent anion is –1 respectively, and those of any neutral compounds are 0. (Regarding Z descriptors, I will in detail study in Chapter 4.) Correspondingly, the newly introduced Z simply denotes the permanent charge and covers partitioning related partial interaction energies for cations and anions, while the system constant *z* shows the system specific quantitative relevance of the Coulomb interaction, which must therefore correspond to an electrostatic potential. The partial interaction energy described by the term Z can therefore be seen as an analogy to the well–known Eq. (2.2) with a different conceptional background.

It may seem simplistic to set the Coulomb constant to ±1 also for cases where the molecular ion possess a delocalized charge or in systems, where ion pairing with the counterion partially compensates the charge. Nevertheless we claim that such effects can either be covered by the remaining terms (i.e. S, A, and B) of the Abraham equation, as in the case of charge delocalization, or should be addressed separately, as in the case of significant ion pairing. This approach ensures that only the specific property of ions to migrate or partition according to an electrostatic potential is covered by the *z*Z term. On the other hand, it supposes that the electrostatic potential is a system property and is not significantly influenced by the solute ion under investigation.

Here it should be noticed that the conceptual approach for ions and ion species is not the same as Abraham's approach, thus experimentally determined solute descriptors in this study cannot be used together with Abraham descriptors and system parameters. [31-33]

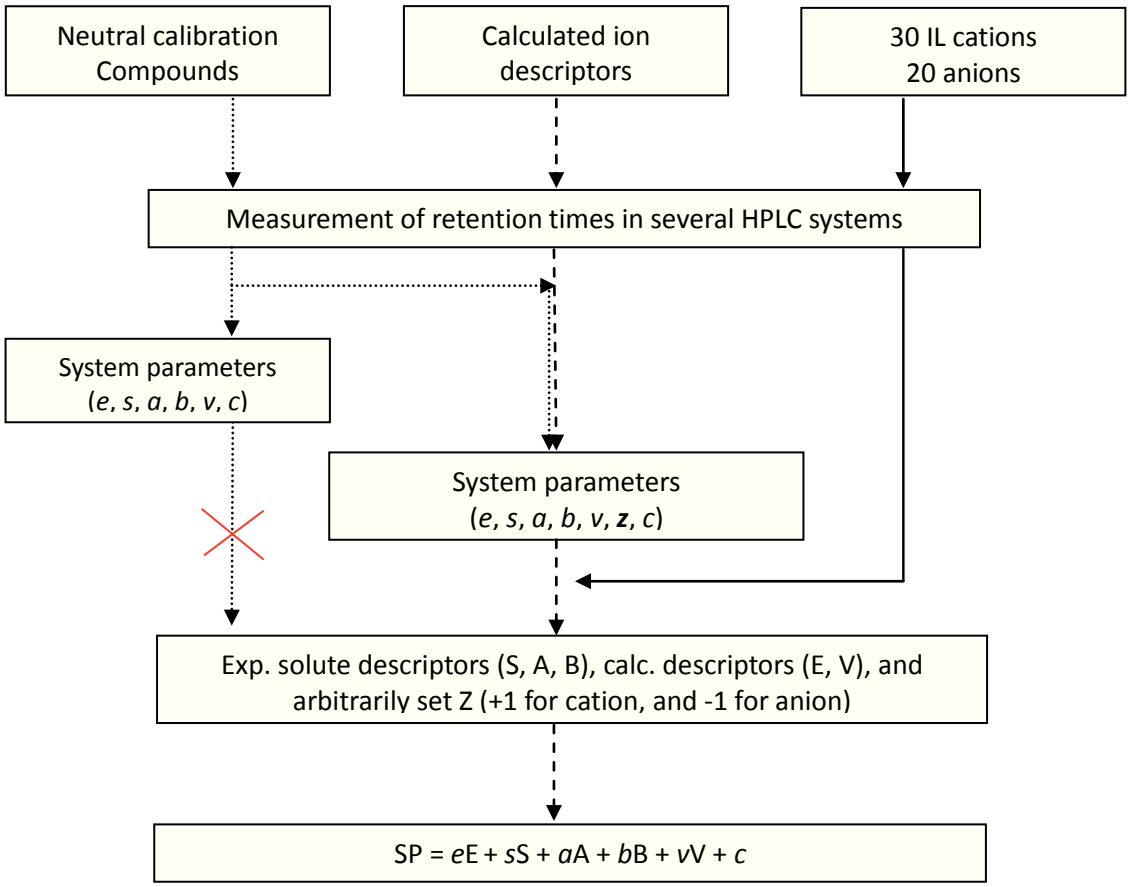

Figure 2.1. A strategy for determination of solute descriptors of IL cations and anions

In summarizing the methodology developed here, the solute descriptors of 30 cations and 20 anions can be determined by the following procedure (As shown in Figure 2.1): As a first step, the retention time of neutral compounds with known descriptors in five different HPLC systems is measured to estimate system parameters (*e, s, a, b, v, c*). As these system parameters will be of limited use for determing solute descriptors of ions, descriptors of "calibration ions" are calculated including *z*Z which is + 1 for monovalent cations, - 1 for monovalent anion and 0 for neutral compounds. After multiple linear regressions including retention time of the calculated ionic descriptors, system parameters can be obtained including *z* coefficient (*e, s, a, b, v, z, c*). Based on the system parameters, retention times of targeted ions, and computable E, V, and artificial Z value, the missing S, A, and B descriptors for cations will be obtained. And then finally the experimentally and computationally determined solute descriptors will be used for prediction of physical and chemical properties.

2.2. Experimental approach for the determination of molecular interaction potentials of ion

There may be a few methods to obtain Gibbs free energy related properties of single ions in a given system. As we mentioned above, one possible experimental method is to estimate the partitioning coefficient of a single ion between water and several solvents using the tetraphenyl arsenate – tetraphenyl borate (TATB) assumption[30] as Abraham and coworkers have done. [31-33] The rationale behind the TATB assumption[30] is that the four phenyl groups effectively shield the central ionic entity from direct interaction with the solvent and that therefore the chemical potential of the salt in solution can be equally attributed to cation and anion. However, this experimental work usually requires the exact quantification of the solute concentration, preferably in both phases, for each system. This can be very time–consuming and introduce a significant error if the solute is predominantly localized in one of the two phases. Also, ion pairing might affect partitioning of salts depending on their concentration.[34]

Another method is to use high performance liquid chromatography (HPLC), which is suitable for estimating retention characteristics of a variety of solutes and available stationary phases. It was successfully used to determine solute descriptors for neutral molecules.[35-36] A wide spectrum of molecular interaction potentials can be covered by various stationary phases. When salts are added to the mobile phase, which is frequently done in order to buffer the pH to the desired value, counterion effects can be neglected in analytical investigations of cations.[37] Again, the presumption of this type of approach is that the solute descriptors are independent of the chemical environment and the influence of the counterion in the buffer is assumed to be appropriately described by the system constants. This has previously been used to derive hydrophobicity parameters for cations that correlate well with cytotoxicity[38] and water solubility of ILs.[39] Therefore, Eq. (2.3) appears appropriate for the determination of solute descriptors of ions by HPLC, provided that the mobile phase contains electrolytes. It must be noted, however, that the partition of ion pairs in such systems is not appropriately described by this approach, as ion pairing is not explicitly included in Eq. (2.3). Therefore, it can be expected that Eq. (2.3) is limited to ions with a low tendency of ion pairing (weakly coordinating ions) as often used in ILs.

- **Step 1. Determination of HPLC system parameters (*e, s, a, b, v, z, c*) using neutral solutes with known descriptors**

Suitable liquid chromatographic systems have to be defined that can be used to generate retention data for as many neutral calibration compounds. Since it would be most convenient to use HPLC conditions that have already been established for pp-LFER correlations, the suitability of isocratic conditions specified in the literature, e.g. in the supporting information supplied by Fenner and co-workers[36] for ionic solutes will be investigated. Possibly, the pH could be adjusted in order to control surface charges of silica carriers, without significantly changing retention behavior of neutral solutes. Here, when establishing the system parameters of Abraham equation for HPLC, the neutral compounds are limited to determine *z* parameters. Thus for determination of z parameters using additional calibration compounds of ions, computational tools should be employed (see Chapter 2.3). Using the retention characteristics of neutral (from Abraham) and ionic compounds (from computational tool), all system coefficients including *z* can be determined. For solute descriptors of ions i.e. cation and anion, five systems were planned for each, even though only three orthogonal systems are required. Thus in total ten different systems will be investigated.

- **Step 2. Determination of solute descriptors (E, S, A, B, V, Z) for IL ions**

In a second step, the retention characteristics of IL cations will be measured in the five HPLC systems with known system parameters determined in step 1. And then the determined system parameters and retention characteristics of cations will be used in order to determine solute descriptors for cations according to the modified Abraham equations (Eq. 2.3). For the determination of solute descriptors of anions, anionic retention characteristics in the new five systems with known system parameters by performing Step 1 again using neutral calibration compounds, cationic calibration compounds (determined by step 1 & 2), and anionic calibration compounds (by computational tool) will be measured. And using them, the solute descriptors will be determined.

2.3 Computational details

There are several computational tools[20, 55] e.g. non-random two liquids (NRTL) [55a], universal quasi-chemical (UNIQUAC),[55a] equation of state (EoS),[55a] CLOGP (calculated logarithmic octanol-water partitioning coefficients),[55b] universal quasi-chemical functional group activity coefficients (UNIFAC),[20] and Monte Carlo methods[55c-f] and continuum solvation models[55g] e.g. COSMO(conductor-like screening model).[40-42] Among them, COSMO[40-42] has been popular owing to its remarkable advantages which are considerable reduction of the numerical demands; therefore having a substantial lower computational effort while increase of numerical robustness.[42d] Thus the COSMO calculation approach is used.

Background of COSMO, COSMO–RS [40-42] and OBPROP[53]

COSMO belongs to the class of dielectric continuum models.[40] This is a calculation method for screening electrostatic interaction of a molecular with a solvent.[42b] The fundamental idea of COSMO is to apply "the simpler boundary conditions of vanishing total potential that holds for a conductor, *i.e.* for a medium with infinite dielectric permittivity $\mathcal{E}$, and to use a scaling function $f(\mathcal{E})$ for the screening charge"[42a] in order to achieve an approximate solution for a finite dielectric.[42a] The polarization charges of the continuum induced by the polarity of the solute is represented by the screening change density σ appearing on the continuum solvent boundary surface and can be calculated by solving the boundary condition problems.[42]

"**COSMO** for **R**eal **S**olvents (COSMO-RS)" is a prediction model for all kinds of thermodynamic equilibrium properties of liquids that are imagined as a dense packing molecule in the reference state *e.g.* activity coefficient, solubility, heat of mixture, and liquid–liquid equilibrium properties.[42a] There are properties that are based on total energy of the molecule in the electrical conductor and the screening charge density on the molecular surface derived by quantum chemical COSMO calculations (see Chapter 2.3.1).[42c] Again the COSMO–RS describes locally contacting interaction of molecular surfaces in a fluid. So, COSMO–RS provides detailed quantative information about the polarity of molecules, namely the so-called σ^2–profile and σ^3–profile which are the values of two screening charge densities. Here most contributing energy modes are electrostatic misfit energy and hydrogen bonding.

OBPRO program is an open chemical toolbox to print a set of standard molecular properties e.g. molecular weight, exact mass, octanol-water partition, topological polar surface area, molar refractivity and number of atoms, bonds, residues, and rings. [53]

2.3.1. COSMO calculation

For the COSMO calculations of all sub–descriptors of ILs (σ2, σ3, HBD3, and HBA3), the structures of the single IL ions were optimized. Firstly, (RI–)BP86/SV(P) optimizations[43-45] in gas phase were carried out with the TURBOMOLE program package (version 5.10) using the Resolution of Identity (RI)[46] for reasonable starting structures. Using AOFORCE,[47,48] the vibrational frequencies of each ion were calculated. These structures were further refined with the TZVP[49] basis set, after which a full optimization with inclusion of COSMO[40] was performed ($\varepsilon_r = \infty$). And then the full optimization with COSMO[40] follows in order to obtain the .cosmo (or ccf), and the file is sent to COSMO–RS. Finally sig 2, sig 3, HBD3, and HBA3 of the optimized ion of ILs were calculated with COSMO–RS[40] using BP_TZVP_C21_0108 parameterization.

2.3.2. Sub–descriptors (sig 2, sig 3, HBD 3, HBA3, MR, and COSMO volume)

From the COSMO calculation, the sub–descriptors *i.e.* sigma–moment (σ^2 and σ^3), hydrogen bonding acidity 3 (HBA3), hydrogen bonding basicity 3 (HBD 3), can be obtained. As well as we could obtain COSMO calculated volume and molar refractivity from COSMO[40] and OBPROP[53] (internet freeware) respectively. The sub-descriptors are provided in Table 2.1 for cations and anions.

Table 2.1. Second sigma moment (σ^2), third sigma moment (σ^3), third hydrogen–bonding donor (HBD3), third hydrogen–bonding acceptor (HBA3) values and scaled COSMO volume for V of IL cations calculated by COSMO–RS and molar refraction (MR) for E calculated by OBPROP.

Cations	σ^2	σ^3	HBD3	HBA3	MR	Scaled Cosmo vol. [nm^3]
$[IM11]^+$	87.351	–84.816	1.929	0	29.353	0.126
$[IM12]^+$	84.733	–81.208	1.934	0	34.16	0.149
$[IM13]^+$	83.868	–79.476	1.962	0	38.967	0.173
$[IM14]^+$	84.047	–78.557	1.895	0	43.774	0.197
$[IM15]^+$	84.682	–78.359	1.903	0	48.581	0.220
$[IM16]^+$	85.452	–78.525	1.936	0	53.388	0.244
$[IM17]^+$	86.154	–78.252	1.925	0	58.195	0.267
$[IM18]^+$	86.741	–78.008	1.925	0	63.002	0.292

$[IM19]^+$	87.668	−78.275	1.961	0	67.809	0.315
$[IM1–10]^+$	88.154	−77.524	1.896	0	72.616	0.338
$[IM1–12]^+$	89.619	−77.325	1.887	0	82.230	0.385
$[IM1–14]^+$	91.274	−77.386	1.903	0	91.844	0.433
$[IM1–16]^+$	92.804	−77.309	1.917	0	102.515	0.482
$[IM1–18]^+$	94.393	−77.219	1.924	0	115.576	0.529
$[IM1–(1Ph–4Me)\ ]^+$	101.958	−87.064	2.096	0	58.806	0.253
$[IM1–1Ph]^+$	96.069	−80.484	1.276	0	53.840	0.229
$[IM1–2Ph]^+$	96.085	−80.462	1.282	0	53.840	0.228
$[IM1–2=1]^+$	90.110	−82.240	1.561	0	38.492	0.167
$[N1,1,\ 10,Bz]^+$	95.496	−69.665	0.396	0	91.466	0.427
$[N,1,1,12,\ Bz]^+$	96.343	−67.713	0.305	0	101.08	0.474
$[IM12O1]^+$	110.148	−73.145	2.344	1.065	40.052	0.187
$[IM13OH]^+$	151.917	−146.106	10.499	2.207	40.129	0.186
$[IM11O2]^+$	91.486	−74.392	1.349	0.038	40.052	0.186
$[Py2]^+$	84.770	−80.982	1.179	0	34.901	0.144
$[Py4]^+$	83.698	−78.040	1.161	0	44.522	0.192
$[Py6]^+$	84.915	−77.588	1.169	0	54.136	0.239
$[Py8]^+$	86.170	−77.234	1.165	0	63.75	0.287
$[Py4–2Me]^+$	76.982	−65.498	0.520	0	49.488	0.214
$[Py4–3Me]^+$	76.989	−67.175	0.921	0	49.488	0.215
$[Py4–4Me]^+$	77.337	−67.757	0.925	0	49.488	0.215
$[Py4–4NMe2]^+$	72.813	−58.095	0.306	0	58.729	0.254
$[Py6–4NMe2]^+$	69.577	−51.067	0.261	0	68.343	0.302
$[Py4–3Me–5Me]^+$	71.235	−56.607	0.379	0	54.454	0.235
$[Py6–3Me]^+$	78.205	−66.784	0.889	0	59.102	0.262
$[Py6–4Me]^+$	78.472	−67.135	0.865	0	59.100	0.263
$[Py8–4Me]^+$	80.048	−67.177	0.916	0	68.716	0.310
$[Pyr14]^+$	73.031	−56.635	0.060	0	44.802	0.212
$[Pyr16]^+$	74.639	−56.952	0.090	0	54.146	0.259
$[Pyr18]^+$	76.083	−56.688	0.098	0	64.030	0.306
$[IM16–2Me]^+$	75.876	−58.275	0.253	0	58.354	0.265
$[Pip14]^+$	71.688	−55.241	0.114	0	54.416	0.231
$[Mor11O2]^+$	111.608	−66.743	0.567	0.889	42.165	0.212
$[Py3OH]^+$	122.940	−80.564	3.4	1.818	40.877	0.180
$[IM12OH]^+$	132.798	−93.644	4.957	2.016	35.322	0.162
$[N4,4,4,4]^+$	67.172	−44.092	0.028	0	81.400	0.391
$[N1,1,1,8]^+$	82.829	−67.152	0.233	0	57.365	0.276
$[N1,1,1,10]^+$	84.379	−66.951	0.234	0	66.979	0.323
$[N1,1,1,12]^+$	85.856	−66.556	0.227	0	76.593	0.370
$[N1,1,1,14]^+$	87.443	−66.408	0.228	0	86.207	0.417

$[N1,1,1,16]^+$	89.164	–66.467	0.235	0	95.821	0.464
$[N1,1,1,18]^+$	90.481	–65.860	0.226	0	111.777	0.515
Na^+	2.60E–03	–6.70E–03	0	0	–	–
$[(CF3SO2)2N]^-$	95.34	98	0	1.40	32.84	0.218
$[B(CN)4]^-$	102.77	108.27	0	3.46	22.93	0.141
$[C(CN)3]^-$	113.23	140.06	0	7.57	20.59	0.104
$[4MEPhSO3]^-$	194.55	311.17	0	30.55	39.42	0.183
$[F4SO3]^-$	215.97	269.74	1.17	25.58	31.24	0.174
$[(CF3SO2)C]^-$	96.67	85.97	0	0.86	48.81	0.324
$[(8OSO3)]^-$	166.48	229.4	0	18.97	50.34	0.259
$[(1OSO3)]^-$	160.81	223.67	0	18.41	16.69	0.093
$[(1O2O2OSO3)]^-$	194.56	247.06	0	19.07	38.09	0.212
$[PF6]^-$	88.13	78.28	0	0	16.69	0.093
$[BF4]^-$	111.18	124.8	0	2.29	4.97	0.059
I^-	147.93	218.82	0	18.88	15.13	-
$[(2–SO2PhCO)N]^-$	178.00	180.04	1.74	14.88	38.39	0.183
$[2OSO3]^-$	163.29	229.32	0	19.11	21.50	0.116
$[6SO3]^-$	194.55	311.17	0	30.55	39.64	0.200
$[(C2F5)2PO2]^-$	104.56	144.29	0	12.68	31.83	0.236
$[AC]^-$	158.33	199.61	0	14.09	29.39	0.150
$[H(C2F4)SO3]^-$	145.79	158.72	0.38	12.63	20.65	0.142
$[4OSO3]^-$	163.92	229.78	0	19.09	31.11	0.164
$[4SO3]^-$	192.69	309.41	0	30.36	30.03	0.153
$[SbF6]^-$	80.01	67.17	0	0	14.24	0.113
F^-	-	0.00E+00	0	1.00E–02	2.22	-
$[HSO4]^-$	181.04	193.56	3.29	18.42	12.37	0.069
$[N(CN)2]^-$	133.01	193.15	0	45.64	14.03	0.070
$[SCN]^-$	128.45	177.43	0	12.28	14.6	0.056
Cl^-	-	358.95	0	36.66	6.92	-
Br^-	-	291.23	0	29.68	3.61	-
$[(2–OPHCOO)2B]^-$	168.58	176.01	0	12.72	38.39	0.183
$[(C2F5)3PF3]^-$	52.94	34.2	0	0.03	44.27	0.327
$[(CF2)2N]^-$	86.01	87.34	0	3.98	16.17	0.112
$[1COO]^-$	204.46	425.93	0	39	11.56	0.059
$[1OSO3]^-$	160.81	223.67	0	18.41	16.69	0.093
$[CF3COO]^-$	136.03	218.09	0	20.23	11.75	0.084
$[CF3SO3]^-$	119.21	157.86	0	10.8	15.8	0.109
$[[Cl4SO3]^-$	216.32	262.89	1.99	25.39	36.00	0.190
$[(C2F5SO2)2N]^-$	89.60	86.34	0	1.07	42.73	0.302
$[SbF6]^-$	81.01	67.17	0	0	14.24	0.113
$[PhBF3]^-$	131.01	142.84	0	6.32	29.19	0.154

$[(6–2Et)2SS]^-$	220.02	282.91	0	24.49	109.51	0.566
$[C8SO4]^-$	166.48	229.40	0	18.97	50.34	0.259
$[C10SO4]^-$	168.40	229.69	0	18.94	59.95	0.307
$[C12SO4]^-$	170.10	230.08	0	19.02	69.57	0.352
$[C14SO4]^-$	171.72	230.46	0	19.06	79.18	0.399
$[Al2Cl7]^-$	54.1752	30.9411	0	0	17.52	0.287

2.3.3. Calculated Abraham descriptors (E, S, A, B, and V) using sub–descriptors

For the investigations, the calculated sub–descriptors *i.e.* σ^2, σ^3, HBD3, HBA3, MR, and COSMO volume were used for calculation of Abraham descriptors *i.e.* E, S, A, B, and V. The McGowan volume of a molecule, given in $cm^3\ mol^{-1}/100$, can be calculated by addition of the volumes of all atoms and subtraction of 6.56 ml/mol for each bond regardless of whether it is a single, double or triple bond: McGowan volume = Σ all atom contributions – Σ 6.56 (number of bonds – 1 + number of rings).[23] However, unlike for neutral compounds, the McGowan volume of ionic compounds cannot be calculated in this way because the volume of ionic compounds can be altered with each loss or gain of electrons. The McGowan characteristic volume is the actual volume of a mole when the molecules are not in motion.[50] In this work, we used the molecular volume V_m, a physical observable as Abraham previously did.[50] It equals the crystallographic unit cell volume divided by the number of formula units and represents the space a molecule or ion pair occupies in the solid state. We have shown that these volumes ($V_m = V_m^+ + V_m^-$) can be reliably modeled by a BP86/TZVP + COSMO gas phase geometry optimization.[51] These calculated COSMO volumes [nm^3] were first compared with the McGowan volumes of neutral compounds to check the validity of the calculation. Literature values and calculated volumes of neutral compounds are given in Table 2.2. The results show an excellent correlation ($R^2 = 0.99$) between calculated and reported values (shown in the Figure 2.2). Equation (2.5) shows that the McGowan volume (V) of cations can be calculated by scaling the COSMO volume:

McGowan volume [$cm^3\ mol^{-1}/100$] = 6.399× scaled COSMO volume [nm^3] – 0.001 Eq. (2.5)

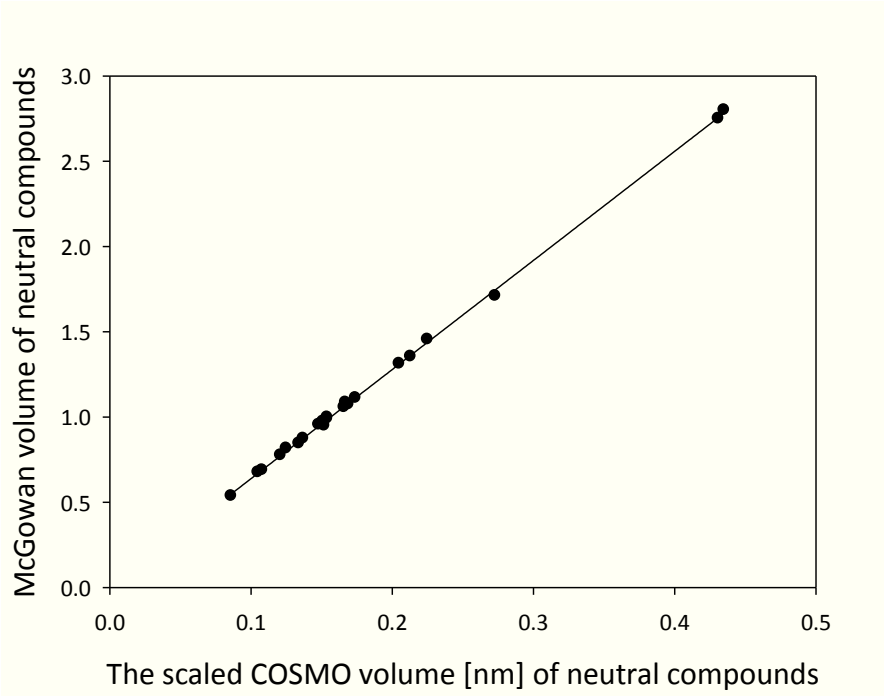

Figure 2.2. Correlation between the scaled COSMO [nm] and McGowan volumes [cm^3 mol^{-1}/100] in R^2 of 0.99 (according to Eq. (2.5))

For the calculation of cationic E values, the molar refractivity (MR) is required. Generally, this quantity can be easily measured or calculated by ACD/Chemsketch (http://www.acdlabs.com/resources/freeware/chemsketch) for neutral compounds as previous researchers mentioned.[36] However, in case of separate ions, neither are the mentioned calculations possible, nor are measurements feasible. As another computational approach, Zissimos *et al.*[52] reported a model for the calculation of E using COSMO–RS. Results, though, were suboptimal, as indicated by the large error range of 0.368 and the low R^2 of 0.504. Thus, as a supplementary method, we employed the OBPROP program[53] that calculates the molar refractivity (MR) based on a group contribution method.[54] The calculated molar refractivity values were scaled by comparison to the values of 22 neutral compounds as presented by Abraham (Figure 2.3). An excellent R^2 of 0.99 resulted. Finally the E values of compounds could be easily calculated using Equation 2.6, which means scaled molar refractivity (0.1015×MR – 0.5218) less the molar refractivity of an alkene with the same volume (–0.525+2.832V).[31] Literature values and calculated molar refractivities of the 22 neutral compounds[27] are given in Table 2.2.

$$E = (0.1015 \times MR - 0.5218) - (-0.525 + 2.832V) \qquad \text{Eq. (2.6)}$$

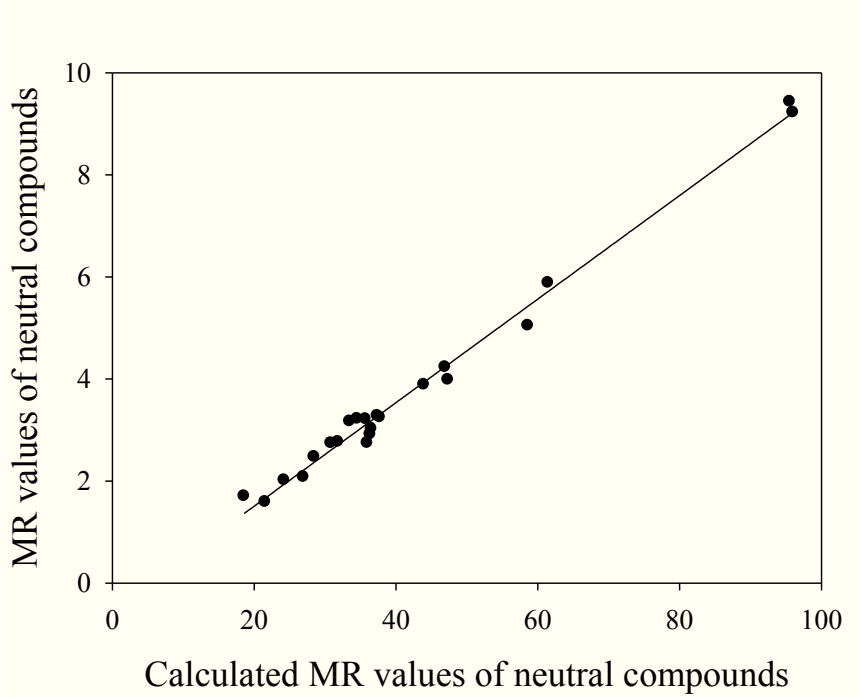

Figure 2.3. Correlation between literature and calculated (OBPROP) molecular refraction (MR) values of neutral compounds in R^2 of 0.99.

Table 2.2. McGowan volume V_{MG}[cm^3/mol] and calculated molar refractivity (MR) from literature,[27] and calculated COSMO volumes V_{cosmo} [nm^3], and molar refractivity from OBPROP of 22 neutral compounds

Chemicals	Structure	V_{MG} [cm^3/mol]	V_{cosmo} [nm^3]	MR from literature[27]	MR from OBPROP[27]
Phenol	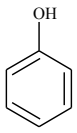	0.775	0.121	2.475	28.465
3–Nitrophenol	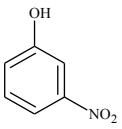	0.949	0.152	3.212	35.707
Salicylic acid	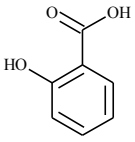	0.990	0.154	3.168	33.482
Cortisone	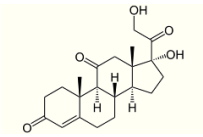	2.75	0.431	9.223	95.990
Hydrocortisone	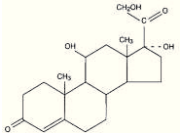	2.80	0.435	9.434	95.534

Diethyl phthalate	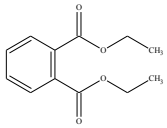	1.71	0.273	5.046	58.615
Ethyl acrylate	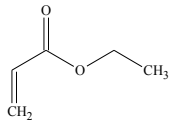	0.845	0.134	2.080	26.960
Propylbenzoate	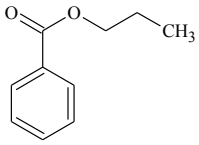	1.354	0.213	3.984	47.336
2–phenylethanol	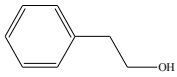	1.057	0.166	3.279	37.377
Methylbenzoate	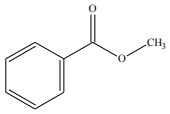	1.073	0.169	3.247	37.722
2–Butanone	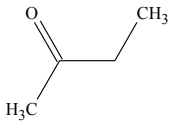	0.688	0.108	1.589	21.542
2–Heptanone	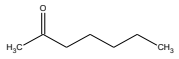	1.111	0.174	2.744	35.963
Benzamide	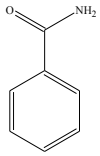	0.973	0.151	3.220	34.537
Naphthalene	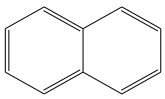	1.085	0.167	3.887	43.948
Ethyl 4–aminobenzoate	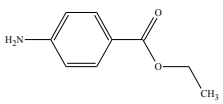	1.313	0.205	4.233	46.933
Anthracene	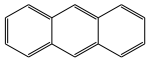	1.454	0.225	5.882	61.454
p–Xylene	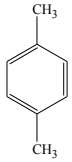	0.998	0.154	2.914	36.372

Styrene	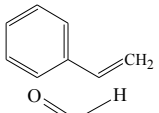	0.955	0.148	3.028	36.533
Benzaldehyde	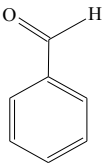	0.873	0.137	2.767	31.830
Pyridine	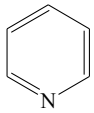	0.675	0.105	2.017	24.237
Imidazole	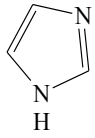	0.536	0.086	1.703	18.588
Aniline	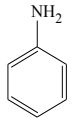	0.816	0.125	2.741	30.846

For the calculation of S, A, and B, the Equations from Zissimos *et al.*[52] were used. They investigated calculation methods for the Abraham descriptors with COSMO–RS program. For a set of 470 compounds with experimentally derived Abraham descriptors, they reported that the S, A, and B parameters can be calculated in COSMO–RS. But the authors mentioned that calculated S values have a large error of 0.215 and a rather poor R^2 value of 0.777. Thus, we attempted to establish a new model for S calculation with small error by performing new regression after adding E descriptor using the data from the supporting information provided by Zissimos *et al.*[52] The newly modified Equation has rather small standard deviation (0.167) and higher R^2 values (0.865) compared to Zissimos Equation indicating its usefulness Eq. (2.7). For A and B values the calculation methods [Eq. (2.8) for A and Eq. (2.9) for B] were used as developed by Zissimos *et al.* [52] with errors close to the experimental error.

$$S = -0.15 + 0.354\times E + 0.016\times sig2 - 0.078\times HBD3 - 0.040\times HBA3 \quad \text{Eq. (2.7)}$$

N=470, R^2=0.865, SD=0.167, F=746.2

$$A = 0.030 - 0.006\times sig\ 3 + 0.085\times HBD3 + 0.074\times HBA3 \quad \text{Eq. (2.8)}$$

N=470, R^2=0.926, SD=0.075, F=1941.5

$$B = -0.033 + 0.006\times sig2 + 0.007\times sig3 + 0.0022\times HBD3 + 0.017\times HBA3 \quad \text{Eq. (2.9)}$$

N=470, R^2=0.879, SD=0.099, F=841.2

The calculated descriptors (E, S, A, B, and V) according to Eq. (2.5) ~ Eq. (2.9) and ion descriptors (Z_c and Z_a) are given in Table 2.3 for cations and Table 2.4 for anions.

Table 2.3. The LFER descriptors of single cations of ionic liquids calculated by COSMO–RS, COSMO and OBPROP.

Cation	E_c	S_c	A_c	B_c	V_c	Z_c
[Choline]$^+$	0.351	1.697	0.969	0.151	0.941	+1
[Gu01111O2]$^+$	1.093	1.147	0.556	–0.020	1.340	+1
[IM]$^+$	0.621	1.106	2.690	–0.734	0.483	+1
[IM01]$^+$	0.668	1.233	1.675	–0.407	0.642	+1
[IM04]$^+$	0.881	1.238	1.602	–0.369	1.083	+1
[IM1–(1Ph–4Me)]$^+$	1.392	1.811	0.731	–0.026	1.617	+1
[IM11]$^+$	0.711	1.349	0.703	–0.098	0.802	+1
[IM1–10]$^+$	1.248	1.554	0.656	–0.043	2.163	+1
[IM1–12]$^+$	1.368	1.621	0.654	–0.032	2.466	+1
[IM1–14]$^+$	1.487	1.688	0.656	–0.023	2.768	+1
[IM1–16]$^+$	1.684	1.781	0.657	–0.013	3.081	+1
[IM1–18]$^+$	2.156	1.974	0.657	–0.003	3.382	+1
[IM11CN]$^+$	1.255	2.037	1.460	–0.091	0.988	+1
[IM11O2]$^+$	0.704	1.456	0.594	–0.001	1.188	+1
[IM1–1Ph]$^+$	1.328	1.758	0.621	–0.017	1.462	+1
[IM12]$^+$	0.771	1.328	0.682	–0.089	0.953	+1
[IM1–2=1]$^+$	0.894	1.487	0.656	–0.065	1.065	+1
[IM1–2C6F13]$^+$	–0.749	1.079	1.095	–0.171	2.556	+1
[IM12O1]$^+$	0.690	1.631	0.747	0.139	1.193	+1
[IM12O2]$^+$	0.770	1.517	0.645	0.041	1.337	+1
[IM12OH]$^+$	0.654	1.739	1.162	0.154	1.036	+1
[IM1–2Ph]$^+$	1.332	1.759	0.622	–0.017	1.461	+1
[IM13]$^+$	0.826	1.331	0.674	–0.082	1.106	+1
[IM13O1]$^+$	0.759	1.713	0.732	0.270	1.341	+1
[IM13OH]$^+$	0.718	1.628	1.962	–0.084	1.186	+1
[IM14]$^+$	0.886	1.361	0.662	–0.074	1.257	+1
[IM14–2Me]$^+$	0.964	1.398	0.446	–0.015	1.408	+1
[IM15]$^+$	0.945	1.391	0.662	–0.069	1.409	+1
[IM16]$^+$	1.007	1.423	0.666	–0.066	1.559	+1
[IM16–2Me]$^+$	1.136	1.446	0.401	0.015	1.692	+1
[IM17]$^+$	1.080	1.461	0.663	–0.060	1.706	+1
[IM18]$^+$	1.111	1.481	0.662	–0.054	1.867	+1
[IM19]$^+$	1.188	1.520	0.666	–0.051	2.012	+1
[IM–1–Ph]$^+$	1.328	1.758	0.621	–0.017	1.462	+1

[IM24]$^+$	0.945	1.335	0.655	–0.068	1.409	+1
[IM26]$^+$	1.058	1.398	0.645	–0.056	1.714	+1
[Melamine]$^+$	1.043	1.913	4.919	–1.059	0.852	+1
[Mor11CN]$^+$	0.375	2.067	1.418	0.048	1.160	+1
[Mor11O2]$^+$	0.444	1.713	0.545	0.186	1.356	+1
[Mor12]$^+$	0.502	1.679	0.530	0.159	1.124	+1
[Mor12O1]$^+$	0.430	2.034	0.656	0.367	1.360	+1
[Mor12O2]$^+$	0.523	2.058	0.640	0.382	1.500	+1
[Mor12OH]$^+$	0.413	2.078	1.044	0.335	1.197	+1
[Mor13O1]$^+$	0.542	1.971	0.540	0.386	1.493	+1
[Mor13OH]$^+$	0.477	2.047	0.863	0.414	1.347	+1
[Mor14]$^+$	0.642	1.715	0.525	0.168	1.419	+1
[N0,1,1,2OH]$^+$	0.386	1.255	2.394	–0.497	0.648	+1
[N1,1,1,1]$^+$	0.362	1.311	0.524	–0.061	0.723	+1
[N1,1,1,10]$^+$	0.951	1.519	0.452	–0.005	2.066	+1
[N1,1,1,12]$^+$	1.072	1.585	0.449	0.017	2.368	+1
[N1,1,1,14]$^+$	1.194	1.654	0.448	0.027	2.669	+1
[N1,1,1,16]$^+$	1.319	1.725	0.449	0.037	2.97	+1
[N1,1,1,18]$^+$	2.022	1.996	0.444	0.049	3.293	+1
[N1,1,1,4]$^+$	0.575	1.315	0.457	–0.027	1.165	+1
[N1,1,1,8]$^+$	0.829	1.451	0.453	–0.006	1.765	+1
[N1,1,14,1Ph]$^+$	1.802	2.032	0.473	0.074	3.333	+1
[N1,1,2,1CN]$^+$	0.411	1.740	1.201	–0.066	1.042	+1
[N1,1,2,1COO2]$^+$	0.514	1.742	0.637	0.120	1.405	+1
[N1,1,2,1O2]$^+$	0.449	1.267	0.46	–0.018	1.248	+1
[N1,1,2,2O1]$^+$	0.499	1.610	0.493	0.184	1.231	+1
[N1,1,2,2O2]$^+$	0.580	1.665	0.414	0.174	1.375	+1
[N1,1,2,3O1]$^+$	0.556	1.645	0.464	0.295	1.383	+1
[N1,1,2,3OH]$^+$	0.617	1.273	0.416	–0.014	1.150	+1
[N1,1,2,4]$^+$	0.665	1.300	0.422	–0.012	1.306	+1
[N1,1,Bz,10]$^+$	1.554	1.897	0.482	0.053	2.731	+1
[N1,1,Bz,12]$^+$	1.675	1.961	0.462	0.072	3.032	+1
[N1,8,8,8]$^+$	1.710	1.724	0.332	0.097	3.865	+1
[N2,2,2,6]$^+$	1.026	1.350	0.340	0.034	1.867	+1
[N4,4,4,4]$^+$	1.189	1.344	0.297	0.062	2.499	+1
[P1i4i4i4]$^+$	1.200	1.377	0.373	0.018	2.217	+1
[P4,4,4,2]$^+$	1.302	1.382	0.305	0.056	2.353	+1
[P4,4,4,4]$^+$	1.517	1.483	0.304	0.061	2.622	+1
[P6,6,6,14]$^+$	2.416	1.961	0.277	0.154	5.061	+1
[Pip11CN]$^+$	0.584	1.725	1.057	–0.017	1.219	+1

$[Pip11O2]^+$	0.666	1.289	0.379	0.036	1.411	+1
$[Pip12O1]^+$	0.673	1.592	0.434	0.213	1.408	+1
$[Pip12O2]^+$	0.752	1.611	0.420	0.222	1.553	+1
$[Pip12OH]^+$	0.631	1.664	0.848	0.203	1.254	+1
$[Pip13O1]^+$	0.736	1.633	0.406	0.324	1.558	+1
$[Pip13OH]^+$	0.687	1.778	0.741	0.376	1.406	+1
$[Pip14]^+$	1.476	1.465	0.359	0.028	1.478	+1
$[Py0]^+$	0.826	2.108	1.789	–0.172	0.613	+1
$[Py1–4NMe2]^+$	1.195	1.457	0.438	–0.023	1.167	+1
$[Py1CN]^+$	0.814	1.875	1.544	–0.155	0.956	+1
$[Py1O2]^+$	0.883	1.631	0.703	–0.008	1.152	+1
$[Py2]^+$	0.935	1.446	0.616	–0.089	0.922	+1
$[Py2–4NMe2]^+$	1.251	1.438	0.421	–0.015	1.320	+1
$[Py2O1]^+$	0.880	1.756	0.782	0.123	1.153	+1
$[Py2O2]^+$	0.958	1.772	0.771	0.136	1.298	+1
$[Py2OH]^+$	0.825	1.835	1.150	0.105	1.003	+1
$[Py3]^+$	0.992	1.445	0.604	–0.081	1.074	+1
$[Py3O1]^+$	0.923	1.696	0.602	0.146	1.310	+1
$[Py3OH]^+$	0.687	1.778	0.741	0.376	1.406	+1
$[Py3SO3H]^+$	0.714	2.365	1.615	0.078	1.484	+1
$[Py4]^+$	1.055	1.472	0.597	–0.075	1.225	+1
$[Py4–2Me]^+$	1.155	1.450	0.467	–0.029	1.367	+1
$[Py4–3Me]^+$	1.138	1.418	0.515	–0.041	1.373	+1
$[Py4–3Me–4Me]^+$	1.278	1.402	0.407	–0.001	1.502	+1
$[Py4–3Me–5Me]^+$	1.153	1.329	0.441	–0.015	1.520	+1
$[Py4–4Me]^+$	1.138	1.418	0.515	–0.041	1.373	+1
$[Py4–4NMe2]^+$	1.370	1.476	0.405	–0.002	1.623	+1
$[Py5]^+$	1.196	1.442	0.501	–0.032	1.525	+1
$[Py6]^+$	1.175	1.534	0.595	–0.064	1.527	+1
$[Py6–3Me]^+$	1.264	1.479	0.506	–0.029	1.673	+1
$[Py6–4Me]^+$	1.242	1.478	0.506	–0.030	1.681	+1
$[Py6–4NMe2]^+$	1.476	1.465	0.359	0.028	1.930	+1
$[Py8]^+$	1.272	1.588	0.592	–0.054	1.837	+1
$[Py8–3Me]^+$	1.366	1.543	0.511	–0.021	1.982	+1
$[Py8–4Me]^+$	1.366	1.543	0.511	–0.021	1.982	+1
$[Pyr11COO2]^+$	0.554	1.675	0.556	0.129	1.457	+1
$[Pyr11O2]^+$	0.523	1.275	0.375	0.045	1.289	+1
$[Pyr12O1]^+$	0.514	1.570	0.420	0.212	1.292	+1
$[Pyr12O2]^+$	0.597	1.593	0.410	0.223	1.435	+1
$[Pyr12OH]^+$	0.480	1.644	0.840	0.205	1.135	+1
$[Pyr13O1]^+$	0.569	1.626	0.414	0.348	1.445	+1

$[Pyr13OH]^+$	0.530	1.722	0.741	0.376	1.289	+1
$[Pyr14]^+$	1.476	1.465	0.359	0.028	1.478	+1
$[Pyr16]^+$	0.808	1.323	0.379	0.016	1.656	+1
$[Pyr18]^+$	0.956	1.398	0.380	0.025	1.959	+1
$[Pyr66]^+$	1.195	1.424	0.329	0.053	2.391	+1
$[Quin4]^+$	1.740	1.700	0.510	–0.030	1.610	+1
$[Quin6]^+$	1.860	1.760	0.510	–0.020	1.910	+1
$[Quin8]^+$	1.976	1.825	0.503	–0.012	2.216	+1
$[S122]^+$	0.846	1.403	0.528	–0.058	0.950	+1
$[S222]^+$	0.932	1.374	0.425	–0.021	1.091	+1
$[TMG]^+$	0.758	1.646	1.272	–0.025	1.042	+1
$[Xn1111]^+$	1.504	2.536	0.805	0.415	1.546	+1
Na^+	-0.020*	–0.157	0.030	–0.033	0.033*	+1

*were referred to Abraham *et al.*[29]

Table 2.4. The LFER descriptors of single anions of ionic liquids calculated by COSMO–RS, COSMO and OBPROP.

Anion	E_a	S_a	A_a	B_a	V_a	Z_a
I^-	0.384*	1.598	0.114	2.773	0.408*	–1
$[(2–OPhO)2B]^-$	1.247	2.228	–0.141	2.023	1.576	–1
$[(2–SO2PhCO)N]^-$	0.595	2.178	0.199	2.552	1.167	–1
$[(6–2Et)2SS]^-$	0.866	2.698	0.144	3.684	3.62	–1
$[(C2F5)2PO2]^-$	–1.042	0.647	0.103	1.82	1.51	–1
$[(C2F5)3PF3]^-$	–1.448	0.183	–0.173	0.525	2.099	–1
$[(C2F5SO2)2N]^-$	–1.124	0.843	–0.409	1.127	1.93	–1
$[(C4F9)SO3]^-$	–1.058	0.923	–0.145	1.824	1.473	–1
$[(CF3)2N]^-$	–0.391	0.929	–0.199	1.162	0.719	–1
$[(CF3SO2)2N]^-$	–0.608	1.104	–0.436	1.228	1.393	–1
$[(CF3SO2)3C]^-$	–0.906	1.041	–0.422	1.163	2.071	–1
$[1COO]^-$	0.112	1.601	0.36	4.838	0.376	–1
$[1O2O2OSO3]^-$	0.025	2.209	–0.041	3.188	1.357	–1
$[1OSO3]^-$	0.014	1.692	0.05	2.811	0.595	–1
$[1SO3]^-$	0.126	1.792	0.422	3.779	0.516	–1
$[2OSO3]^-$	0.086	1.729	0.068	2.877	0.741	–1
$[4MePhSO3]^-$	0.692	1.986	0.424	3.832	1.169	–1
$[8OSO3]^-$	0.428	1.907	0.058	2.894	1.654	–1
$[Al2Cl7]^-$	-3.417	-0.493	–0.156	0.509	1.838	–1
$[B(CN)4]^-$	–0.212	1.281	–0.364	1.400	0.898	–1
$[BF4]^-$	–0.566	1.337	–0.549	1.547	0.379	–1
$[C10SO4]^-$	0.528	1.974	0.053	2.973	1.964	–1
$[C12SO4]^-$	0.691	2.056	0.057	2.987	2.251	–1
$[C14SO4]^-$	0.812	2.123	0.058	3.001	2.553	–1
$[C8SO4]^-$	0.429	1.907	0.058	2.960	1.654	–1
$[Cap]^-$	0.475	1.785	0.324	4.817	1.281	–1
$[CF3COO]^-$	–0.234	1.481	0.364	4.844	0.498	–1
$[CF3SO3]^-$	–0.366	1.196	–0.118	1.971	0.697	–1
$[CH3COO]^-$	–0.234	1.481	0.364	4.844	0.498	–1
$[Cl4SO3]^-$	0.217	2.217	0.501	3.541	1.215	–1
$[F4SO3]^-$	0.023	2.199	0.404	3.588	1.113	–1
$[FeCl4]^-$	–1.416	0.491	–0.285	0.763	0.900	–1
$[HCOO]^-$	0.085	1.474	0.404	4.281	0.227	–1
$[HSO4]^-$	0.020	1.760	0.511	2.729	0.438	–1
$[N(CN)2]^-$	0.162	0.21	2.248	2.893	0.447	–1
$[NO3]^-$	0.193	1.531	0.075	2.769	0.269	–1

$[PF6]^-$	–0.189	1.193	–0.44	1.044	0.592	–1
$[PhBF3]^-$	0.169	1.753	–0.359	1.86	0.988	–1
$[SbF6]^-$	-0.597	0.919	–0.373	0.923	0.724	–1
$[SCN]^-$	0.478	1.583	–0.126	2.189	0.356	–1
Br^-	0.17*	1.453	0.482	3.534	0.307*	–1
Cl^-	0.06*	1.436	0.593	4.25	0.228*	–1

*were referred to Abraham *et al.*[29]

2.4. Application of LFER descriptors for prediction

The understanding of the molecular interactions of chemicals in various environments is a prerequisite for predicting their physical and chemical properties, and in the face of sustainable development their environmental properties should be predicted. For these objectives, the prediction studies using the experimentally (see Chapter 2.1) and computationally (see Chapter 2.3) determined solute descriptors will be used, because the LFER descriptors (solute descriptors) can be express the chemical behaviors of solute. As shown Figure 2.4, for examples of the applications for determined LFER descriptors in this study, toxicity, water solubility, octanol-water partitioning coefficient, and CMC of ILs, and hydrophobicity, and activity coefficient of IL anion will be predicted.

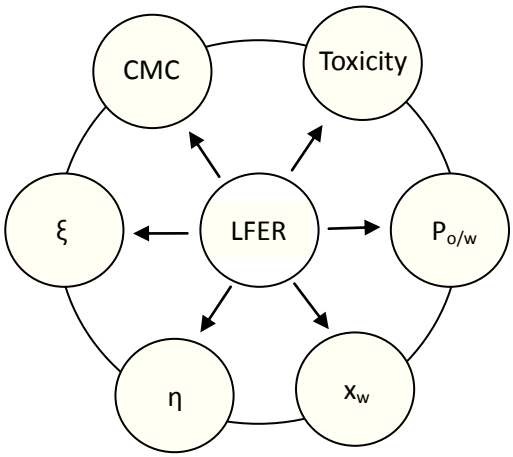

Figure 2.4. Schematic diagram of the applications of the linear free energy relationships in this study. (ξ-hydrophobicity, η –activity coefficient, x_w – water solubility, $P_{o/w}$ – octanol/water partitioning coefficient, CMC –critical micelle concentration in water)

2.5 Multiple linear regression[56]

Multiple linear regression (MLR) is a multivariate statistical techniques to model the linear relationship between single dependence variable (predictand) and one or more independence variables (predictors).[56] In this approach, the data are modeled based on the linear function. From the data, the unknown parameters are estimated. The linear function is based on the methods of least squares: the model is fit such that the sum–of–squares of differences of observed and predicted values is minimized.[56b] The MLR model forms:

$$Y_{Pred} = c + b_1X_1 + b_2X_2 + b_3X_3 + b_4X_4 + + b_nX_n \qquad \text{Eq. (2.10)}$$

where, Y_{pred} is the predictand on the criterion variable, the X_s are the predictor variables, and the b_s are coefficients related with the predictors.[57] These b_s are also referred to as *partial regression coefficients* (Kachigan, 1986)[57] because each reflects the relative contribution of its independent variable when we are statistically predicting for the effects of all the other predictors. [57] Because this is a raw score equation, it also contains a constant, shown as *c* in the equation 2.10, representing the *Y* intercept. For this statistic, I used SPSS package (version 12.0K window).

3. Determination of LFER parameters of 30 cations of ionic liquids – Progress in understanding of their molecular interaction potentials

3.1. Experiment

As I mentioned in methodology part (Chapter 2.2.), the HPLC enables to investigate molecular interaction between only single ion and system. Thus for this study, I employed five systems *i.e.* RP-select B-ACN, RP-select B-MeOH, Cyan-MeOH, Diol-ACN, and Diol-MeOH, which we deem sufficient to assess these LFER descriptors.

The HPLC measurements were carried out under isocratic conditions and operated at two different aqueous phase pHs, adjusted to pH 2.5 using 15 mM KH_2PO_4, 30 mM H_3PO_4, and to pH 10 using 1mM KOH. A basic mobile phase condition (pH 10) was only used for basic compounds, which are ionizable compounds at pH 2.5. A detection wavelength of 211 nm was used for imidazolium-based IL cations. The wavelength for the neutral calibration compounds, pyridinium-based cations, and ammonium-based cations with a benzene ring was set to 254 nm. Depending on their solubility and detectability, calibration and target compounds were injected at concentrations between 50 and 200 µM. The dead time of HPLC systems with RP-select B was determined by injecting thiourea at pH 2.5. The dead time of systems with diol and cyano groups was determined using clearly visible solvent peaks. In Table 3.1, the mobile phase conditions of the five HPLC systems and specifications for each column are provided. And the 30 cations i.e. $[IM12]^+$, $[IM13]^+$, $[IM14]^+$, $[IM15]^+$, $[IM16]^+$, $[IM17]^+$, $[IM18]^+$, $[IM19]^+$, $[IM1\text{-}10]^+$, $[IM1\text{-}1Ph]^+$, $[IM1\text{-}(1Ph\text{-}4Me)]^+$, $[IM1\text{-}2Ph]^+$, $[IM1\text{-}2\text{=}1]^+$, $[IM12O1]^+$, $[IM13OH]^+$, $[Py2]^+$, $[Py4]^+$, $[Py6]^+$, $[Py8]^+$, $[Py4\text{-}3Me]^+$, $[Py4\text{-}2Me]^+$, $[Py4\text{-}4Me]^+$, $[Py4\text{-}3Me\text{-}5Me]^+$, $[Py6\text{-}3Me]^+$, $[Py6\text{-}4Me]^+$, $[Py8\text{-}4Me]^+$, $[Py6\text{-}4NMe2]^+$, $[Py4\text{-}4NMe2]^+$, $[N1,1,10,Bz]^+$ and $[N1,1,12,Bz]^+$ will be investigated.

HPLC system

A Hewlett Packard system Series 1100 HPLC with a binary pump, online degasser, and auto sampler was used. All columns used in this study are commercially available. The columns types and analytical condition for estimating the retention characteristics of ions *i.e.* cations and anions are in detail provided in Chapter 3 & 4 respectively.

Determination of retention characteristics as given solute property

The retention factors of IL cations and calibration compounds were measured in the HPLC system. The retention factor (log *k*) as given solute property can be calculated from:

$$\text{Log } k = (t_r - t_o)/t_o \qquad \text{Eq. (3.1)}$$

where t_r is the measured retention time, t_o is the system dead time (system hold–up time). In this study, we have three missing solute parameters, *i.e.* S, A, and B as shown in Eq. (2.3).

Table 3.1. Mobile phase conditions of five HPLC systems and specification of each column

Name	Stationary phase	Particle size (µm)	Pore size (nm)	Mobile phase	Flow rate [ml/min]	Column dimensions [mm]	Supplier
RP-Select B-ACN	Particles of silica with octyl derivative	5	6	ACN/buffer 40%/60%	1	125 * 4	Merck
RP select-B-MeOH		5	6	MeOH/buffer 65%/35%	1	125 * 4	Merck
Cyan-MeOH	Particles of silica with g-cyanopropyl function	5	10	MeOH/buffer 35%/65%	1	125 * 4	Merck
DIOL-ACN	Particles of silica with diol function	5	10	ACN/ buffer 25%/75%	1	125 * 4	Merck
DIOL-MeOH		5	10	MeOH/buffer 30%/70%	1	125 * 4	Merck

3.2. Determination of the *z* parameter

The ionic parameter z_c in our study is essential in order to obtain solute descriptors for ions. For comparison, previously Abraham and Zhao[29] fixed their system parameter j^+ for ionic interactions with cations as +3 for all solvents and the system parameter j^- for ionic interactions with anions to 0 for aprotic solvents and as -3 for the alcohol solvents in the Eq. (2.3). Later, the j^+ and j^- were recalculated using more data and fixing the other system parameters *e*, *s*, *a*, *b*, and *v*.[31-34] Since in our attempt we try to capture the partitioning tendency of ions caused simply and solely by their permanent charge, we fixed the ionic solute descriptors Z_c and Z_a as +1 for monovalent cations and as -1 for monovalent anions respectively, while Abraham *et al.*[31-34] have addressed specific values for their ionic descriptor of each ion. In this study we approached the z_c parameter of the system by adding calculated descriptors of three cations to our former set of 45 neutral calibration compounds with known solute descriptors[27] in a multiple linear regression.

Table 3.2. The list of calibration compounds presented by Abraham et al. [27]

Chemicals	E	S	A	B	V
Phenol	0.805	0.89	0.6	0.3	0.775
3-Nitroaniline	1.2	1.71	0.4	0.35	0.99
4-Nitroaniline	1.22	1.83	0.45	0.38	0.99
3-Nitrophenol	1.05	1.57	0.79	0.23	0.949
4-Nitrophenol	1.07	1.72	0.82	0.26	0.949
p-Toluidine	0.923	0.95	0.23	0.45	0.957
3-Fluorophenol	0.667	0.98	0.68	0.17	0.793
Salicylic acid	0.89	0.84	0.71	0.38	0.99
Caffeine	1.5	1.63	0	1.29	1.36
Cortisone	1.96	3.5	0.36	1.87	2.75
Hydrocortisone	2.03	3.49	0.71	1.9	2.8
Diethyl phthalate	0.729	1.4	0	0.86	1.71
Propiophenone	0.8	0.95	0	0.51	1.155
Ethyl acrylate	0.212	0.64	0	0.42	0.845
4-Chloroanilin	1.06	1.13	0.3	0.31	0.939
2-phenylethanol	0.811	0.91	0.3	0.64	1.057
Methylbenzoate	0.733	0.85	0	0.46	1.073
Propyl benzoate	0.675	0.80	0	0.46	1.354
2-Heptanone	0.123	0.68	0	0.51	1.111
Acetophenone	0.818	1.01	0	0.48	1.014
1-Naphthylamine	1.67	1.26	0.2	0.57	1.185
Benzophenone	1.447	1.5	0	0.46	1.481
Acetanilide	0.87	1.4	0.5	0.67	1.113
Ethyl 4-aminobenzoate	1.04	1.52	0.32	0.59	1.313
Resorcinol	0.98	1	1.1	0.58	0.834
o-Xylene	0.663	0.56	0	0.16	0.998
m-Xylene	0.623	0.52	0	0.16	0.998
p-Xylene	0.613	0.52	0	0.16	0.998
Biphenyl	1.36	0.99	0	0.22	1.324
Benzaldehyde	0.82	1	0	0.39	0.873
2-Nitroaniline	1.18	1.37	0.3	0.36	0.991
Nitrobenzene	0.871	1.11	0	0.28	0.891
1-Naphthol	1.52	1.05	0.61	0.37	1.144
Benzyl alcohol	0.803	0.87	0.33	0.56	0.916
Pyridine	0.631	0.84	0	0.52	0.675
2-Butanone	0.166	0.70	0	0.51	0.688
Benzamide	0.99	1.50	0.49	0.67	0.973
Naphtalene	1.340	0.92	0	0.20	1.085
Anthrancene	2.29	1.34	0	0.26	1.454
Benzoic acid	0.73	0.9	0.59	0.4	0.932

4-Chlorophenol	0.915	1.08	0.67	0.2	0.898
Fluorobenzene	0.477	0.57	0	0.1	0.734
Aniline	0.955	0.96	0.26	0.41	0.816
Cyclohexanone	0.403	0.86	0	0.56	0.861
Benzothiazole	1.33	1.1	0	0.42	0.969

3.3. Results and discussion

3.3.1. *Determination of system parameters using neutral solutes (e, s, a, b, v)*

The LFER parameters for five HPLC systems – RP-select B-ACN, RP-select B-MeOH, Cyan-MeOH, Diol-ACN, and Diol-MeOH – were determined using a set of 45 neutral calibration compounds (Table 3.2) where solute descriptors were available from the literature and the calculated parameters for three ionic compounds (Table 3.3) as explained in methodology part in Chapter 2. The result on determination of system parameters of five systems showed that the standard error of the regressions ranged from 0.064 to 0.087 log units (Table 3.4). This is deemed reasonably low and is comparable to the error range of a 78 compound training set measured on eight HPLC systems as presented by Tülp *et al.*[36] All *e* values are in the range between 0.065 and 0.723 log units. Among them, the *e* values of the Diol column systems are generally larger than for other systems, while the *e* value of the RP-Select B system with ACN is close to zero. The *s* values of all systems are negative, which means that the dipolarity/polarizability of their stationary phases are smaller than of their mobile phases. The *a* and *b* coefficients are negative, which indicates that the stationary phases are weaker H-bonding acids and bases than the mobile phases. The positive *v* coefficient is partially a result of the higher energy required to create a given-sized cavity in the mobile phase and partially of the difference in dispersive interaction potential of mobile and stationary phase.

3.3.2. Determination of system parameter z using calculated descriptors for three cations

For the investigation of molecular interaction potentials of monovalent cations, the system parameters including z (*e*, *s*, *a*, *b*, *v*, and *z*) should be determined. All parameters except of z can be determined using only neutral calibration compounds with known descriptors Z = 0 for positively monovalent charged compounds, however, Z_c = +1. By calculating solute descriptors of three cations ($[IM14]^+$, $[IM16]^+$, and $[IM18]^+$) - only allow for an indirect determination of these solute descriptors introducing an error of around 0.077 to 0.167 as shown in a previous study for neutral compounds[52] and using the three compounds additionally for calibration, now z can be determined.

After performing multiple linear regressions, we could obtain the z_c parameter in reasonable standard deviations, less than 0.087 (Table 3.4). With the exception of the Diol-ACN system, the z_c

parameters are all negative, indicating that a positive charge generally decreased partitioning to the mobile phase, while the opposite appears to be true in the Diol-ACN system.

Table 3.3. The LFER descriptors of cations of ionic liquids calculated which are used for calibration compounds by COSMO, COSMO-RS and OBPROP.

	E	S	A	B	V	Z_c
$[IM14]^+$	0.886	1.361	0.662	-0.074	1.257	+1
$[IM16]^+$	1.007	1.423	0.666	-0.066	1.559	+1
$[IM18]^+$	1.111	1.481	0.662	-0.054	1.867	+1

Table 3.4. System descriptors (*e*, *s*, *a*, *b*, *v*, and z_c) determined with sets of calibration compounds including calculated solute descriptors of cation of ionic liquids. Here n and SD stand for number of calibration compounds and standard deviation respectively.

Systems	*e*	*s*	*a*	*b*	*V*	z_c	*c*	N	SD	R^2	F
RP-Select B –ACN	0.065±0.036	-0.298±0.041	-0.396±0.043	-1.658±0.068	1.593±0.060	-1.571±0.072	-0.014±0.036	43	0.064	0.983	343.9
RP-Select B –MeOH	0.118±0.044	-0.295±0.055	-0.376±0.054	-1.080±0.073	1.224±0.069	-0.745±0.083	-0.386±0.043	46	0.087	0.950	122.4
Cyano —MeOH	0.331±0.042	-0.191±0.046	-0.178±0.044	-1.172±0.062	1.074±0.060	-1.391±0.070	-0.482±0.036	42	0.070	0.959	137.5
DIOL —ACN	0.557±0.039	-0.402±0.044	-0.117±0.044	-0.660±0.072	0.421±0.063	0.044±0.077	-0.722±0.037	45	0.069	0.961	155.3
DIOL —MeOH	0.723±0.049	-0.446±0.055	-0.300±0.056	-0.938±0.092	0.616±0.081	-0.745±0.097	-0.405±0.047	43	0.086	0.964	162.1

n stands for number of calibration compounds, SD is standard deviation in the unit of log, F is Fisher F-Statistic, and R^2 is correlation coefficient. ACN is acetonitrile and MeOH is methanol.

3.3.3. *Experimentally determined S, A, and B*

For the experimental determination of solute descriptors (S, A, B), we measured retention factor (Eq. 2.3) and rely on the calculated descriptors V and E (Eqs. (2.5) and (2.6) respectively) as well as the system parameter z estimated as described above. In the extended Abraham Eq. (2.3), they can be shifted to the left hand for convenient multiple linear regression:

$$\log k - c - v\,V - e\,E - z\,Z = s\,S + a\,A + b\,B \qquad \text{Eq. (3.2)}$$

Here, the B^U values of some target compounds without functional groups such as ether, hydroxyl, dimethylamino was artificially set to 0 because B should be small or zero for cations.[31-34] Measured

dipolarity/polarizability, hydrogen bonding acidity and basicity, calculated McGowan volume, and excess molar refraction are shown in Table 3.5.

Table 3.5. Experimentally determined (S, A and B) (standard deviation) and calculated (E and V) LFER solute descriptors. NS stands for number of system used.

Cation	S	A	B	E	V	R^2	SD	NS
$[IM12]^+$	0.944±0.354	0.755±0.406	0.000	0.771	0.953	0.969	0.122	5
$[IM13]^+$	1.363±0.087	-0.010±0.101	0.000	0.826	1.106	0.997	0.030	5
$[IM14]^+$	1.432±0.107	0.485±0.123	0.000	0.886	1.257	0.990	0.037	5
$[IM15]^+$	1.493±0.068	0.535±0.078	0.000	0.945	1.410	0.999	0.023	5
$[IM16]^+$	1.562±0.031	0.570±0.034	0.000	1.006	1.559	1.000	0.011	5
$[IM17]^+$	1.414±0.107	0.707±0.123	0.000	1.080	1.706	0.998	0.037	5
$[IM18]^+$	1.165±0.248	1.128±0.276	0.000	1.112	1.867	0.991	0.088	5
$[IM19]^+$	1.037±0.378	1.332±0.421	0.000	1.188	2.012	0.980	0.134	5
$[IM1\text{-}10]^+$	0.604±0.460	1.774±0.513	0.000	1.247	2.163	0.969	0.163	5
$[IM1\text{-}1Ph]^+$	2.189±0.294	0.494±0.328	0.000	1.328	1.462	0.991	0.104	5
$[IM1\text{-}(1Ph\text{-}4Me)]^+$	2.008±0.266	0.840±0.297	0.000	1.392	1.617	0.993	0.094	5
$[IM1\text{-}2Ph]^+$	2.272±0.235	0.232±0.262	0.000	1.332	1.460	0.994	0.083	5
$[IM1\text{-}2=1]^+$	1.896±0.373	-0.086±0.417	0.000	0.895	1.065	0.972	0.132	5
$[Py2]^+$	1.247±0.233	0.614±0.267	0.000	0.937	0.922	0.989	0.080	5
$[Py4]^+$	1.272±0.315	0.966±0.362	0.000	1.055	1.224	0.986	0.108	5
$[Py6]^+$	1.377±0.229	1.047±0.263	0.000	1.175	1.527	0.994	0.079	5
$[Py8]^+$	1.543±0.098	0.816±0.113	0.000	1.273	1.837	0.999	0.034	5
$[Py4\text{-}4NMe2]^+$	1.097±0.700	1.227±0.398	0.162±0.349	1.370	1.623	0.973	0.235	5
$[Py6\text{-}4NMe2]^+$	1.076±0.689	1.725±1.375	0.079±0.343	1.476	1.930	0.976	0.232	5
$[Py4\text{-}2Me]^+$	1.480±0.424	1.115±0.487	0.000	1.157	1.366	0.981	0.146	5
$[Py4\text{-}3Me]^+$	1.331±0.397	1.165±0.458	0.000	1.139	1.373	0.981	0.137	5
$[Py4\text{-}4Me]^+$	1.330±0.397	1.175±0.443	0.000	1.137	1.373	0.982	0.137	5
$[Py4\text{-}3Me\text{-}5Me]^+$	1.635±0.555	1.130±0.638	0.000	1.275	1.502	0.972	0.191	5
$[Py6\text{-}3Me]^+$	1.315±0.378	1.346±0.434	0.000	1.264	1.673	0.985	0.130	5
$[Py8\text{-}4Me]^+$	1.528±0.214	1.048±0.246	0.000	1.366	1.982	0.995	0.074	5
$[Py6\text{-}4Me]^+$	1.315±0.378	0.895±0.333	0.000	1.264	1.673	0.991	0.100	5
$[IM12O1]^+$	1.156±0.322	-0.184±0.642	0.389±0.160	0.690	1.193	0.992	0.108	5
$[IM13OH]^+$	1.346±0.752	0.003±1.500	0.458±0.375	0.718	1.186	0.973	0.253	5
$[N1,1,10,Bz]^+$	1.427±0.415	2.388±0.549	0.000	1.553	2.731	0.993	0.132	4
$[N1,1,12,Bz]^+$	1.038±0.184	2.891±0.244	0.000	1.676	3.032	0.999	0.059	4

NS stands for the number of HPLC system, R^2 is the determination coefficient and SD is the standard deviation in the dependent variable

3.3.4. Dipolarity/polarizability (S)

It is shown that the dipolarities/polarizabilities depend on the cation structure, especially on tail group length, functionalization, and number and position of substituents on the head group. The S of imidazolium increases as increasing alkyl chain length in the side chain from 2 to 6 due to the lower overall symmetry of the cation.[58] However, a side chain with more than seven carbon atoms leads to a decrease of the S value, as attractive van der Waals interaction between the alkyl chain start outweighing the symmetric effect.[58] The S of ammonium cations decreases with increasing alkyl chain lengths from 10 to 12, while that of S of pyridinium ions increases with increasing alkyl chain lengths from 2 to 8. Functionalization (ether and hydroxyl) in the alkyl chain vaguely affects S. The S value (1.156) of the ether-functionalized imidazolium cation ($[IM12O1]^+$) is slightly higher than that (0.944) of non-functionalized $[IM12]^+$, but remarkably lower than that (1.432) of $[IM14]^+$. Hydroxyl functionalization has no influence on S; it is almost same with a hydroxyl group than without ($[IM13OH]^+$ vs. $[IM13]^+$). On the other hand $[IM1\text{-}2=1]^+$ with a double bond in the alkyl chain has an increased S compared to other non-functionalized imidazolium cations.

The substitution of benzyl and methyl groups, and number and position of methyl substitutions also has a critical influence on S. Phenyl substitution in the imidazolium cations ($[IM1\text{-}1Ph]^+$, $[IM1\text{-}(1Ph\text{-}4Me)]^+$, and $[IM1\text{-}2Ph]^+$) extraordinarily increases the dipolarity/polarizability, which might be due to the charge-rich region of the benzene ring. Methyl substitution on the 1-methylpyridinium cation has also positive influence on the increase of the S values, due to enriching the electron density in the electron-delocalized area by the inductively electron-donating methyl group. Therefore, two methyl substitutions ($[Py4\text{-}3Me\text{-}5Me]^+$) increase S much more than one substituent does ($[Py4\text{-}2Me]^+$, $[Py4\text{-}3Me]^+$, $[Py4\text{-}4Me]^+$) and $[Py4]^+$. While substituting methyl in the hexyl- and octylpyridinium cation has a negligible effect on S, the introduction of a dimethylamino group ($[Py4\text{-}4NMe2]^+$ and $[Py6\text{-}4NMe2]^+$) remarkably decreases dipolarity/polarizability, if compared to $[Py4]^+$ and $[Py6]^+$, respectively.

3.3.5. Hydrogen bonding acidity (A) and basicity (B)

Hydrogen bonding acidity and basicity of a cation are dependent on its alkyl chain length and possible functional substituent respectively. For both, imidazolium and pyridinium cations, hydrogen bonding acidities steeply increase with increasing alkyl chain length, except for $[IM12]^+$ and $[Py8]^+$, which are out of the pattern. For ammonium based cations with stronger Lewis acidic character, it is clearly observed that the A values increase with the alkyl chain lengths. By adding a substituent to the pyridinium cations ($[Py4\text{-}2Me]^+$, $[Py4\text{-}3Me]^+$, $[Py4\text{-}4Me]^+$, $[Py4\text{-}3Me\text{-}5Me]^+$, $[Py6\text{-}3Me]^+$, $[Py8\text{-}4Me]^+$) with the exception of $[Py6\text{-}4Me]^+$, hydrogen bonding acidity slightly increases. However, a clear effect of the position of the substituent is not observed. In case of the olefinic $[IM1\text{-}2=1]^+$, ether-functionalized $[IM12O1]^+$, and hydroxylated cation $[IM13OH]^+$, the hydrogen bonding acidity is not different from 0 within standard error, while substituting the pyridinium cation with dimethylamino-residues leads to higher A values, especially introducing the dimethylamino-residue to $[Py6]^+$ increases the A value (1.725) to around twice that of $[Py6]^+$ (1.047). On the other hand the basicity of ILs is strongly related to the nature of the anion. Nevertheless, there's a small but considerable cation effect. In the investigation for B, only functionalized cations were considered, because the basicity of non-functionalized cations is negligible. The results showed that hydroxyl functionalized imidazolium ($[IM13OH]^+$) leads to a larger hydrogen-bonding basicity (0.458) than ether (0.389), while substitution of dimethylamino to $[Py6]^+$ and $[Py8]^+$ results in small B values of 0.162 and 0.079, respectively.

3.4. Conclusion

I have for the first time demonstrated that HPLC can be used to experimentally determine LFER descriptors of IL cations. For the study, we determined five HPLC systems *i.e.* RP-select B-ACN, RP-select B-MeOH, Cyan-MeOH, Diol-ACN, and Diol-MeOH using 45 types of calibration compounds and three calculated descriptors of cations for the determination of the newly introduced zZ model parameter.

These HPLC methods can be ideally used to measure retention factor of cations with less 270 g/mol for determination of solute descriptors, while the hydrophobic system - especially RP-select B-MeOH in this study - was restricted to compounds with above weights 270 g/mol. Moreover, the computationally established models for E and V allow us to obtain easily molar refractivity and McGowan volume of ions.

Our characterization of cationic LFER descriptors is helpful to understand physicochemical properties of ILs. The S descriptor is of important for microwave synthesis. Large organic cations with high polarizability can lead to a very high reaction rate and significantly shorter reaction times, due to their excellent microwave absorbing ability.[60] From our results, we suggest that ILs with imidazolium-based, phenyl-substituted cations ($[IM1\text{-}1Ph]^+$, $[IM1\text{-}(1\text{-}Ph\text{-}4Me)]^+$, $[IM1\text{-}2Ph]^+$) can be used as a desirable media in microwave-assisted reactions. Also, ILs with highly polarizability can cause rapid solvation and dynamic properties such as low viscosity and high self-diffusion behavior.[61,62] From our results it appears that cations with benzyl, hydroxyl, and methyl substitution/functionalization could lead to rapid initial solvation and affect the properties, *e.g.* lower viscosity and significantly higher diffusion constant. Especially, the hydrogen bonding basicity of ILs is related to solvating materials. For example, cellulose is more readily dissolved in more basic ILs.[12] Although it was reported that hydrogen basicity is moderate and dominated by the nature of anion,[12] our results indicate a possible increased basicity by coupling functionalized cations ($[IM12O1]^+$, $[IM13OH]^+$). In the light of relationships between the characterized parameters and physicochemical properties of ILs, the characterized descriptors may provide many possibilities for predictions and therefore may prove valuable tools to design ILs. However, our *z*Z term introduced in the Abraham equation, with Z being + 1 for monovalent cation differs from the ionic interaction terms proposed by Abraham and co-workers.[31-34] Our approach aims at capturing the energetic contribution of a permanent charge in an electric field, caused by a difference in the electrostatic potential across an interface between two phases. Therefore, the *z*Z term should not be applied for the equations of ionic transfer from water

to organic solvents, as also established by Abraham and coworkers.[31-34] In such systems, ionic liquid ions are not expected to partition independent of their respective counterion.

In this study, we could clear up the dipolarity/polarizability, hydrogen bonding acidity, and basicity of IL cations according to their various substituent, head group and functionalization. These presented results will be essential and helpful to design the cationic structure and to predict physicochemical properties of cation *e.g.* solubility, partition in binary system, critical micelle concentrations (CMC), toxicity, sorption, and mobility in various environment.

4. Determination of molecular interaction potentials of anions

4.1. Background

In an independent approach, our group recently studied the chemical and physical behavior of single IL ions on the same scale using HPLC in Chapter 3. In general, anions typically do not have retention characteristics, because they are mostly of low lipophilicity. In order to determine their retention characteristics, anion-exchange columns are a good option; however, it is in general not suitable to retain cationic and neutral compounds to determine the system parameters, because of repulsion for cations and weak stationary phase for neutral compounds. Thus, we used special columns with multiple stationary mechanisms, *i.e.* anion and cation exchange and hydrophobic or hydrophobic functionalization.

4.2. Experimental

For measuring retention time of a set of IL anion, we used:

- lithium bis(trifluoromethylsulfonyl)amide Li[(CF3SO2)2N], sodium iodide NaI, sodium 1-butanesulfonate Na[4SO3], sodium hexafluorophosphate Na[PF6], and sodium tetrafluoroborate Na[BF4] (Lancaster Synthesis, UK);
- sodium octylsulfate Na[8OSO3] (Fluka, Buchs, Switzerland);
- potassium tetracyanoborate K[B(CN)4], potassium tricyanomethide K[C(CN)3], sodium 1-hexanesulfonate Na[6SO3], 1-ethyl-3-methylimidazolium butylsulfate [IM12][4OSO3], and potassium 1,1,2,2-tetrafluoroethanesulfonate K[H(C2F4)SO3], 1-ethyl-3-1-methylimidazolium ethyl sulfate [IM12][2OSO3] (IoLiTec GmbH, Heilbronn, Germany);
- ethyl-3-methylimidazolium bis(pentafluoroethyl)phosphinate [IM12][(C2F5)2PO2], and 1-ethyl-3-methylimidazolium 4-fluoro-1-butanesulfonate [IM12][F4SO3] (Ms. Wei Wei in group of Prof. Wasserscheid, Universität Erlangen-Nürnberg, Germany);
- 1-butyl-3-methylimidazolium methylsulfate [IM14][1OSO3], and 1-butyl-3-methylimidazolium 2-(2-methoxyethoxy)ethylsulfate [IM14][1O2O2OSO3] 1-butyl-3-methylimidazolium 4-methylbenzenesulfonate [IM14][4MePhSO3], 1-hexyl-3-methylimidazolium tris(trifluoromethylsulfonyl)methanide [IM16][(CF3SO2)3C], 1-hexyl-3-methylimidazolium 6-methyl-2,2-dioxo-1,2,3-oxathiazin-4-onate [IM16][AC], 1-hexyl-3-methylimidazolium 1,1-dioxo-1,2-dihydrobenzo[d]isothiazol-3-onate [IM16][(2-SO2PhCO)N] (Merck, Darmstadt Germany);
- Neutral compounds for the determination of system parameters were purchased from

Merck (Darmstadt, Germany) and Fluka.

All neutral calibration compounds were purchased from Merck and Fluka. All chloride ($[IM14]^+$, $[IM16]^+$, $[IM18]^+$, $[IM19]^+$, $[IM1\text{-}10]^+$, $[IM1\text{-}1Ph]^+$, $[IM1\text{-}(1\text{-}Ph\text{-}4Me)]^+$, $[IM1\text{-}2Ph]^+$, $[IM1\text{-}2\text{=}1]^+$, $[IM12O1]^+$, $[IM13OH]^+$, $[Py2]^+$, $[Py4]^+$, $[Py6]^+$, $[Py8]^+$, $[Py4\text{-}4NMe2]^+$, $[Py6\text{-}4NMe2]^+$, $[Py4\text{-}2Me]^+$, $[Py4\text{-}3Me]^+$, $[Py4\text{-}4Me]^+$, $[Py4\text{-}3Me\text{-}5Me]^+$, $[Py6\text{-}3Me]^+$, $[Py8\text{-}4Me]^+$, $[Py6\text{-}4Me]^+$, $[N1,1,10,Bz]^+$, and $[N1,1,12,Bz]^+$) and bromide-based ILs ($[IM12]^+$ and $[IM13]^+$) were supplied by Merck;[IM15]Br was supplied by Prof. Dr. Bernd Ondruschka from the Universität Jena, Germany. The list of neutral compounds and 29 cations are provided in Table 4.1.

The eluents (methanol and acetonitrile) for HPLC measurements were bought from Fluka, and phosphate salts, ammonium formate $[NH_4][HCO_2]$, and formic acid for buffer solution which is available in mass spectrometer were purchased from Roth (Karlsruhe, Germany).

Table 4.1. The list of neutral and cationic compounds for calibration of systems

Chemicals	E	S	A	B	V	Z_c
Phenol	0.805	0.89	0.6	0.3	0.775	0
3-Nitroaniline	1.2	1.71	0.4	0.35	0.99	0
4-Nitroaniline	1.22	1.83	0.45	0.38	0.99	0
3-Nitrophenol	1.05	1.57	0.79	0.23	0.949	0
4-Nitrophenol	1.07	1.72	0.82	0.26	0.949	0
Propylbenzene	0.604	0.5	0	0.15	1.139	0
3-Fluorophenol	0.667	0.98	0.68	0.17	0.793	0
Salicylic acid	0.89	0.84	0.71	0.38	0.99	0
Fluorene	1.588	1.06	0	0.2	1.357	0
Cortisone	1.96	3.5	0.36	1.87	2.75	0
Hydrocortisone	2.03	3.49	0.71	1.9	2.8	0
Diethyl phthalate	0.729	1.4	0	0.86	1.71	0
Propiophenone	0.8	0.95	0	0.51	1.155	0
Ethyl acrylate	0.212	0.64	0	0.42	0.845	0
2-Phenylethanol	0.811	0.91	0.3	0.64	1.057	0
Methylbenzoate	0.733	0.85	0	0.46	1.073	0
Propyl benzoate	0.675	0.80	0	0.46	1.354	0
2-Heptanone	0.123	0.68	0	0.51	1.111	0
2-butanone	0.166	0.7	0	0.51	0.688	0
diphenylmethane	1.22	1.04	0	0.28	1.465	0
Cyclohexanone	0.403	0.86	0	0.56	0.861	0
2-heptanone	0.123	0.68	0	0.51	1.111	0
Acetophenone	0.818	1.01	0	0.48	1.014	0
1-Naphthylamine	1.67	1.26	0.2	0.57	1.185	0
Iodobenzene	1.188	0.82	0	0.12	0.975	0

Benzophenone	1.447	1.5	0	0.46	1.481	0
Benzamide	0.99	1.5	0.49	0.67	0.973	0
Acetanilide	0.87	1.4	0.5	0.67	1.113	0
Naphtalene	1.34	0.92	0	0.2	1.085	0
Ethyl-4-aminobenzoate	1.04	1.52	0.32	0.59	1.313	0
Chlorobenzene	0.718	0.65	0	0.07	0.839	0
Resorcinol	0.98	1	1.1	0.58	0.834	0
Toluene	0.601	0.52	0	0.14	0.857	0
o-Xylene	0.663	0.56	0	0.16	0.998	0
m-Xylene	0.623	0.52	0	0.16	0.998	0
p-Xylene	0.613	0.52	0	0.16	0.998	0
Biphenyl	1.36	0.99	0	0.22	1.324	0
Benzaldehyde	0.82	1	0	0.39	0.873	0
2-Nitroaniline	1.18	1.37	0.3	0.36	0.991	0
Nitrobenzene	0.871	1.11	0	0.28	0.891	0
1-Naphthol	1.52	1.05	0.61	0.37	1.144	0
Benzyl alcohol	0.803	0.87	0.33	0.56	0.916	0
Benzoic acid	0.73	0.9	0.59	0.4	0.932	0
Paraldehyde	0.136	0.68	0	0.68	1.022	0
Fluorobenzene	0.477	0.57	0	0.1	0.734	0
Benzothiazole	1.33	1.1	0	0.42	0.969	0
4-Nitrobenzoic acid	0.99	1.43	0.68	0.51	1.172	0
$[IM12]^+$	0.771	0.944	0.755	0	0.953	1
$[IM13]^+$	0.826	1.363	-0.01	0	1.106	1
$[IM14]^+$	0.886	1.432	0.485	0	1.257	1
$[IM15]^+$	0.945	1.493	0.535	0	1.41	1
$[IM16]^+$	1.006	1.562	0.57	0	1.559	1
$[IM18]^+$	1.112	1.165	1.128	0	1.867	1
$[IM19]^+$	1.188	1.037	1.332	0	2.012	1
$[IM1\text{-}10]^+$	1.247	0.604	1.774	0	2.163	1
$[IM12O1]^+$	0.69	1.156	-0.184	0.389	1.193	1
$[IM13OH]^+$	0.718	1.346	0.003	0.458	1.186	1
$[BzMIM]^+$	1.328	2.189	0.494	0	1.462	1
$[PMBzMIM]^+$	1.392	2.008	0.84	0	1.617	1
$[EBzMIM]^+$	1.332	2.272	0.232	0	1.46	1
$[AIMIM]^+$	0.895	1.896	-0.086	0	1.065	1
$[BzMMDA]^+$	1.553	1.427	2.388	0	2.731	1
$[BzMMDdA]^+$	1.676	1.038	2.891	0	3.032	1
$[Py4\text{-}4NMe2]^+$	1.37	1.097	1.227	0.162	1.623	1
$[Py6\text{-}4NMe2]^+$	1.476	1.076	1.725	0.079	1.93	1
$[Py2]^+$	0.937	1.247	0.614	0	0.922	1
$[Py4]^+$	1.055	1.272	0.966	0	1.224	1
$[Py6]^+$	1.175	1.377	1.047	0	1.527	1
$[Py8]^+$	1.273	1.543	0.816	0	1.837	1
$[Py4\text{-}4Me]^+$	1.137	1.33	1.175	0	1.373	1

$[Py4\text{-}3Me]^+$	1.139	1.331	1.165	0	1.373	1
$[Py4\text{-}2Me]^+$	1.157	1.48	1.115	0	1.366	1
$[Py4\text{-}3Me\text{-}5Me]^+$	1.275	1.635	1.13	0	1.502	1
$[Py6\text{-}3Me]^+$	1.264	1.315	1.346	0	1.673	1
$[Py6\text{-}4Me]^+$	1.264	1.315	0.895	0	1.673	1
$[Py8\text{-}4Me]^+$	1.366	1.528	1.048	0	1.982	1

4.2.1. HPLC Measurement

A Hewlett Packard system series 1100 HPLC with a binary pump, online degasser, and auto sampler was connected to a mass spectrometer (MS). Most anions, except for I^-, $[AC]^-$, $[4MePhSO3]^-$ and $[(2\text{-}SO2PhCO)N]^-$, cannot be detected by UV, thus their retention times were determined with MS. As mentioned above, we used commercially available columns with multi-stationary phases (Obelisc R, Obelisc N, and Acclaim Trinity P1) with retain of anions, cations, and neutral compounds. The specifications for each column are given in Table 4.2. The buffer condition was set to 30mM ammonium formate and 0.5 vol-% formic acid to adjust a pH of 3.0. All samples were injected into the columns with a 5µL sample loop of a concentration between 50 and 200 µM. The ion trap mass spectrometer was operated with the electrospray source in positive ion mode for the 29 calibration cations and in negative ion mode for the targeted anions. In order to sensitively detect the ions, the mass detection range was restrained to the mass of the of target compound ± 10 m/z. The dead time for system 1 and system 2 was estimated by injecting urea, while that of other systems was determined by the solvent peak.

Table 4.2. Mobile phase condition of six HPLC systems and specifications of each column

system number	name	stationary mechanism	particle size (µm)	mobile phase	flow rate [ml/min]	column dimensions [mm]	supplier
1	Obelisc R	hydrophobic phase, anionic and cationic exchange	5	ACN/buffer 31%/69%	1	4.6 × 100	SIELC
2				MeOH/buffer 45%/55%	1		
3	Obelisc N	hydrophilic phase, anionic and cationic exchange	5	ACN/buffer 45%/55%	1	4.6 × 100	
4				MeOH/buffer 60%/40%	1		
5	Acclaim Trinity P1	reverse phase, anionic and cationic exchange based on silica	5	MeOH/buffer 75%/25%	0.4	3.0 × 100	Dionex

4.3. Investigating the ion–pairing effect

When analyzing salts in an HPLC system, there is the possibility of ion-pairing, destabilizing the retention time. The problem can be avoided using buffer solutions. For confirmation, we measured the retention times of the anions with different cations. For this experiment, we used [BF4] and [PF6] combined with [IM1n] (n = 2, 4, 6, 8), and [(CF3SO2)2N], [B(CN)4] and [C(CN)3] combined with [IM1n] (n = 2, 6, 8). The results (Table 4.3) show that the retention characteristics stay nearly constant. Therefore, we conclude that there is no ion-pairing effect influencing the retention time.

Table 4.3. The retention time of anions i.e. $[BF4]^-$, $[PF6]^-$, $[(CF3SO2)2N]^-$, $[B(CN)4]^-$ and [B(CN)4] according to different cations i.e. [IM12], [IM14], [IM16], and [IM18] to investigate the ion-paring effect

		[BF4]	[PF6]	[(CF3SO2)2N]	[B(CN)4]	[C(CN)3]
System 1	[IM12]	2.8	5.6	14.3	9.3	5.2
	[IM14]	2.8	5.6	-	-	-
	[IM16]	2.8	5.6	14.4	9.3	5.2
	[IM18]	2.8	5.6	14.3	9.3	5.2
System 2	[IM12]	3.4	7.0	28.3	11.9	9.4
	[IM14]	3.4	7.0	28.5	-	-
	[IM16]	3.5	7.0	28.0	11.9	9.4
	[IM18]	-	7.0	28.7	11.9	9.2
System 3	[IM12]	2.6	4.9	10.4	7.4	4.2
	[IM14]	2.6	4.9	-	-	-
	[IM16]	2.6	4.9	10.4	7.4	4.2
	[IM18]	2.6	4.9	10.4	7.4	4.2
System 4	[IM12]	8.5	8.2	13.8	9.4	10.3
	[IM14]	8.5	8.2	-	-	-
	[IM16]	8.5	8.2	13.8	9.4	10.3
	[IM18]	8.5	8.2	13.8	9.4	-
System 5	[IM12]	3.4	6.4	24.6	11.1	8.6
	[IM14]	3.4	6.4	-	-	-
	[IM16]	3.4	6.4	25.2	11.1	8.7
	[IM18]	3.4	6.4	25.3	11.2	8.7

4.4. Results and discussions

4.4.1. Determination of system parameters using neutral solutes and cations

The system parameters for five HPLC systems (Obelisc R - ACN, Obelisc R – MeOH, Obelisc N – ACN, Obelisc N – MeOH, and Acclaim Trinity P1 – MeOH) were determined using the retention characteristics of calibration compounds – both neutral and cationic (Table 4.1) – under isocratic conditions. A calibration compound was excluded as outliers if the characteristic retention value (log *k*) was lower than -1.0 after estimating the system parameters by multiple linear regression. After this, we could observe that the standard deviation ranges of the five systems are reasonably low (between 0.070 and 0.124 log unit) (see Table 4.4); thereby, it is shown that the interaction potential of the columns used can be modeled by linear free energy relationship descriptors of cationic and neutral compounds.

Table 4.4. System descriptors for the zZ term model determined with solute descriptors of cationic and neutral compounds. n = number of calibration compounds, SD = standard deviation in logarithmic units, F = Fisher F-statistic, R^2 = squared correlation coefficient.

system	*e*	*S*	*a*	*b*	*v*	*z*	*c*	n	SD	R^2	F
1	0.225±0.043	-0.223±0.030	-0.171±0.023	-0.954±0.051	0.891±0.035	-0.923±0.038	-0.492±0.028	70	0.070	0.967	304.5
2	0.185±0.060	-0.166±0.042	-0.035±0.039	-1.591±0.087	1.457±0.065	-1.967±0.084	-0.772±0.044	57	0.089	0.965	227.6
3	0.361±0.089	-0.086±0.052	-0.205±0.039	-0.037±0.083	-0.241±0.062	0.916±0.059	-0.406±0.049	67	0.115	0.927	126.1
4	0.529±0.086	-0.157±0.052	-0.208±0.041	-0.362±0.110	-0.194±0.069	1.218±0.058	-0.586±0.078	60	0.113	0.967	257.2
5	0.078±0.072	0.045±0.044	-0.096±0.034	-0.331±0.071	-0.031±0.051	0.734±0.050	-0.546±0.041	63	0.098	0.954	192.6

4.4.2. Determination of solute descriptors of anions

The coefficients in Table 4.4 allow us to estimate the solute descriptors of the target anions as mentioned in our assumption in the introduction (Chapter 2). Because the E and V can be calculated,[59] and we assume that zZ can cover both cationic and anionic interaction with the system, we shift *c*, *e* E, *v* V, and *z* Z in Eq. (3.2) to the left for convenient calculation of the missing terms S, A, and B. The modified Equation then reads:

$$\text{Log k} - c - e\,\text{E} - v\,\text{V} - z\,(\text{Z}_a = -1 \text{ for monovalent anion}) = s\,\text{S} + a\,\text{A} + b\,\text{B} \qquad \text{Eq. (4.1)}$$

By performing multiple linear regression, the missing descriptors can then be obtained. Table 4.5 shows the solute descriptors of 20 anions. However, the large standard deviation shows that zZ

cannot cover both cation and anion although the charges are the same size but with opposite signs. Therefore the zZ term is not suited to describe with the opposite signs.

Table 4.5. Solute descriptors of anions for the zZ^U term model obtained by using the system parameters from Table 4.4. N stands for number of system.

Anion	E	S	A	B	V	R^2	SD	N
[(CF3SO2)2N]$^-$	-0.6083	4.15(10.17)	-17.80(7.71)	1.31(1.42)	1.3929	0.750	1.78	5
[B(CN)4]$^-$	-0.2132	3.55(8.05)	-15.02(6.10)	1.10(1.12)	0.8984	0.773	1.41	5
[C(CN)3]$^-$	0.22	4.38(8.09)	-13.28(6.13)	0.86(1.13)	0.6614	0.706	1.42	5
[4MePhSO4]$^-$	0.6923	3.91(10.01)	-11.97(7.59)	1.16(1.39)	1.1693	0.585	1.75	5
[F3SO3]$^-$	0.0176	3.83(9.29)	-11.85(7.04)	1.55(1.29)	1.1145	0.656	1.63	5
[(CF3SO2)3C]$^-$	-0.9073	3.48(10.84)	-20.57(8.22)	1.79(1.51)	2.0708	0.792	1.90	5
[8OSO3]$^-$	0.4282	3.05(11.77)	-14.74(8.93)	1.32(1.64)	1.6541	0.617	2.06	5
[1OSO3]$^-$	0.0136	4.71(8.99)	-11.66(6.82)	1.02(1.25)	0.5945	0.608	1.57	5
[1O2O2OSO3]$^-$	0.0252	4.42(9.53)	-12.48(7.23)	1.77(1.33)	1.3573	0.683	1.67	5
[PF6]$^-$	0.0204	7.73(9.05)	-15.95(6.86)	0.52(1.26)	0.5921	0.701	1.58	5
[BF4]$^-$	-0.5664	-10.45(9.54)	-3.09(6.86)	2.38(1.14)	0.3792	0.847	1.07	4
I$^-$	0.38	5.31(9.45)	-11.70(7.17)	0.68(1.32)	0.408	0.554	1.65	5
[(2-SO2PhCO)N]$^-$	0.595	4.45(9.73)	-12.42(7.38)	1.30(1.36)	1.1669	0.622	1.70	5
[2OSO3]$^-$	0.0862	4.43(9.17)	-11.59(6.95)	1.10(1.28)	0.7412	0.605	1.61	5
[6SO3]$^-$	0.4084	2.83(10.25)	-12.30(7.77)	1.34(1.43)	1.2777	0.607	1.61	5
[(C2F5)2PO2]$^-$	-1.0424	1.33(10.84)	-16.06(8.22)	1.66(1.51)	1.51	0.719	1.90	5
[AC]$^-$	0.2674	4.55(9.25)	-12.63(7.01)	1.13(1.29)	0.9601	0.637	1.62	5
[H(C2F4)SO3]$^-$	-0.4647	4.25(9.61)	-14.30(7.29)	1.20(1.34)	0.9055	0.678	1.68	5
[4OSO3]$^-$	0.1991	3.80(9.89)	-12.43(7.50)	1.23(1.38)	1.046	0.612	1.73	5
[4SO3]$^-$	0.2871	3.50(9.27)	-11.35(7.03)	1.29(1.29)	0.9759	0.615	1.62	5

As a solution, we attempted to separate the zZ descriptors to z_cZ_c for cation and z_aZ_a for anion as Abraham did:[31-34]

$$SP = c + e\,E + s\,S + a\,A + b\,B + v\,V + z_cZ_c + z_aZ_a \qquad \text{Eq. (4.2)}$$

For determination of the z_aZ_a descriptors, we add the calculated descriptors (E, S, A, B, and V) of five anions because measured solute descriptors of anion in our theoretical background are not available so far. The equations previously established by our group[59] and by Abraham and Klamt,[52] respectively, are repeated below (Eqs. (2.5)~(2.9)). The calculated descriptors are shown in Table 4.6.

Table 4.6. The calculated solute descriptors of five anions for calibration compounds

Anion	E	S	A	B	V	Z_a
$[(CF3SO2)2N]^-$	-0.6083	1.104	-0.454	1.249	1.3929	-1
$[B(CN)4]^-$	-0.2132	1.281	-0.364	1.400	0.8984	-1
$[C(CN)3]^-$	0.22	1.437	-0.250	1.756	0.6614	-1
$[(CF3SO2)3C]^-$	-0.9073	1.041	-0.422	1.164	2.0708	-1
$[PF6]^-$	0.0204	1.267	-0.440	1.044	0.5921	-1

After adding the calculated descriptors of the anions, we performed a multiple linear regression including neutral and cationic compounds. Thereby, we could obtain the system parameters of five HPLC systems with a reasonably low standard deviation range of 0.090 ~ 0.157 (Table 4.7).

Table 4.7. System descriptors (standard deviation) including z_c and z_a of five HPLC systems determined with calibration sets (cations and neutral compounds) and the calculated solute descriptors of five anions. n = number of calibration compounds, SD = standard deviation in logarithmic units, F = Fisher F-Statistic, R^2 = squared correlation coefficient.

System	*e*	*s*	*a*	*b*	*v*	z_c	z_a	*c*	n	SD	R^2	F
1	0.335(0.044)	-0.287(0.036)	-0.158(0.029)	-0.794(0.057)	0.786(0.033)	-0.826(0.044)	-1.864(0.077)	-0.476(0.036)	75	**0.090**	0.960	230.2
2	0.488(0.072)	-0.336(0.060)	-0.099(0.062)	-1.040(0.105)	1.061(0.065)	-1.504(0.105)	-2.481(0.139)	-0.630(0.066)	62	**0.145**	0.936	112.2
3	-0.032(0.088)	0.042(0.062)	-0.229(0.051)	-0.259(0.094)	0.049(0.057)	0.760(0.069)	-1.325(0.140)	-0.405(0.064)	69	**0.152**	0.905	84.7
4	0.153(0.090)	-0.034(0.066)	-0.258(0.056)	-0.438(0.132)	0.139(0.068)	1.087(0.071)	-1.670(0.186)	-0.673(0.105)	65	**0.157**	0.939	125.8
5	0.009(0.067)	0.087(0.048)	-0.110(0.040)	-0.446(0.072)	0.038(0.044)	0.670(0.053)	-2.411(0.104)	-0.555(0.048)	68	**0.116**	0.969	263.8

For the estimation of the missing terms S, A, B, we shifted the computed descriptors (*e*E, *v*V, z_cZ_c, and z_aZ_a) to the left as shown in Eq.(4.3).

$$\text{Log k} - c - e\,\text{E} - v\,\text{V} - z_cZ_c - z_aZ_a = s\,\text{S} + a\,\text{A} + b\,\text{B} \qquad \text{Eq. (4.3)}$$

Here, for anions, $Z_c = 0$; for monovalent anions, $Z_a = -1$. We artificially set A = 0 for anions devoid of hydrogen atoms in order to obtain chemically more reasonable values. However, in the case of three anions ($[(CF3SO2)3C]^-$, $[PF6]^-$, I^-), multiple linear regression was done without this because the statistical coefficient might be low. This might be due to the difference between the actual magnitude of the Coulomb interaction and the fixed charge of –1. Both cases are shown above and below (Table 4.8). With this, we determined the solute descriptors of 20 anions (Table 4.8).

Table 4.8. Solute descriptors (S, A, B) of anions using the system parameters from Table 4.7.

Anion	E	S	A	B	V	Z_c	Z_a	R^2	SD	N
$[(CF3SO2)2N]^-$	-0.61	1.94(0.25)	0	0.95(0.08)	1.3929	0	-1	0.997	0.065	5
$[B(CN)4]^-$	-0.21	0.22(0.56)	0	1.54(0.17)	0.8984	0	-1	0.988	0.147	5
$[C(CN)3]^-$	0.22	0.09(0.22)	0	1.78(0.07)	0.6614	0	-1	0.999	0.059	5
$[4MePhSO4]^-$	0.69	2.22(0.85)	2.78(0.83)	1.15(0.37)	1.1693	0	-1	0.995	0.176	5
$[F4SO3]^-$	0.02	1.42(0.74)	2.82(0.73)	1.81(0.32)	1.1145	0	-1	0.997	0.154	5
$[(CF3SO2)3C]^-$	-0.91	2.97(1.20)	0	0.60(0.37)	2.0708	0	-1	0.938	0.316	4
*		1.36 (0.34)	-2.55(0.34)	1.53 (0.15)		0	-1	0.998	0.071	5
$[8OSO3]^-$	0.43	2.94(0.98)	1.82(0.97)	0.66(0.43)	1.6541	0	-1	0.989	0.204	5
$[1OSO3]^-$	0.01	1.58(0.83)	3.25(0.81)	1.28(0.36)	0.5945	0	-1	0.995	0.172	5
$[1O2O2OSO3]^-$	0.03	2.07(0.79)	2.83(0.77)	1.90(0.34)	1.3573	0	-1	0.997	0.164	5
$[PF6]^-$	0.02	2.15(1.04)	0	1.04(0.32)	0.5921	0	-1	0.962	0.276	5
*		3.40 (0.78)	1.98 (0.77)	0.31 (0.34)		0	-1	0.991	0.163	5
$[BF4]^-$	-0.57	-2.51(0.84)	0	2.56(0.27)	0.3792	0	-1	0.994	0.138	4
I^-	0.38	0.28(1.69)	0	2.01(0.51)	0.408	0	-1	0.941	0.442	5
*		2.50(0.64)	3.51(0.63)	0.73(0.28)		0	-1	0.996	0.132	5
$[(2\text{-}SO2PhCO)N]^-$	0.60	2.31(0.71)	2.38(0.70)	1.40(0.31)	1.1669	0	-1	0.997	0.148	5
$[2OSO3]^-$	0.09	1.59(0.79)	3.27(0.78)	1.32(0.34)	0.7412	0	-1	0.996	0.164	5
$[6SO3]^-$	0.41	1.60(0.74)	2.29(0.72)	1.35(0.32)	1.2777	0	-1	0.996	0.153	5
$[(C2F5)2PO2]^-$	-1.04	0.12(0.45)	0	1.56(0.14)	1.51	0	-1	0.992	0.118	5
$[AC]^-$	0.27	1.77(0.54)	2.39(0.53)	1.31(0.23)	0.9601	0	-1	0.998	0.113	5
$[H(C2F4)SO3]^-$	-0.47	1.57(0.41)	1.93(0.40)	1.18(0.18)	0.9055	0	-1	0.998	0.084	5
$[4OSO3]^-$	0.20	1.88(0.60)	2.72(0.59)	1.23(0.26)	1.046	0	-1	0.997	0.124	5
$[4SO3]^-$	0.29	1.22(0.58)	2.76(0.57)	1.58(0.25)	0.9759	0	-1	0.998	0.119	5

*in this case, the multiple linear regression was done without artificially setting (i.e. set 0 for anions without hydrogen).

In this study, molecular interaction potentials of these anions with fixed Z_a value are reported for the first time. Thus, it is impossible to validate the descriptors, because systems for comparison are not available. For internal validation, we attempted to predict retention characteristics of all calibration compounds (cationic and neutral) and target anions in five systems with their experimentally determined descriptors (Tables 4.7 and 4.8). Predicted and measured values are shown in Figures 4.1 for the five columns.

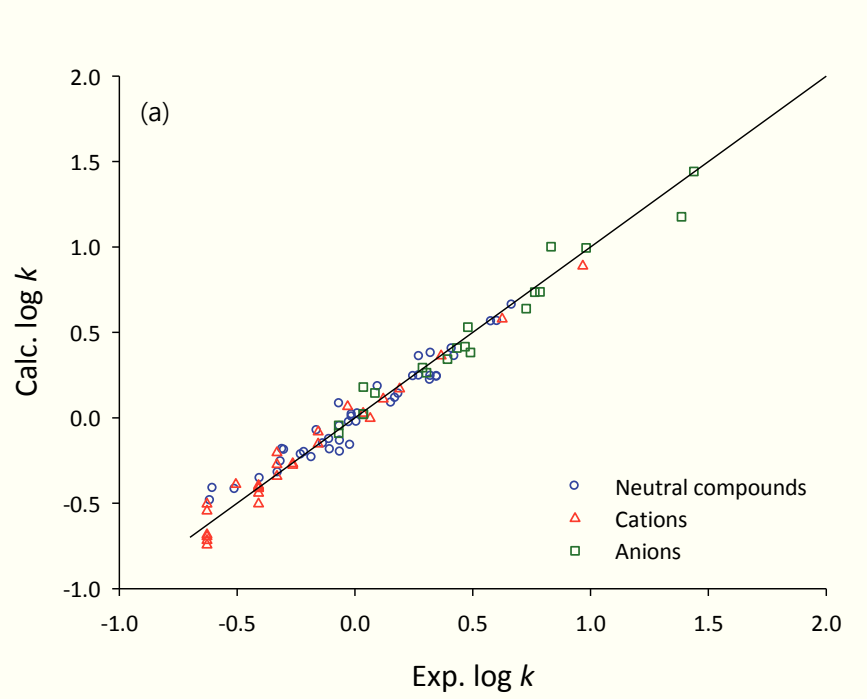
(a)
Calc. log k
Exp. log k
Neutral compounds
Cations
Anions
2.0
1.5
1.0
0.5
0.0
-0.5
-1.0
-1.0
-0.5
0.0
0.5
1.0
1.5
2.0

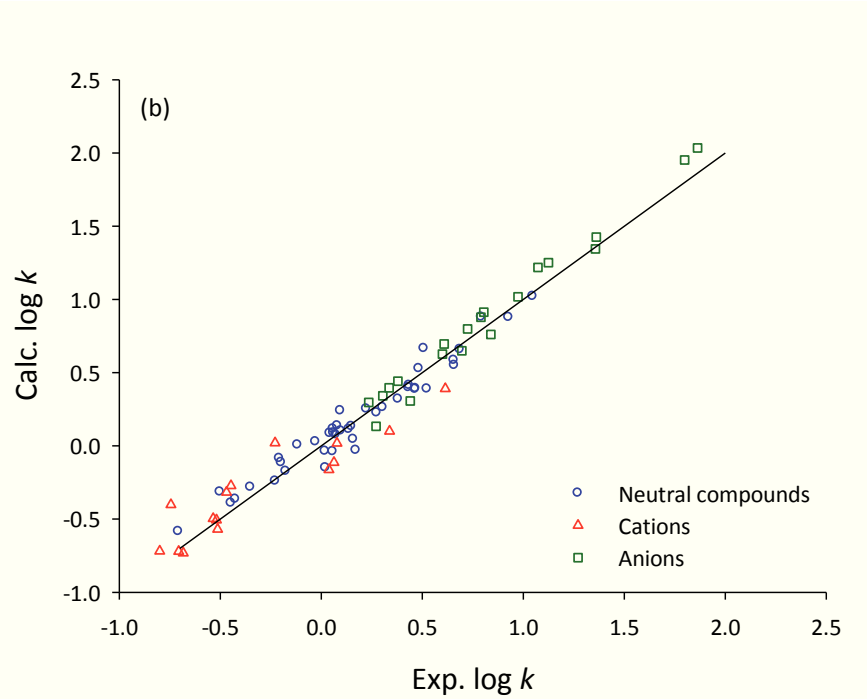
(b)
Calc. log k
Exp. log k
Neutral compounds
Cations
Anions
2.5
2.0
1.5
1.0
0.5
0.0
-0.5
-1.0
-1.0
-0.5
0.0
0.5
1.0
1.5
2.0
2.5

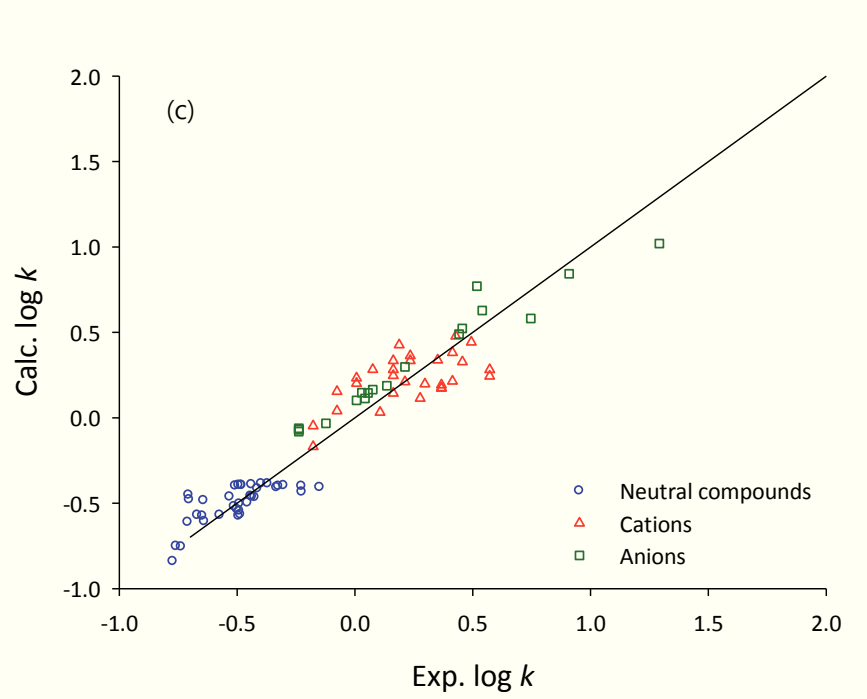
(c)
Calc. log k
Exp. log k
Neutral compounds
Cations
Anions
2.0
1.5
1.0
0.5
0.0
-0.5
-1.0
-1.0
-0.5
0.0
0.5
1.0
1.5
2.0

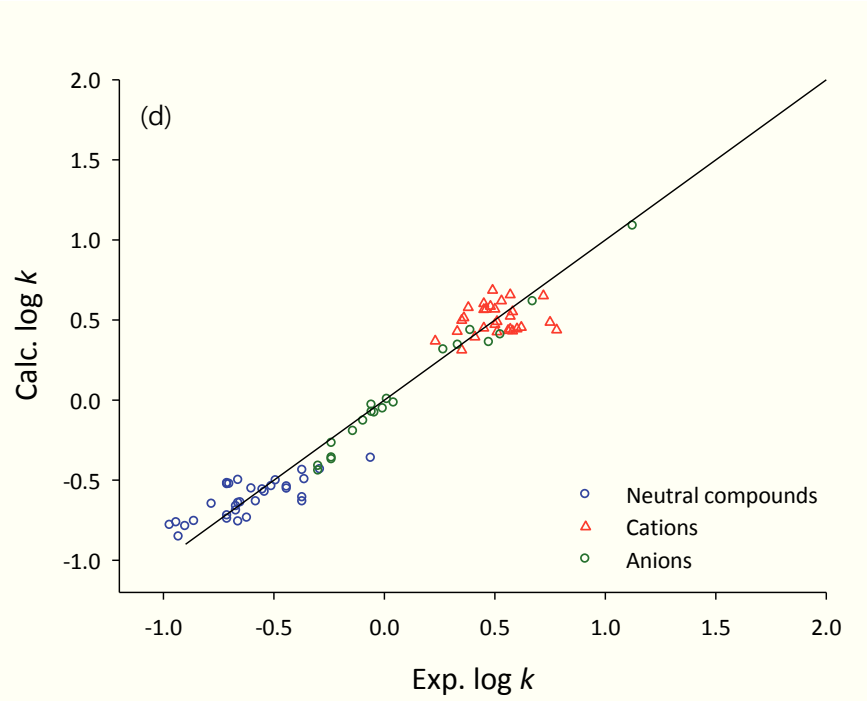
(d)
Calc. log k
Exp. log k
Neutral compounds
Cations
Anions
2.0
1.5
1.0
0.5
0.0
-0.5
-1.0
-1.0
-0.5
0.0
0.5
1.0
1.5
2.0

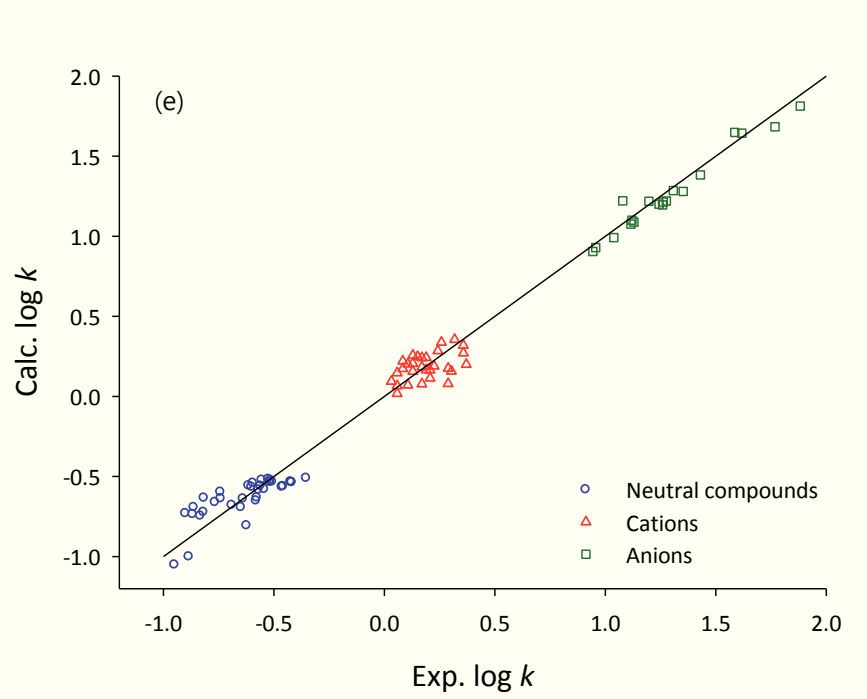

Figure 4.1. Predicted and measured retention characteristics in system 1(a), 2(b), 3(c), 4(d), and 5(e).

Figures 4.1 and the high R^2 values (0.92 ~ 0.99) show that the descriptors can now be predicted with a high reliability. Also, we can observe that the solute descriptors of anions can be used together with those of cations and neutral compounds. This fact is very helpful to predict the retention characteristics of anions in HPLC and ion chromatography systems. To our knowledge, a prediction using molecular interaction potentials was not yet performed for anions. The results will provide an advantage to chromatographically separate charged and neutral compounds. Moreover the measured descriptors of the anions will allow us to understand their molecular interactions, in various environments, *e.g.* partition in water-octanol, activity coefficient, and aggregation in water.

4.5. Conclusions

In this study, we developed a new method for the determination of the molecular interaction potentials of 20 anions which are important to understand the behavior of ionic liquids in various environments. We employed three multiple stationary phase columns in which anions, cations, and neutral compounds can be retained. Cations and neutral compounds were used to determine the system parameters in order to make a separate investigation of the anions possible. With knowing the retention characteristics of the cationic, neutral compounds and calculated five anions in five

systems based on Eq. (2.3), we could determine parameters of the systems with a large R^2 of 0.927 ~ 0.967. However, we realized that the single ionic zZ term we previously used (in Chapter 3) is not suited for charge interaction of cation and anion at the same time. Therefore, we separated zZ into z_aZ_a and z_cZ_c in Eq. (4.2). A reasonably high R^2 of 0.905 ~ 0.969 resulted. With this approach, we could estimate the solute descriptors of 20 anions in isocratic and buffered conditions with an excellent R^2 of 0.988 ~ 0.999 and a low standard deviation of 0.059 ~ 0.204 log units. We validated the reproducibility of the approach by comparing measured and predicted retention characteristics in five systems.

The solute descriptors of these 20 anions can prove useful to set up further predictive models for retention characteristics of anions in analytical chemistry. They could also provide an advantage in understanding the chemical and physical behavior (e.g. sorption, partition, toxicity, activity) of ionic liquids in various environments. Moreover, we assume that these descriptors can also be used to estimate further molecular interaction potentials of other ions.

In addition, our conceptual approach to the ionic terms represents an improvement upon Abraham and coworkers.[31-34] Their method is useful to understand the ionic forces of single ions, while our approach is more convenient and easier accessible as simply considering Z = ±1 for monovalent ions. However, further studies are needed to check whether our theoretical model is also valid for multiply-charged ions.

5. Ionic Liquids: Predictions of physicochemical properties with experimental and/or DFT-calculated LFER parameters to understand molecular interactions in solution

5.1. Introduction

Using the experimentally and computationally determined LFER descriptors of the representative ion set (Chapter 2 & 3), system parameters for the prediction of the octanol-water partitioning coefficient, water solubility, critical micelle concentration of ILs, anionic activity coefficient in water and anionic hydrophobicity in octanol-water were established.

The octanol-water partitioning coefficient (log P) as the ratio of the concentrations of a compound in two phases (*n*-octanol/ water) at the Equilibrium indicates hydrophobicity. Like log $P_{O/W}$, the water solubility is also a useful quantity, since it influences release, transport, environmental fate, and risk of a compound. These properties can be strongly related to the adsorption of a drug in the human body as well as bioaccumulation and migration of dissolved hydrophobic compounds in soil, sediments and groundwater.[63-67] And the critical micelle concentration (CMC) is a basic parameter of surface chemistry as well as colloid and environmental science. Specifically, it influences biological properties like toxicity and biodegradability. The process of micellization can be directly correlated to the interaction of amphiphiles with apolar surfaces such as micelles or cell membranes. Therefore, to choose an IL with a specific behavior in the environment, it is necessary to establish a prediction model.

5.2. Experiment

As one part of this study, we measured the log P values of 25 chloride-based ILs (see the list of log P in Table 5.1). Three 15 ml conical tube with cap were filled with 3 ml of octanol and water respectively, and 15.0 mM of IL were added. The vials were vigorously shaken for 10 min and allowed to stabilize for at least an hour and then centrifugation was performed to eliminate the emulsion created by shaking process prior to injection into the HPLC system. Then, samples of 5 µL from each phase were carefully withdrawn with a syringe. The withdrawn samples were diluted by a factor of 10 or 100 prior to HPLC analysis.

For analyzing the quantity of ILs in each phase, we employed a Hilic stationary phase with acetonitrile (99.9 %, Fluka) and buffer (15 mM KH_2PO_4 and 30 mM H_3PO_4) as eluent in the HPLC (Hewlett Packard System Series 1100), because cation has a good retention characteristic in Hilic system and applying phosphate buffer into the mobile phase allows us to neglect influence of anion in the chromatographic system.[37] The detection wavelengths were 211 nm for imidazolium based ILs and 254 nm for pyridinium based ILs and ammonium based compounds with benzyl substituents. The partitioning coefficients of ILs were determined as the ratio of the solute peak area in both phases Eq. (5.1). The tests for partition coefficient of ILs were triplicate. C^i_o is the concentration of ILs in octanol phase, and C^i_w is the concentration of ILs in water phase.

$$\text{Log } P = \text{Log } C^i_o/C^i_w \qquad \text{Eq. (5.1)}$$

5.3. Results and discussions

5.3.1. Extraction and prediction of anionic hydrophobicity from log $P_{o/w}$ of ionic liquids

For the partitioning behavior of salts including ILs, we assumed that both cationic (log k_o) and anionic hydrophobicity (H_a) play an important role. The cationic hydrophobicity can be assessed by HPLC with a lipophilic stationary phase,[38] while it is difficult to directly measure anionic hydrophobicity, because most anions are rather small and therefore do not show a significant retention in the stationary phase. Thus, in order to determine anionic hydrophobicity for the typical IL anions [(CF3SO2)2N]$^-$, [PF6]$^-$, [BF4]$^-$, [SbF6]$^-$, [CF3SO3]$^-$, Cl$^-$, [NO3]$^-$, Br$^-$, and [CH3COO]$^-$), we applied Eq. (5.2), as established by Ranke et al.,[39] to the model set. This model is based on the idea that the excess molar free energy of dissolving the ILs in water can be expressed as the sum of cationic and anionic contributions, where the former one is given by the capacity factor, and the latter one is extracted by a least squares fit of the model to the data.

$$\text{Log P} = m \log k_o + H_a + c \qquad \text{Eq. (5.2)}$$

where k_o is the cationic capacity factor representing hydrophobicity defined by Stepnowski and Storoniak,[37] m is the slope that ideally equals unity, if all model assumptions are satisfied, and c is a constant. For the determination of the anionic contribution, cationic capacity factors were collected from literature [38,69] (Table 5.1). In Figure 5.1, log P data are plotted against the hydrophobicity of the cation. It turned out that the slopes are all equal, confirming the linear model specified in equation (5.2). By correlating the log P values of 45 ILs with log k_o of cations (Table 5.1), we obtained m = 1.423, c = –3.039. Results are given in Table 5.2.

Table 5.1. Hydrophobicity values of cations (log k_o), log P, and average log P values of ionic liquids

Ionic liquids	Log P values of ionic liquids	Average log P of ionic liquids	log k_o
[IM14]Cl	-2.77 ± 0.068[a], -2.40[70, 71]	-2.590	0.63
[IM16]Cl	-1.73 ± 0.003[a]	-1.730	1.21
[IM18]Cl	-0.60 ± 0.003 [a]	-0.600	1.85
[IM19]Cl	-0.13 ± 0.005[a]	-0.130	2.1
[IM1–10]Cl	0.311 ± 0.030[a]	0.311	2.37
[IM1–1Ph]Cl	-2.35 ± 0.008[a]	-2.350	0.83
[IM1–(1Ph–4Me)]Cl	-1.80 ± 0.010[a]	-1.800	1.12
[IM1–2Ph]Cl	-1.99 ± 0.017[a]	-1.990	1.01
[IM1–2=1]Cl	-3.25 ± 0.007[a]	-3.250	–
[N1,1,10, Bz]Cl	1.04 ± 0.014[a]	1.040	2.93
[N1,1,12, Bz]Cl	1.73 ± 0.017[a]	1.730	3.49
[IM12O1]Cl	-3.77 ± 0.060[a]	-3.770	–0.02
[IM13OH]Cl	-3.691 ± 0.010[a]	-3.691	–0.23
[IM11O2]Cl	-3.31 ± 0.005[a]	-3.310	0.21
[Py4–4NMe2]Cl	-2.13 ± 0.008[a]	-2.130	1.08
[Py6–4NMe2]Cl	-1.15 ± 0.011[a]	-1.147	1.80
[Py4–3Me–5Me]Cl	-2.38 ± 0.003[a]	-2.380	0.57
[Py2]Cl	-3.55 ± 0.011[a]	-3.546	–
[Py4]Cl	-2.82 ± 0.017[a]	-2.820	0.57
[Py8]Cl	-0.72 ± 0.001[a]	-0.720	–
[Py4–2Me]Cl	-2.78 ± 0.002[a]	-2.780	0.71
[Py4–4Me]Cl	-2.57 ± 0.020[a]	-2.572	0.73
[Py4–3Me]Cl	-2.62 ± 0.007[a]	-2.623	0.73
[Py6–3Me]Cl	-1.58 ± 0.005[a]	-1.580	–
[Py6–4Me]Cl	-1.65 ± 0.008[a]	-1.650	1.37
[IM14][NO_3]	-2.42[70, 71],-2.9[72]	-2.660	0.63
[IM14]Br	-2.48[71]	-2.480	0.63

[IM11][$(CF_3SO_2)_2N$]	-1.35 ± 0.040[73]	-1.350	–
[IM12][$(CF_3SO_2)_2N$]	-1.18 ± 0.03[73]; -1.01(-1.05 ~ -0.95)[71]	-1.120	0.22
[IM13][$(CF_3SO_2)_2N$]	-0.88 ± 0.02[73]	-0.880	0.42
[IM14][$(CF_3SO_2)_2N$]	-0.50 ± 0.03[73]; -0.58 (-0.96 ~ -0.208) [71]	-0.540	0.63
[IM15][$(CF_3SO_2)_2N$]	-0.11 ± 0.03[73]	-0.110	0.92
[IM16][$(CF_3SO_2)_2N$]	0.16 ± 0.02[73] ; 0.19 (0.15 ~ 0.22)[71]	0.180	1.21
[IM17][$(CF_3SO_2)_2N$]	0.57 ± 0.02[73]	0.570	1.57
[IM18][$(CF_3SO_2)_2N$]	0.79 ± 0.03[73] ; 0.93 (0.80 ~ 1.05)[71]	0.860	1.85
[IM12][PF_6]	-2.36 ± 0.08[73]	-2.360	0.22
[IM14][PF_6]	-1.72 ± 0.06[73]; -1.66[70,74], -2.39[72]	-1.920	0.63
[IM16][PF_6]	-1.20 ± 0.05[73]	-1.200	1.21
[IM18][PF_6]	-0.35 ± 0.04[73]	-0.350	1.85
[IM12][BF_4]	-2.66 ± 0.10[73]	-2.660	0.22
[IM14][BF_4]	-2.40 ± 0.08[73]; -2.52[70,74]	-2.460	0.63
[IM16][BF_4]	-1.58 ± 0.08[73]	-1.580	1.21
[IM18][BF_4]	-0.68 ± 0.06[73]	-0.680	1.85
[IM14][SbF_6]	-2.39 ± 0.08[73]	-2.390	0.63
[IM14][CF_3SO_3]	-1.61 ± 0.05[73]	-1.610	0.63
[IM14][CH_3COO]	-2.77 ± 0.08[73]	-2.770	0.63

[a] Measured for this study

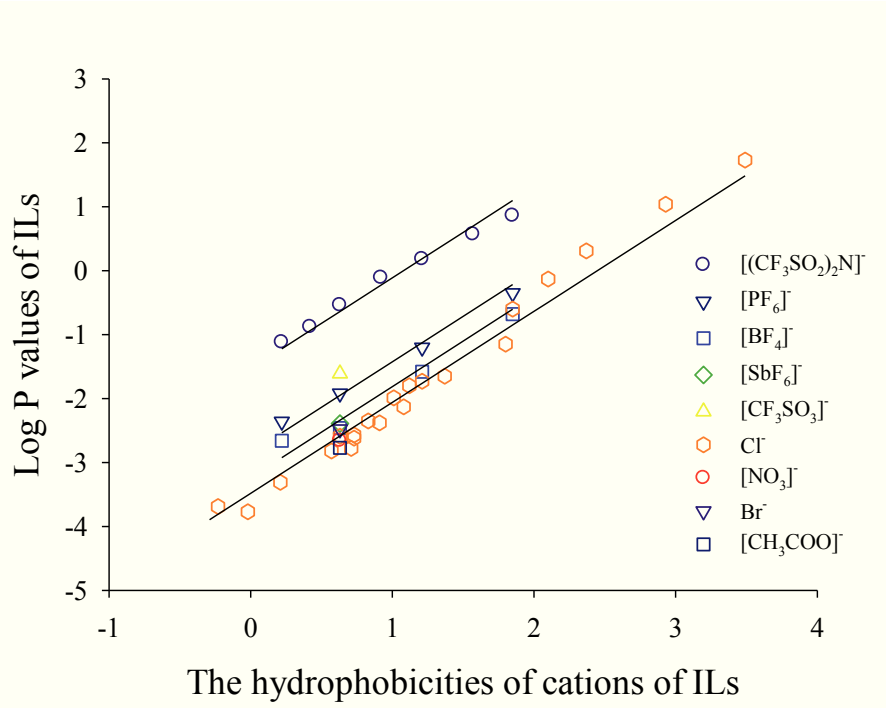

Figure 5.1. Measured octanol-water partitioning coefficient (log P) of ionic liquids as a function of the measured hydrophobicities of the cations[38,69] of various ionic liquids.

Table 5.2. The dimensionless hydrophobicity of anions in the octanol-water partitioning system.

Anions	Measured hydro-phobicity (from Eq. 5.2)	Predicted hydrophobicity (from Eq. 5.3)
$[(CF3SO2)2N]^-$	1.504 ± 0.135	1.423
$[PF6]^-$	0.191 ± 0.136	0.211
$[BF4]^-$	–0.197 ± 0.177	–0.186
$[SbF6]^-$	–0.248	–
$[CF3SO3]^-$	0.533	0.509
Cl^-	–0.443 ± 0.220	–0.537
$[NO3]^-$	–0.518	–0.561
Br^-	–0.338	–0.261
$[CH3COO]^-$	–0.628	–0.609

5.3.2. Prediction of hydrophobicity of anion in water-octanol

In order to establish a prediction of the anionic hydrophobicity without any experimental input, we employed the LFER with the five computed[52] parameters E, S, A, B, and V, for the prediction based on the Abraham model. One data point ($[SbF6]^-$) had to be excluded, because Sb is not parameterized in OBPROP's atomic contribution method.

The results show that the full Abraham model with our calculated parameters can be used for prediction of the anion hydrophobicity with a standard deviation (SD) of 0.079 (dimensionless), which has the expected statistical and physicochemical meaning (Table 5.3). For a better understanding of the contribution of each parameter of the anion, we systematically simplified the Abraham Equation to find the most important contributions for the molecular interactions. First of all, it is not surprising that the hydrophobicity correlates well with V_a according to Eq. (5.4) in Table 5.3 for which SD = 0.261. Here we found that acetate with its strong hydrogen-bonding basicity ability forms a large exception. In order to also include similarly basic anions, the hydrogen basicity values were added as parameter. For the combination of V_a and B_a, we found SD to decrease to 0.211 with all data points coming closer to the best-fit axis Eq. (5.5). In the next step, the hydrogen bonding acidity A_a was added Eq. (5.6). Indeed, the SD decreased to 0.143. We then also added the refractive index (E_a) and dipolarity/polarizability (S_a), which further enhanced the accuracy Eq. (5.7). E_a only slightly increased the accuracy (SD = 0.067) and S_a has very little importance, but in combination with V_a, B_a, and A_a, Eq. (5.3), they contribute to reaching the best prediction (R^2 of 0.997). The fitting is shown in Figure 5.2.

Table 5.3. The system parameters (standard deviation) for predicting the anionic hydrophobicity with calculated LFER parameters of anion.

Eq.	c	e_a	s_a	a_a	b_a	v_a	R^2	SD	F	N
(5.3)	0.298(0.742)	–0.841(0.312)	0.263(0.660)	1.691(0.388)	–0.571(0.121)	1.319(0.149)	0.997	0.079	116.1	8
(5.4)	–0.956(0.169)					1.778(0.260)	0.886	0.261	46.7	8
(5.5)	–0.449(0.283)				–0.135(0.066)	1.503(0.249)	0.938	0.211	37.9	8
(5.6)	0.136(0.293)			0.844(0.246)	–0.370(0.100)	1.575(0.171)	0.977	0.143	57.5	8
(5.7)	0.581(0.178)	–0.756(0.193)		1.586(0.242)	–0.532(0.062)	1.288(0.108)	0.996	0.067	201.7	8

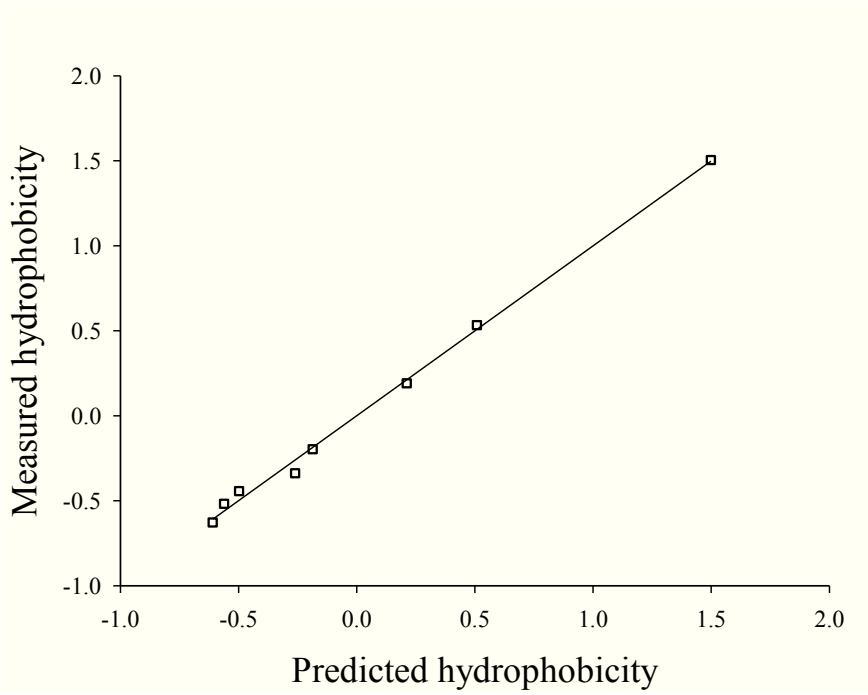

Figure 5.2. The relationship of experimental and predicted hydrophobicity values determined using calculated LFER parameters according to Eq. 5.3

5.3.3. Octanol-water partitioning coefficient of ionic liquids

For predicting the octanol-water partitioning coefficient of ILs, I used measured as well as calculated descriptors were used. Experimentally determined log $P_{O/W}$ values measured between very dilute condition and around 15 mM were collected from literatures[70-74] because log $P_{O/W}$ is dependent on concentration [35] and, for 25 chloride-based ILs, measured as part of this work. From theoretical considerations, I modified the Abraham Equation by adding the anionic hydrophobicity parameter (H_a, dimensionless) Eq. (5.8).

$$\text{Log } P_{O/W} = c + e_c E_c + s_c S_c + a_c A_c + b_c B_c + v_c V_c + d H_a \qquad \text{Eq. (5.8)}$$

With the measured cationic LFER descriptors presented (Chapter 3) and the experimentally determined anionic hydrophobicity constants, log $P_{O/W}$ was predicted according to Eq. (5.8) using a multiple linear regression with an SD of 0.182 log units and $R^2 = 0.984$ [Eq. (5.9)].

Table 5.4. The system parameters (standard deviation) for predicting the octanol-water partitioning coefficient (log $P_{O/W}$) of ionic liquids with measured cationic LFER parameters and including anionic hydrophobicity.

Eq.	c	e_c	s_c	a_c	b_c	v_c	d	R^2	SD	N	F
(5.9)	-4.678 (0.190)	0.118 (0.344)	-0.710 (0.178)	-0.529 (0.161)	-3.310 (0.373)	2.985 (0.139)	0.983 (0.044)	0.984	0.182	44	373.3
(5.10)	-5.543 (0.177)	-	-	-	-	2.653 (0.113)	1.127 (0.068)	0.947	0.315	44	363.2
(5.11)	-5.372 (0.137)	-	-	-	-2.274 (0.402)	2.576 (0.086)	1.074 (0.052)	0.970	0.234	44	435.9
(5.12)	-4.958 (0.175)	-0.885 (0.268)	-	-	-2.686 (0.381)	2.932 (0.133)	1.007 (0.051)	0.977	0.213	44	410.4
(5.13)	-4.693 (0.213)	-0.653 (0.282)	-0.229 (0.113)	-	-2.722 (0.367)	2.803 (0.143)	1.010 (0.049)	0.979	0.204	44	355.6

As shown by Eq. (5.10), the cationic volume term combined with the anionic hydrophobicity are the most important parameters for the log $P_{O/W}$ prediction of ILs, which already has a high accuracy with R^2 = 0.947, SD = 0.315. The next important term is the hydrogen bonding basicity [R^2 = 0.970, SD = 0.234 in Eq. (5.11)], and then excess molar refraction, which both enhance the predicting accuracy to R^2 = 0.977 and SD = 0.213 Eq. (5.12). Inclusion of S_c and A_c contributes very slightly to the prediction quality as shown by the small reduction of the SD values in Eq. (5.13) and Eq. (5.9), respectively. The system parameters according to Eq. (5.9) ~ (5.13) for predicting Log $P_{O/W}$ with measured LFER parameters and anionic hydrophobicity are shown in Table 5.3. Here [IM11O2][Cl] and [IM11][$(CF_3SO_2)_2N$] were not investigated because their LFER parameters were not measured so far.

Using only calculated cationic LFER descriptors (including the calculated anionic hydrophobicity), the log $P_{O/W}$ values of ILs were predicted following Eq. (5.8) giving a SD of 0.217 log units (Table 5.4). The order of importance of the contribution factors is similar to as with the measured parameters. The system parameters according to Eq. (5.14) ~ (5.18) are shown in Table 5.4. Measured and predicted values using experimentally and computationally determined parameters are provided in Table 5.5 and fitted in Figure 5.3.

Table 5.5. The system parameter (standard deviation) for predicting octanol-water partitioning coefficient (log $P_{O/W}$) of ionic liquids with calculated cationic LFER descriptors and including anionic hydrophobicity.

Eq.	c	e_c	s_c	a_c	b_c	v_c	d	R^2	SD	N	F
(5.14)	-6.239 (0.481)	-0.603 (0.347)	0.794 (0.458)	-0.901 (0.235)	-6.765 (1.130)	2.976 (0.143)	1.007 (0.049)	0.977	0.217	45	272.1
(5.15)	-5.514 (0.168)	-	-	-	-	2.671 (0.109)	1.114 (0.0624)	0.949	0.309	45	387.9
(5.16)	-6.104 (0.182)	-	-	-	-4.911 (1.013)	2.914 (0.101)	1.032 (0.053)	0.967	0.250	45	404.9
(5.17)	-5.702 (0.197)	-	-	-0.558 (0.160)	-5.529 (0.916)	2.874 (0.090)	1.024 (0.047)	0.975	0.221	45	389.2
(5.18)	-5.544 (0.273)	-0.262 (0.294)	-	-0.633 (0.181)	-5.573 (0.920)	2.977 (0.146)	1.009 (0.050)	0.975	0.222	45	309.9

Table 5.6. Measured and predicted log $P_{O/W}$ values of ionic liquids with calculated (calc.) and measured (exp.) LFER parameters.

Chemicals	Measured Log $P_{O/W}$	Predicted Log $P_{O/W}$ with	
		(calc. LFER parameters) according to Eq. (5.14)	(exp. LFER parameters) according to Eq. (5.9)
[IM14]Cl	-2.77 ± 0.068[a], -2.40[70, 71]	-2.59	-2.53
[IM16]Cl	-1.73 ± 0.003[a]	-1.77	-1.75
[IM18]Cl	-0.60 ± 0.003 [a]	-0.95	-0.83
[IM19]Cl	-0.13 ± 0.005[a]	-0.56	-0.41
[IM1–10]Cl	0.311 ± 0.030[a]	-0.16	0.12
[IM1–1Ph]Cl	-2.35 ± 0.008[a]	-2.28	-2.41
[IM1–(1Ph–4Me)]Cl	-1.80 ± 0.010[a]	-1.89	-1.99
[IM1–2Ph]Cl	-1.99 ± 0.017[a]	-2.29	-2.33
[IM1–2=1]Cl	-3.25 ± 0.007[a]	-3.12	-3.13
[N1,1,10, Bz]Cl	1.04 ± 0.014[a]	1.12	0.95
[N1,1,12, Bz]Cl	1.73 ± 0.017[a]	1.89	1.87
[IM12O1]Cl	-3.77 ± 0.060[a]	-3.96	-3.48
[IM13OH]Cl	-3.691 ± 0.010[a]	-3.57	-3.96
[IM11O2]Cl	-3.31 ± 0.005[a]	-2.04	--
[Py4–4NMe2]Cl	-2.13 ± 0.008[a]	-1.96	-1.87
[Py6–4NMe2]Cl	-1.15 ± 0.011[a]	-1.27	-1.02
[Py4–3Me–5Me]Cl	-2.38 ± 0.003[a]	-2.63	-2.24

[Py2]Cl	-3.55 ± 0.011[a]	-3.41	-3.46
[Py4]Cl	-2.82 ± 0.017[a]	-2.64	-2.75
[Py8]Cl	-0.72 ± 0.001[a]	-0.99	-1.01
[Py4–2Me]Cl	-2.78 ± 0.002[a]	-2.49	-2.54
[Py4–4Me]Cl	-2.57 ± 0.020[a]	-2.44	-2.45
[Py4–3Me]Cl	-2.62 ± 0.007[a]	-2.45	-2.44
[Py6–3Me]Cl	-1.58 ± 0.005[a]	-1.65	-1.62
[Py6–4Me]Cl	-1.65 ± 0.008[a]	-1.61	-1.38
[IM14][NO_3]	-2.42[70, 71],-2.9[72]	-2.61	-2.60
[IM14]Br	-2.48[71]	-2.31	-2.43
[IM11][$(CF_3SO_2)_2N$]	-1.35 ± 0.040[73]	-1.67	--
[IM12][$(CF_3SO_2)_2N$]	-1.18 ± 0.03[73]; -1.01(-1.05 ~ -0.95)[71]	-1.32	-1.33
[IM13][$(CF_3SO_2)_2N$]	-0.88 ± 0.02[73]	-0.93	-0.76
[IM14][$(CF_3SO_2)_2N$]	-0.50 ± 0.03[73]; -0.58 (-0.96 ~ -0.208) [71]	-0.54	-0.62
[IM15][$(CF_3SO_2)_2N$]	-0.11 ± 0.03[73]	-0.13	-0.22
[IM16][$(CF_3SO_2)_2N$]	0.16 ± 0.02[73] ; 0.19 (0.15 ~ 0.22)[71]	0.28	0.16
[IM17][$(CF_3SO_2)_2N$]	0.57 ± 0.02[73]	0.66	0.64
[IM18][$(CF_3SO_2)_2N$]	0.79 ± 0.03[73] ; 0.93 (0.80 ~ 1.05)[71]	1.11	1.08
[IM12][PF_6]	-2.36 ± 0.08[73]	-2.61	-2.62
[IM14][PF_6]	-1.72 ± 0.06[73]; -1.66[70,74], -2.39[72]	-1.83	-1.91
[IM16][PF_6]	-1.20 ± 0.05[73]	-1.02	-1.13
[IM18][PF_6]	-0.35 ± 0.04[73]	-0.19	-0.21
[IM12][BF_4]	-2.66 ± 0.10[73]	-3.01	-3.01
[IM14][BF_4]	-2.40 ± 0.08[73]; -2.52[70,74]	-2.23	-2.29
[IM16][BF_4]	-1.58 ± 0.08[73]	-1.42	-1.51
[IM18][BF_4]	-0.68 ± 0.06[73]	-0.59	-0.59
[IM14][SbF_6]	-2.39 ± 0.08[73]	--	-2.34
[IM14][CF_3SO_3]	-1.61 ± 0.05[73]	-1.53	-1.57
[IM14][CH_3COO]	-2.77 ± 0.08[73]	-2.66	-2.71

[a] Measured for this study

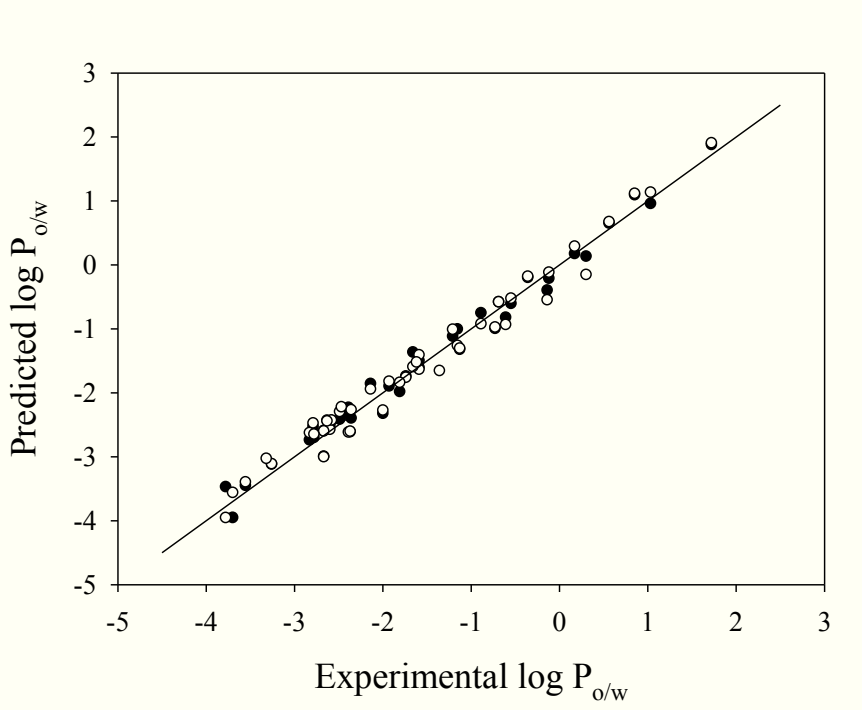

Figure 5.3. The relationship of experimental and predicted log $P_{O/W}$ values determined using measured (●) and calculated LFER parameters (○).

5.3.4. Activity coefficient of anions in water

Like log $P_{O/W}$, the water solubility is a useful quantity, since it influences release, transport, environmental fate, and risk of a compound. For its prediction, experimental values at 293 - 298 K were collected from literature[39,75-86] and the anionic activity coefficients (C_a, determined by Ranke *et al.*[39] and given in Table 5.7) were combined with the Abraham model.

Table 5.7. Dimensionless activity coefficients of ionic liquid anions in water measured (exp. data from Ranke *et al*)[39] and predicted with the calculated LFER parameters (calc.) according to Eq. (5.19).

Anions	Measured activity coefficient of anion in water	Predicted activity coefficient of anion in water [calc., Eq. (5.19)]
$[(6\text{-}2Et)2SS]^-$	0.521	0.501
$[BF4]^-$	-1.268	-1.219
$[CF3SO3]^-$	-1.343	-1.268
$[PhBF3]^-$	-1.853	-1.837
$[B(CN)4]^-$	-2.264	-2.209
$[PF6]^-$	-2.280; -2.178	-2.414
$[(C4F9)SO3]^-$	-2.610	-2.700
$[(CF3SO2)2N]^-$	-2.911; -2.868	-2.814

$[AsF6]^-$	-3.165	--
$[(C2F5SO2)2N]^-$	-3.363	-3.556
$[(CF3SO2)3C]^-$	-3.902; -3.841	-3.722
$[(C2F5)3PF3]^-$	-4.883, -4.803	-4.788

The dimensionless activity coefficient of the anion in IL-saturated water[39] (Table 5.7) was correlated with the calculated anionic LFER descriptors to establish a prediction model. We modified the model by adding an anionic charge density term $f_\alpha(-1/V_a)$ (f_α is a system parameter):

$$\text{Log } C_a \text{ [dimentionless]} = c + e_aE_a + s_aS_a + \alpha_aA_a + b_aB_a + v_aV_a + f_a(-1/V_a) \quad \text{Eq. (5.19)}$$

This modified equation can be used to predict anionic activity coefficient with a SD of 0.174 Eq. (5.20), which is better than when using the conventional Abraham model Eq. (5.21, SD = 0.389). Table 5.8 gives the system parameters for all predictions of the activity coefficients using calculated parameters according to Eq. (5.20) and (5.26).

Table 5.8. System parameters (standard deviation) according to Eq. (5.20) – Eq. (5.26) for the prediction of the anionic activity coefficient in IL-saturated water using the calculated LFER parameters (calc.). f_a stands for system parameter for anionic charge density.

Eq.	c	e_a	s_a	a_a	b_a	v_a	f_a	R^2	SD	N	F
(5.20)	-3.103 (0.760)	4.110 (1.287)	-7.084 (2.524)	-7.543 (2.712)	4.783 (1.233)	0.670 (0.303)	-0.715 (0.157)	0.994	0.174	11	112.0
(5.21)	-2.651 (1.679)	3.654 (2.861)	-6.287 (5.613)	-7.404 (6.044)	4.710 (2.748)	-0.136 (0.623)		0.963	0.389	11	26.2
(5.22)	-4.811 (0.490)				1.549 (0.279)			0.775	0.719	11	30.9
(5.23)	-4.389 (0.304)				1.923 (0.186)	-0.690 (0.162)		0.931	0.421	11	54.0
(5.24)	-5.880 (0.278)				1.655 (0.125)		-0.898 (0.146)	0.961	0.319	11	97.6
(5.25)	-4.913 (0.401)	0.556 (0.198)			1.287 (0.160)		-0.789 (0.114)	0.981	0.234	11	123.5
(5.26)	-4.151 (0.790)	1.518 (0.709)	-2.016 (1.412)	-2.183 (1.621)	2.401 (0.800)		-0.582 (0.193)	0.987	0.233	11	75.1

The anionic activity coefficient B_a is the most contributing factor and already leads to $R^2 = 0.775$, SD = 0.721 Eq. (5.22). C_a increases with B_a. As shown in Eq. (5.23), inclusion of the two terms B_a and V_a leads to an improvement (SD = 0.421). However, exchanging the volume for f_a ($-1/V_a$), the anionic charge density further reduces the SD value to 0.319 Eq. (5.24). The parameter E is also critical and leads to a significant increase in anionic activity, as shown in Eq. (5-25) (SD = 0.234). Adding S and A terms further slightly enhances the accuracy Eq. (5.26). The fitting is shown in Figure 5.4. Again, one data point ($[AsF_6]^-$) had to be excluded because As is not parameterized in OBPROP's atomic contribution method.

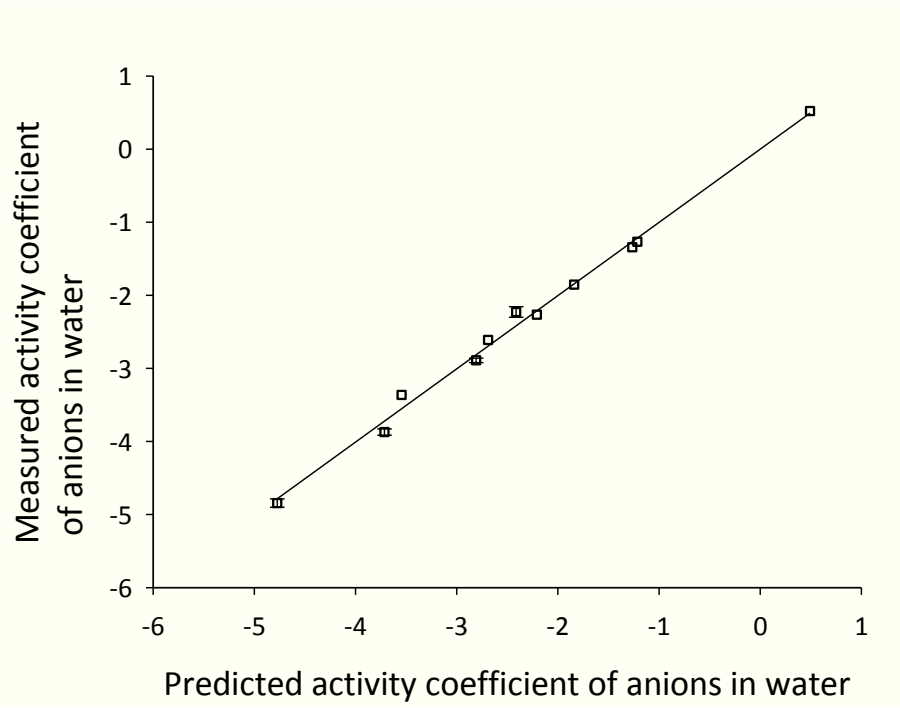

Figure 5.4. The relationship of experimental and predicted activity coefficient values (with standard error bar) of anion according to Eq. (5.26)

5.3.5. Water solubility of ionic liquids

Using the experimental and calculated LFER descriptors of the cation, the water solubility of ILs was predicted. Like for the log P prediction model, we assumed that the cationic LFER parameters and the anionic contribution, expressed by *d*Ca (C_a is the anionic activity coefficient in water and *d* is system parameter), should be combined in one model as shown in Equation (5.27).

$$\text{Log water solubility [g L}^{-1}\text{]} = c + e_c E_c + s_c S_c + a_c A_c + b_c B_c + v_c V_c + f_c(1/V_c) + dC_a \qquad \text{Eq. (5.27)}$$

When using measured LFER parameters of the cation and activity coefficients of the anion, the water solubility of ILs can be predicted within the small error range of 0.138 log units Eq. (5.28) (Figure 5.5).

Table 5.9. System parameters (standard deviation) for predicting the water solubility of ILs determined using measured LFER descriptor and anion activity according to Eq. (5.18) and (5.29). f_c stands for system parameter for cationic charge density.

Eq.	c	e_c	s_c	a_c	v_c	f_c	d	R^2	SD	N	F
(5.28)	1.395 (0.265)	-0.429 (0.453)	0.431 (0.307)	0.280 (0.206)	-1.769 (0.170)	-	1.038 (0.040)	0.979	0.138	27	198.9
(5.29)	1.662 (0.183)	-	-	-	-1.734 (0.081)	-	1.023 (0.035)	0.976	0.135	27	513.8
(5.30)	6.061 (2.078)	0.646 (0.603)	-0.443 (0.478)	-0.169 (0.274)	-3.235 (0.667)	-2.886 (1.276)	1.043 (0.036)	0.984	0.126	27	199.1

Naturally, the molar fraction of ILs in water increases with decreasing cation volume and increasing anion activity coefficient. Therefore, with just the two terms, we can predict the water solubility with R^2 = 0.976 and SD = 0.135 Eq. (5.29). Other parameters (E_c, S_c, and A_c) only slightly enhance the accuracy. B_c is not statistically important. The introduction of the $f_c(1/V_c)$ charge density term slightly reduces the SD values further Eq. (5.30). This means that the charge effect that accounts for IL-IL interactions plays a more important role in water than in the octanol-water system, where no IL phase is present and therefore, IL-IL interactions can be neglected. In the water solubility prediction with measured LFER parameters, 10 data points had to be excluded because their LFER parameters are not available so far. The system parameters according to Eq. (5.28) ~ Eq. (5.30) are provided in Table 5.8.

On the other hand, the water solubility of ILs was assessed using the predicted anion activity coefficient and the calculated cationic LFER descriptors according to Eq. (5.30). The system parameters of Eq. (5.31) ~ Eq. (5.36) are tabulated in Table 5.10.

Table 5.10. System parameters (standard deviation) for predicting the water solubility of ILs determined using calculated LFER parameters and anion activity according to Eq. (5.31) – (5.36).

Eq.	c	e_c	s_c	a_c	b_c	v_c	f_c	d	R^2	SD	N	F
(5.31)	4.586 (1.548)	0.340 (0.240)	-1.661 (0.651)	1.166 (0.359)	4.552 (0.943)	-2.099 (0.398)	-0.996 (0.852)	1.085 (0.041)	0.976	0.166	37	165.8
(5.32)	2.923 (0.613)	0.289 (0.237)	-1.405 (0.617)	1.018 (0.337)	4.205 (0.900)	-1.660 (0.132)		1.062 (0.035)	0.974	0.167	37	190.9
(5.33)	2.536 (0.518)		-0.907 (0.457)	0.795 (0.283)	3.433 (0.632)	-1.598 (0.122)		1.067 (0.035)	0.973	0.168	37	214.1
(5.34)	1.677 (0.298)			0.390 (0.205)	2.474 (0.427)	-1.734 (0.105)		1.075 (0.036)	0.970	0.176	37	256.5
(5.35)	2.074 (0.216)				2.537 (0.443)	-1.835(0.094)		1.082 (0.038)	0.966	0.183	37	315.6
(5.36)	2.084 (0.301)					-1.835 (0.131)		1.102 (0.052)	0.933	0.254	37	236.1

The system parameters in Tables 5.9 and 5.10 that were obtained using the measured and calculated descriptors respectively are different each other. This is likely due to the different statistical relation of measured and calculated parameters, as already noted by Klamt and Abraham in their pioneering study[52] on neutral molecules. By contrast, the interactions due to dispersion, volume, anion activity, and anionic charge density in water are almost the same as when using measured values. This implies that only one independently derived set of LFER descriptors should be used, i.e. experimental or calculated LFER values. The measured and predicted water solubility with measured and calculated LFER parameters according to Eq. (5.30) and Eq. (5.36), respectively, are provided in Table 5.11.

Table 5.11. The measured water and predicted log water solubility [g L^{-1}] of ionic liquids with measured (exp.) and calculated (calc.) LFER parameters according to Eq. (5.30) and (5.36), respectively.

Ionic liquids	Measured log water solubility	Predicted log water solubility with	
		(exp. LFER parameters)	(calc. LFER parameters)
[IM12][B(CN)4]	-2.46[49]	-2.39	-2.41
[IM12][(CF3SO2)2N]	-3.12[76]; -3.1[76]; -3.08[78], -3.08[76],-3.1[75]	-3.04	-3.07
[IM13][(CF3SO2)2N]	-3.29[76]; -3.28[76];-3.27[76]	-3.26	-3.21
[IM14][(CF3SO2)2C]	-4.44[75]	-4.55	-4.41
[IM14][(CF3SO2)2N]	-3.51[76]; -3.51[76]; -3.54[76]; -3.53[76]; -3.49[76]; -3.46[76]; -3.5[76]; -3.5[84]	-3.55	-3.42
[IM14][(C4F9)SO3]	-3.15[77]	-3.24	-3.30
[IM14][PF6]	-3.0[79]; -2.92[79]; -2.96[79]; -2.93[82]; -2.89[80]; -2.87[80]; -2.8[78]; -2.9[84]; -2.9[75]	-2.91	-2.99
[IM15][(CF3SO2)2N]	-3.73[76]; -3.71[76]; -3.74[76]	-3.74	-3.66
[IM16][(C2F5)3PF3]	-5.93[84]	-5.99	-6.06
[IM16][(CF3SO2)3C]	-5.04[84]	-5.00	-4.91
[IM16][(CF3SO2)2N]	-4.02[76]; -4.18[84]; -3.86[78]; -4.03[75]; -4.05[76]; -4.05[76]	-4.00	-3.92
[IM16][PF6]	-3.41[79]; -3.45[79]; -3.35[84]; -3.36[79]	-3.36	-3.49
[IM17][(CF3SO2)2N]	-4.31[76]; -4.3[76]; -4.29[76]	-4.19	-4.19
[IM18][(CF3SO2)2N]	-4.7[85]; -4.6[85]; -4.59[84]; -4.14[75]; -4.1[77]; -4.1[85]; -4.5[76]; -4.49[76]; -4.47[76]	-4.49	-4.48
[IM18][(C4F9)SO3]	-4.23[77]	-4.18	-4.35
[IM18][PF6]	-3.93[84]; -3.92[79]; -3.9[79]; -3.46[81]; -3.95[79]	-3.85	-4.04
[IM18][BF4]	-2.93[79]	-2.83	-2.75
[Py4-3Me][(CF3SO2)2N]	-3.7[75]	-3.67	-3.66
[Py4-4Me][(CF3SO2)2N]	-3.69[77]	-3.66	-3.63
[Py4-4Me][(C4F9)SO3]	-3.03[77]	-3.35	-3.51
[Py8-4Me][(C2F5SO2)2N]	-5.4[84]	-5.18	-5.53
[Py8-4Me][(CF3SO2)2N]	-5.09[84]	-4.72	-4.73

[Py8-4Me][(C4F9)SO3]	-4.63[84]	-4.42	-4.60
[Py8-4Me][PhBF3]	-3.6[84]	-3.66	-3.67
[Py8-4Me][CF3SO3]	-3.09[84]	-3.14	-3.05
[Py8-4Me][BF4]	-2.98[84]	-3.07	-3.00
[Pyr14][(C2F5)3PF3]	-5.43[84]	--	-5.57
[Pyr14][(CF3SO2)2N]	-3.59[84]; -3.57[84]	--	-3.43
[Pyr16][(CF3SO2)2N]	-4.12[84]	--	-3.95
[Pyr18][(CF3SO2)2N]	-4.71[84]	--	-4.53
[Py6-4NMe2][(CF3SO2)2N]	-4.53[84]; -4.53[75]	-4.66	-4.42
[IM16-2Me][(CF3SO2)2N]	-4.15[75]	--	-4.09
[Pip14][(CF3SO2)2N]	-3.78[81]	--	-3.73
[Mor11O2][(CF3SO2)2N]	-3.19[84]	--	-3.26
[Py3OH][(CF3SO2)2N]	-2.43[84]	--	-2.52
[IM12OH][(CF3SO2)2N]	-2.34[75]	--	-2.21
[N4444][(6-2Et)2SS]	-1.52[83]	--	-1.71

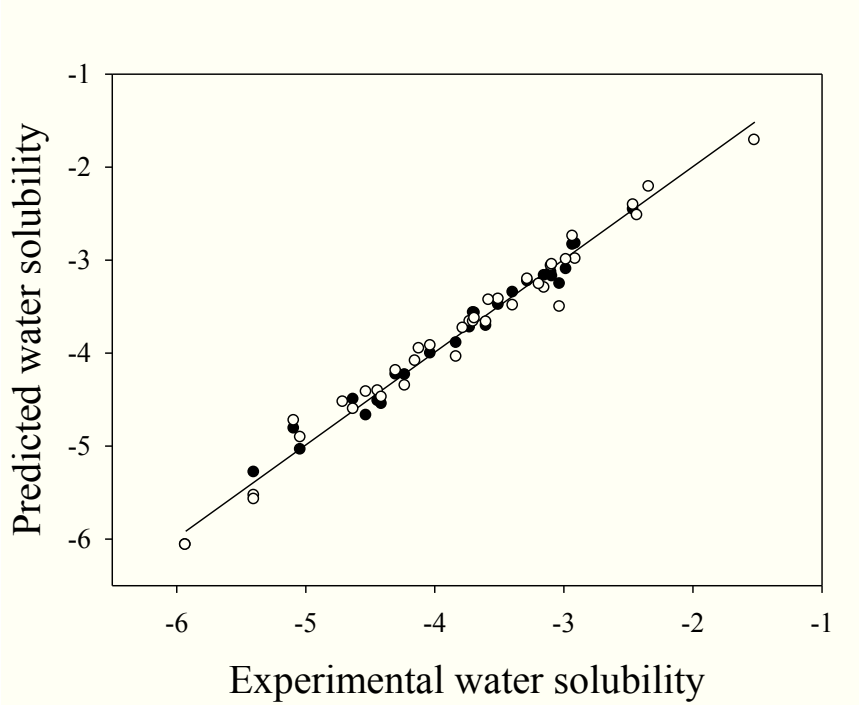

Figure 5.5. The relationship of experimental and predicted water solubility values determined with measured (●) and calculated LFER parameters (○) according to Eq. (5.30) and Eq. (5.31) respectively.

5.3.6. Critical micelle concentration of ionic liquids in water

The critical micelle concentration (CMC) is a basic parameter of surface chemistry as well as colloid and environmental science. Specifically, it influences biological properties like toxicity and biodegradability. The process of micellization can be directly correlated to the interaction of amphiphiles with apolar surfaces such as micelles or cell membranes. Therefore, the CMC was predicted in order to investigate the molecular interaction at a rather high concentration in water. Since we assumed that cations and anions are forming aggregates, we used each parameter as the sum of cationic and anionic contributions Eq. (5-37). The CMC values of ILs at 293 - 298 K were collected from literature [87-111] and are given in Table 5-13.

$$\text{Log CMC [mmol L}^{-1}\text{]} = e(E_c+E_a) + s(S_c+S_a) + a(A_c+A_a) + b(B_a+B_c) + v(V_c+V_a) + c \qquad \text{Eq. (5.37)}$$

Here, the prediction was carried out exclusively with calculated descriptors. The results show that the CMC can be predicted within an error range of about 0.179 log units according to Equation (5.37). However, there are some remarkable exceptions ([IM12]Br, [IM14]Br, [IM14][CF3SO4], and [IM14][C8SO4]). In order to include them, we introduced the charge density term ($1/V_c$ and $-1/V_a$ for cation and anion, respectively). In combination Eq. (5.38), the correlation was improved to $R^2 = 0.989$.

$$\text{Log CMC [mmol L}^{-1}\text{]} = 0.754(0.283)(E_c+E_a) - 1.174(0.704)(S_c+S_a) - 0.993(0.365)(A_c+A_a) + 0.531(0.169)(B_a+B_c) - 1.965(0.062)(V_c+V_a) - 0.123(0.033)1/V_c - 0.364(0.067)(-1/V_a) + 9.518(1.721) \qquad \text{Eq. (5.38)}$$

$$R^2=0.989,\ SD=0.128,\ N=36,\ F=345.7$$

In another approach, we rewrote Eq. (5.30) as Eq. (5.39) with the assumption that each parameter of cation and anion is different.

$$\text{Log CMC} = c + e_cE_c + s_cS_c + a_cA_c + b_cB_c + v_cV_c + e_aE_a + s_aS_a + a_aA_a + b_aB_a + v_aV_a \qquad \text{Eq. (5.39)}$$

The results showed that the CMC can be predicted with an SD of 0.168 log units, which is similar to Equation (5.37), but with different system constants. To further reduce the SD, the charge density terms of cation and anion were added. Consequently, we found that this model can predict the CMC with the smallest error of 0.104 log units. The system parameters according to Eq. (5.40) and Eq. (5.41) are given in Table 5.12 and predicted and measured CMC values are given in Table 5.13.

Table 5.12. System parameters (standard deviation) for predicting the critical micelle concentration of ILs using calculated LFER parameters.

Eq.	c	e_c	s_c	a_c	b_c	v_c	e_a	s_a	a_a	b_a	v_a	g_c	f
(5.40)	4.838	-0.369	1.327	0.580	0.673	-2.010	0.212(0.368)	0.376	0.544	-0.299	-1.633		
	(1.161)	(0.257)	(0.263)	(0.765)	(1.864)	(0.200)		(1.014)	(0.673)	(0.282)	(0.247)		
		R^2=0.982	SD=0.168	N=36	F=139.3								
(5.41)	16.721	3.058	-7.647	-2.601	1.696	-1.648	0.796	-2.024	-2.731	1.452	-2.099	-0.411	0.623
	(0.265)	(0.814)	(2.046)	(0.868)	(1.189)	(0.141)	(0.263)	(0.802)	(0.803)	(0.400)	(0.184)	(0.095)	(0.130)
		R^2=0.994	SD=0.104	N=36	F=307.3								

Table 5.13. The experimentally measured and predicted log CMC values [mmol L^{-1}] of ionic liquids assessed with calculated LFER parameters according to Eq. (5.41).

Chemicals	Surface tension	Conductivity	Other	Predicted
[N1,1,1,8]Br			2.352[88]	2.388
			2.462[89]	
[N1,1,1,10]Cl	1.845[90]	1.976[91]		1.988
[N1,1,1,10]Br		1.797[92]	1.792[88]	1.807
			1.780[92]	
[N1,1,1,12]Cl	1.255[90]	1.346[91]		1.400
		1.328[93]		
[N1,1,1,12]Br			1.155[60]	1.218
			1.176[94]	
[N1,1,1,14]Cl	0.740[95]	0.751[91]		0.793
	0.653[90]	0.740[96]		
[N1,1,1,14]Br		0.580[96]	0.544[94]	0.612
[N1,1,1,16]Cl	0.114[90]	0.164[90]		0.168
[N1,1,1,16]Br			-0.046[94]	-0.013
[N1,1,1,18]Cl			-0.456[97]	-0.221
[IM12]Br	3.398[98]	3.279[98]		3.442
[IM14]Br	2.903[98]	2.954[98]		3.225
[IM14][BF_4]	2.903[99]	2.914[99]		3.090
	3.137[87]			
[IM14][CF_3SO_3]	2.893[87]			2.970
[IM14][C_8SO_4]	1.608[87]	1.491[100]		1.632
[IM16]Cl	2.954[90]			2.873
[IM16]Br	2.778[98]	2.602[98]	2.945[101]	2.692
	2.672[103]		2.903[101]	
[IM18]Cl	2.342[103]	2.369[103]	2.301[90]	2.316
	2.000[99]	1.954[99]		
	2.342[90]			
[IM18]Br	2.176[98]	2.176[98]	2.255[101]	2.135

	2.083[103]		2.279[101]	
[IM18]I	2.000[99]	2.176[99]		2.156
[IM19]Br	1.602[98]	1.477[98]		1.845
		1.869[104]		
[IM1-10]Cl	1.777[103]	1.731[103]	1.653[90]	1.756
	1.740[90]	1.607[105]	1.740[90]	
	1.601[105]			
[IM1-10]Br	1.301[102]	1.602[106]	1.623[101]	1.575
	1.467[107]	1.613[104]	1.663[101]	
		1.517[107]		
[IM1-12]Cl	1.176[90]	1.129[105]	0.845[90]	1.267
	1.120[105]		1.114[90]	
[IM1-12]Br	0.634[102]	0.991[104]	1.000[101]	1.086
		0.929[110]	1.079[101]	
		0.978[108]		
[IM1-12][BF_4]	0.964[107]	0.881[107]		0.952
[IM1-14]Cl	0.602[90]	0.498[93]	0.477[90]	0.652
	0.532[103]	0.566[105]	0.602[90]	
	0.474[105]			
[IM1-14]Br		0.398[104]		0.471
		0.415[107]		
[IM1-16]Cl	0.114[103]	0.057[103]		0.060
	-0.056[109]	-0.066[105]		
	-0.061[105]			
[IM1-16]Br		-0.097[102]		-0.121
		-0.215[104]		
		-0.187[108]		
[IM1-18]Cl	-0.398[103]	-0.347[103]		-0.427
[Py_8]Cl		2.439[103]		2.334
Na[C_8SO_4]			2.127[110]	2.094
Na[$C_{10}SO_4$]			1.477[110]	1.480
Na[$C_{12}SO_4$]			0.881[111]	0.892
Na[$C_{14}SO_4$]			0.301[110]	0.269

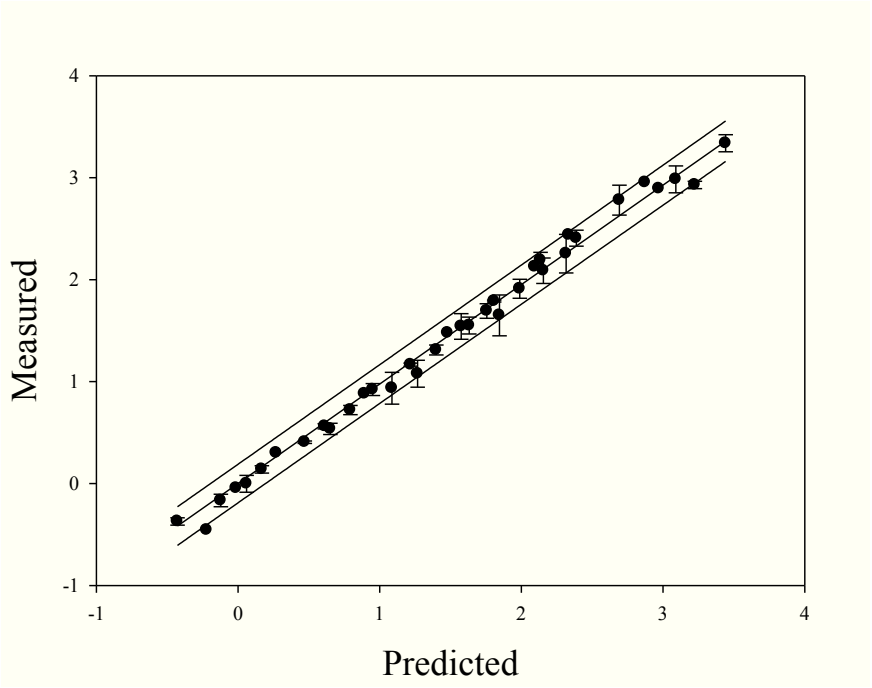

Figure 5.6. The relationship of experimental and predicted log critical micelle concentration [mmolL^{-1}] determined with calculated parameters according to Eq. (5.41).

Recently, we introduced a CMC prediction method for ILs using the cubed molecular radius, the solvent-accessible surface, and COSMO-RS interactions such as hydrogen bonding, van der Waals, and misfit enthalpies.[87] The results give an R^2 of 0.994, equal to that in the present study. However, in order to use this method, it is necessary to calculate the enthalpies for each IL, because the values change with the combination of cation and anion, while the present approach may be more comfortable, as the needed parameters can be easily derived by combining cation- and anion-specific LFER parameters without any quantum chemical calculation.

5.4. Conclusions

The extended models based on the Abraham Equation can satisfactorily model log P, water solubility, and CMC of rather concentrated aqueous solutions of ILs using measured as well as calculated LFER parameters. Activity coefficient and hydrophobicity of the anion in water and octanol-water can equally be modeled using the calculated LFER descriptors. For the prediction of log P and water solubility, it is slightly advantageous to use the measured LFER descriptors over the calculated ones. However, the calculated parameters are much easier accessible and provide an easy approach to investigate parameters for ILs, which are experimentally not yet available.

In our prediction studies, the volume term (V) is the most important factor to determine physicochemical properties of ILs in solution. B is the second-most important contribution parameter, and other terms (E, S, and A) have only slight - but not ignorable - contributions. The combination of all parameters can enhance the predictability of the ILs' behavior in solution. For the anionic hydrophobicity hydrogen bonding basicity as a second key parameter in combination with V significantly contributes to the anionic molecular interaction in the octanol-water system. Similarly, both cationic volume and hydrogen bonding basicity with anionic hydrophobicity cause importantly ILs to partition in octanol-water. On the other hand, for the anionic activity coefficient in water, the single anionic hydrogen-bonding basicity term gives a better correlation than the volume, and changing the charge density term from V_c to $1/V_a$ with inclusion of the hydrogen-bonding basicity of the anion improves the prediction. In the case of the cationic contribution to the solubility in water, unlike the anionic activity coefficient, the $1/V_c$ term includes more molecular interaction than hydrogen-bonding basicity of cation: this might be attributed to the fact that cations (*e.g.* imidazolium and pyridinium) have larger volumes and are less functionalized than anions. Moreover, the CMC at high concentrations was predicted with the assumption of ion-paring and as well for the ion-dissociated form. In both cases, a good agreement was demonstrated, but the prediction using the ion-dissociated form is more accurate. The CMC also correlates readily with the volume term, but to include amphiphiles, the consideration of hydrogen bonding is required.

6. *In silico* modelling for predicting cationic hydrophobicity and cytotoxicity of ionic liquids towards *Leukaemia rat cell line*, *Vibrio fisheri* and *Scenedesmus vacuolatus* based on molecular interaction potentials of ions

6.1. Background

Since ionic liquids can be designed and tailor-made by the selective combination of cation and anion or by modifying their chemical structure, they theoretically could be infinitely applied in industrial processes. However, their different chemical structures and their innumerous possible combinations might evoke unforeseen toxic effects in the environment if ILs are released into different environmental compartments.

Studying the environmental behavior of ILs, many researchers have been enthusiastically progressing and steadily report their observed toxic effects toward bacteria,[38,112-115] algae,[116-124] human cell lines,[125-128] crustaceans.[38,129,130] Furthermore, there is some comprehensive review available dealing with toxicological effect of ILs. However, it is difficult to estimate the toxic effect of all ILs using toxicological and/or ecotoxicological test systems because it is time- and resource-consuming. This becomes obvious if one considers that the theoretically synthesizable number of ILs is around 10^5–10^6. Therefore it is extremely necessary to establish sound prediction models.

Recent reviews provide a comprehensive overview on existing (eco)toxicological and biodegradability data of ILs[131-138] It is difficult, however, to estimate the toxic effect of all possible ILs using toxicological and/or ecotoxicological test systems because these assessments are time- and resource-consuming. This becomes obvious if one considers that several hundred ILs are commercially available at the moment, several thousand are described in literature and millions of IL structures are theoretically synthesizable. Therefore it is of high concern to establish sound prediction models to facilitate the selection of ILs that are favorable to the environment according to the “benign-by-design” approach.

To predict IL toxicity several researchers[38,130, 138-144] have developed models based on QSARs (Quantative–Structure Activity Relationships) combining experimental and computational approaches.

Our group reported for the first time that cationic hydrophobicity values (log k_o) derived by high performance liquid chromatography (HPLC) is highly correlated (statistical coefficient of 0.78) with their measured acute cytotoxicity towards the mammalian cell line IPC-81.[38]

In 2006, Couling et al.[130] developed computationally a QSAR model using four calculated molecular descriptors by MOPAC *i.e.* electropological state indices for atoms, partial negative and positive solvent–accessible surface area, and shadow–v (assuming van der Waals radii for atoms). Their predictive models can predict log EC_{50} of IL to *Vibrio fischeri* and *Daphnia magna* showing statistical coefficients (R^2) of 0.78 to 0.88 log units respectively.

A group contribution method to estimate log EC_{50} values towards *Vibrio fischeri* by using the contribution of artificial numbers designated according to the type of cation and anion and the length of the substituting alkyl chain was presented by Luis et al.[138, 139] Their prediction model has a very good accuracy with a R^2 of 0.92 based on a set 96 log EC_{50} involving 9 types of cation and 17 anions.

Garcia–Lorenzo et al.[140] predicted the logEC_{50} values of imidazolium based ILs in human Caco–2 cell line using several parameters from the Topological sub–Structural Molecular Design approach (www.modeslab.com). These parameters are standard dipole moments, the bond distance, and atomic properties i.e. partition coefficient, polar surface area, polarizability, Gasteiger–Marsilli atomic charges, van der Waals atomic radii, and molar refractivity.

Torrecilla et al.[141] estimated four models by principal component analysis using easily available values – empirical formula (elemental composition) and molecular weight– for predicting toxicity of ILs towards *leukaemia rat cell line* and inhibition to the isolated enzyme acetylcholinesterase. Furthermore, they established a non–linear model for predicting the effective concentrations of ILs towards the IPC-81 cell line using quantum–chemical $S_{s-profile}$ descriptors of IL compounds derived from COSMO–RS.[142] In the study, they developed a new concept Quantitative–Structure–Activity Map (QSAM) because they stated that the toxicity of ILs cannot be systematically estimated as the sum of intrinsic toxicities of cations and anions.[142]

In 2011, Fetami and Izadiyan[143] developed linear and nonlinear models to predict the cytotoxicity of ILs to *rat leukaemia cells* using quantitative structure – toxicity relationships (QSTR). Additionally, Alverez–Guerra and Irabien[144] presented an application of Partial Least Squares–Discriminant Analysis (PLS–DA) to help identifying whether the combination of specific IL cations and anions is lower in toxicity than traditional industrial solvents, i.e. toluene and chloroform.

In our studies we pursue two innovative approaches to predict the acute toxicity of ILs towards the mammalian cell line IPC-81, to unicellular green algae *Scenedesmus vacuolatus*, and marine bacteria *Vibrio fischeri* solely based on *in silico* methods. Firstly, a model will be proposed to predict the HPLC derived hydrophobicity parameter log k_o using multi–linear free energy relationships (m–LFER). This

well established log k_o value was used to predict toxic effects of the IL cations towards the above mentioned cells.[38] Secondly, we will apply an extended Abraham equation that considers calculated descriptors for cation and anions to predict EC_{50} values the selected toxicological test systems using huge toxicity dataset and m-LFER. The approach of m-LFER is very accessible concept to predict the toxicity values if the solute descriptors are known. And especially compared to other prediction studies, [38, 130,138-144] this method using descriptors based on molecular interaction potentials are very useful to link other physical-chemical properties of ILs. For example, with these LFER descriptors, our group has successfully predicted water solubility, partitioning coefficient in octanol-water, activity coefficient of anions in IL saturated water phases, and anionic hydrophobicity in IL equilibrated octanol-water.[59] Moreover, it allows also at investigating the most prominent molecular-interaction-potentials contributing to the cationic hydrophobicity and cytotoxicity of IL cations and anions toward three toxicity test systems. These facts indicate that the LFER concept can be useful to understand the physical and chemical properties and environmental behaviors of ILs and at the same time to reach the 4th principle of the 12 principles of Green Chemistry "Chemical products should be designed to preserve efficiency of function while reducing toxicity".[4]

6.2. A concept of LFER for toxicity prediction

Since we assume complete dissolution of an IL, the cation and anion of ILs can be treated separately. Thus, we separate the descriptors for the cation and anion and remark them with the subscription 'c' for cations and 'a' for anions:

$$SP = c + e_c E_c + s_c S_c + a_c A_c + b_c B_c + v_c V_c + e_a E_a + s_a S_a + a_a A_a + b_a B_a + v_a V_a \quad \text{Eq. (6.1)}$$

The extended Eq. (6.1) has been used to investigate the partitioning behavior of neutral compounds in a water–ILs system.[145,146] In that study the IL ions form part of a binary system (small letters in the above cited equation), while in our study the IL ions represent the solutes (descriptors with the capital letters in the above cited equation).

6.3. Results and discussion

6.3.1. Prediction of cationic hydrophobicity (log k_o)

The hydrophobicity of a molecule is very important in environmental research because it is the predominant property involved in sorption, toxicity and solubility of a substance. To determine the IL cationic hydrophobicity (log k_o), Stepnowski and Storoniak[37] have successfully correlated the retention characteristics of hydrophobic stationary phase in HPLC with Log P values (octanol-water partitioning coefficient) of ILs based on the work of Eadsforth & Moser[147] and introduced by Klein et al.[148] into the OECD guideline 117.[149] Our group used the log k_o for correlating cytotoxicity,[38,112,150] water solubility[39] and the octanol–water partitioning coefficient[59] of ILs. Additionally, we could derive activity coefficients of IL anions in water saturated with the corresponding IL and we could estimate the hydrophobicity of IL anions at Equilibrium conditions of ILs in an octanol–water system.[59] To understand cationic molecular interaction potentials based on the log k_o values and to predict them without further experimental work, we attempted to predict the log k_o using calculated LFER descriptors.

For the prediction of the log k_o we collected 66 log k_o values[38,112,151] from the literature or from the UFT Merck Ionic Liquids Database. By multiple linear regressions of the calculated descriptors of all cations with measured log k_o, values we detected two prominent outliners, $[IM14]^+$ and $[IM16]^+$. Here the calculated values are less than measured values. For a more accurate prediction model, we excluded the outliners and then we were able to reasonably predict the log k_o values with a statistical coefficient (R^2) of 0.985 and a standard deviation (SD) of 0.150 log units [Eq. (6.2)]. In this prediction, we observed that V seems to be the most important parameter to describe the log k_o correlating with a R^2 of 0.943 [Eq. (6.3)]. The B parameter seems to be of secondary importance and therefore its addition to the prediction model helps to increase R^2 to 0.981 [Eq. (6.4)]. The A descriptor only slightly contributes to the enhancement of accuracy from 0.981 to 0.985 of R^2 [Eq. (6.4)] and its addition to the model decreased the SD from 0.167 to 0.150. Finally, the remaining parameters E and S are statiscally not important. Each system parameter of Eq. (6.2) ~(6.4) is given in Table 6.1. The preceding sign of the system parameters shows that either the LFER descriptors contributed positively or negatively to the given property. As shown by the most accurate Eq. (6.2), increasing hydrogen bonding acidity and basicity (A and B) yields a decrease in the log k_o values while the McGowan volume is increasing. The correlation is shown in Figure 6.1, the measured and the predicted hydrophobicity values are given in Table 6.2.

Table 6.1. System parameters (with standard deviation in parentheses) for predicting cationic hydrophobicity

Eq.	*c*	*a*	*b*	*V*	R^2	SD	N	F
(6.2)	–1.602 (0.082)	–0.278 (0.071)	–1.735 (0.154)	1.766 (0.032)	0.985	0.150	64	1305.9
(6.3)	–1.851 (0.058)		–1.856 (0.168)	1.814 (0.032)	0.981	0.167	64	1580.2
(6.4)	–1.867 (0.099)			1.755 (0.055)	0.943	0.286	64	1031.7

R^2 is the statistical coefficient. SD is standard deviation. N is the number of data points. F is the Fisher stastics.

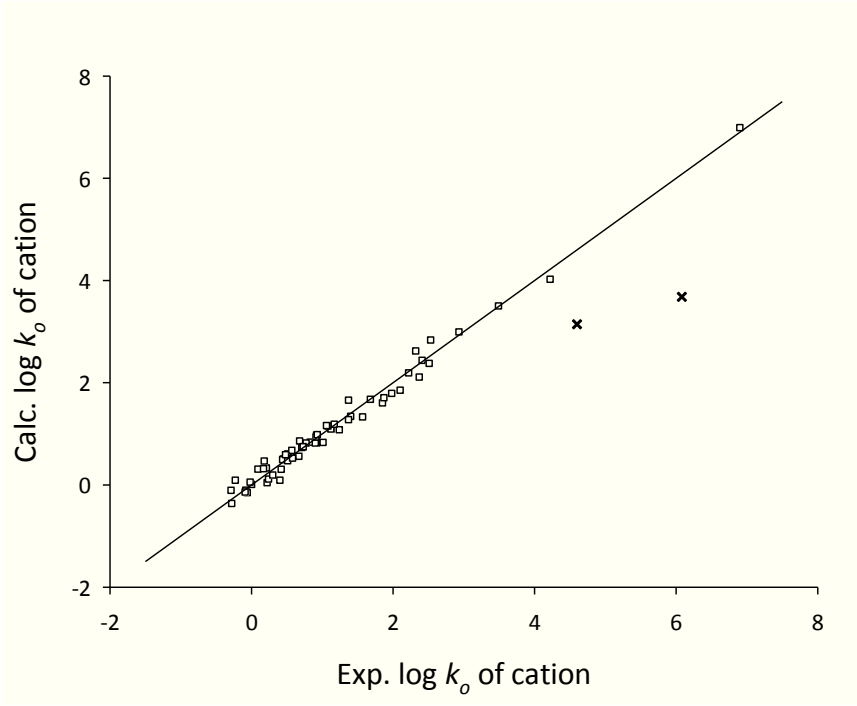

Figure 6.1. The relationship of experimental and predicted cationic hydrophobicity values (log k_o) according to Eq. (6.2). x is outlier.

Table 6.2. The measured (Exp.) and calculated (Calc.) log k_o of 64 cations.

Cations	Exp. Log k_o	Calc. Log k_o
$[IM1–(1Ph–4Me)]^+$	1.12	1.11
$[IM1–10]^+$	2.37	2.10
$[IM11CN]^+$	–0.29	–0.10
$[IM11O2]^+$	0.21	0.34
$[IM1–1Ph]^+$	0.83	0.84
$[IM1–1Ph–4Me]^+$	1.12	1.11
$[IM12]^+$	0.22	0.04

$[IM1–2CO–1]^+$	0.00	0.01
$[IM12O1]^+$	–0.02	0.05
$[IM12O2]^+$	0.45	0.52
$[IM12OH]^+$	–0.28	–0.35
$[IM1–2Ph]^+$	1.01	0.84
$[IM13]^+$	0.42	0.31
$[IM13COOH]^+$	–0.08	–0.09
$[IM13O1]^+$	0.40	0.09
$[IM13OH]^+$	–0.23	0.09
$[IM14]^+$	0.67	0.56
$[IM14OH]^+$	–0.06	–0.15
$[IM15]^+$	0.92	0.83
$[IM16]^+$	1.24	1.09
$[IM16–2Me]^+$	1.37	1.65
$[IM17]^+$	1.57	1.34
$[IM17COOH]^+$	0.92	0.98
$[IM18]^+$	1.85	1.60
$[IM18OH]^+$	0.90	0.82
$[IM19]^+$	2.10	1.85
$[IM2–10]^+$	2.51	2.39
$[IM22]^+$	0.09	0.31
$[IM23]^+$	0.56	0.56
$[IM24]^+$	0.77	0.83
$[IM26]^+$	1.40	1.34
$[Mor11O2]^+$	0.17	0.32
$[Mor14]^+$	0.18	0.47
$[N11–10–1Ph]^+$	2.93	3.00
$[N11–12–1Ph]^+$	3.49	3.50
$[N11–14–1Ph]^+$	4.22	4.03
$[N1121COO2]^+$	0.44	0.50
$[N1122O1]^+$	0.24	0.12
$[N1124]^+$	0.51	0.61
$[N4444]^+$	2.32	2.63
$[P4444]^+$	2.53	2.84
$[P666–14]^+$	6.9	7.00
$[Pip13O1]^+$	0.51	0.48
$[Pip14]^+$	0.68	0.86

[Py2–4NMe2]$^+$	0.51	0.61
[Py3OH]$^+$	–0.09	–0.15
[Py4]$^+$	0.58	0.54
[Py4–2Me]$^+$	0.71	0.74
[Py4–3Me]$^+$	0.73	0.74
[Py4–3Me–4Me]$^+$	0.91	0.93
[Py4–3Me–5Me]$^+$	0.93	0.99
[Py4–4Me]$^+$	0.73	0.75
[Py4–4NMe2]$^+$	1.08	1.14
[Py6–4Me]$^+$	1.37	1.28
[Py8–4Me]$^+$	1.98	1.79
[Pyr11COO2]$^+$	0.48	0.60
[Pyr12O1]$^+$	0.3	0.20
[Pyr14]$^+$	0.57	0.68
[Pyr16]$^+$	1.17	1.19
[Pyr18]$^+$	1.87	1.70
[Pyr66]$^+$	2.41	2.44
[Quin4]$^+$	1.06	1.15
[Quin6]$^+$	1.68	1.66
[Quin8]$^+$	2.22	2.20

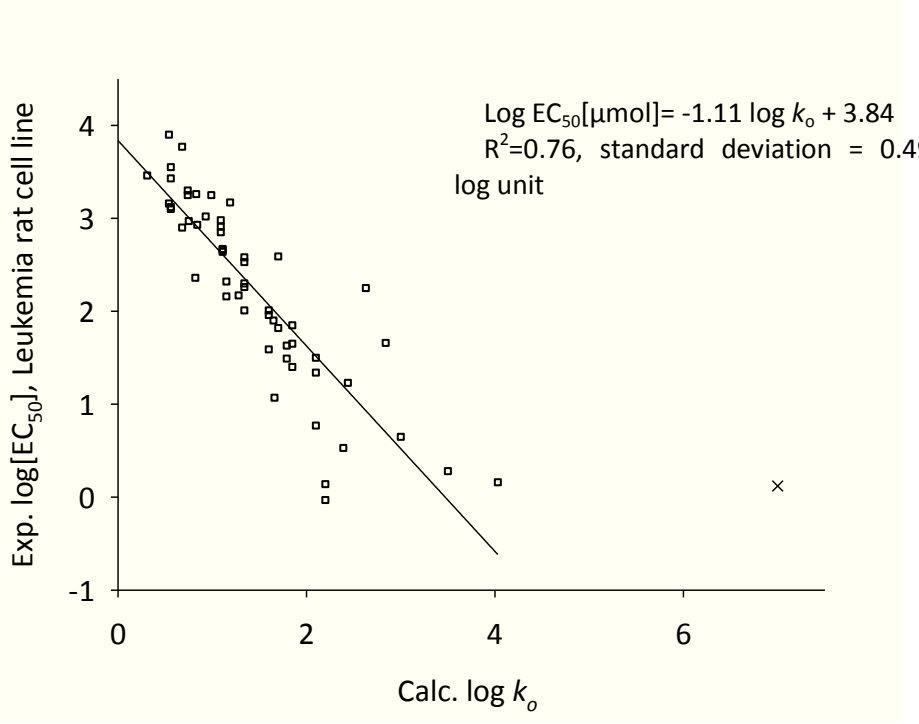

Figure 6.2. Correlation the calculated log k_o values against experimentally determined log EC_{50} values of ionic liquids with anions i.e. Cl^-, Br^-, $[BF_4]^-$, and $[PF_6]^-$ towards Leukaemia rat cell line. A linear fitting, statistical coefficient (R^2), standard deviation was calculated excluding outlier i.e. [P666-16] $[BF_4]$

In order to clarify the applicability of the calculated log k_o for prediction of toxicity of ILs, they were fitted with toxicity dataset tested towards *Leukaemia rat cell line* of ILs- used previously by Ranke et al.[38] The used ILs are comprised of various cations i.e. imidazolium, pyridinium, ammonium, phosphonium, pyrrolidinium, and quinolinium with four different anions i.e. Cl^-, Br^-, $[BF_4]^-$, and $[PF_6]^-$. The result showed that the correlation has almost similar a linear model (Figure 6.2) and statistical coefficient of 0.76 compared to outcomes (R^2 of 0.78, Log EC_{50}[µmol]= -1.11 log k_o + 3.91) from Ranke et al. [38]

6.3.2. Prediction of IL cytotoxicity towards IPC-81 rat leukaemia cells

In order to predict EC_{50} values of ILs towards IPC-81 cells we attempted to model cytotoxicity using Eq. (6.1) based on calculated descriptors of IL cations and anions. For the modeling 200 cytotoxicity data (EC_{50} values) are available in the UFT / Merck Ionic Liquids Database[69] and tabulated in Table 6.5. For the modeling the ILs with high hydrophobicity (4 < calculated log k_o; the calculated log k_o of cations for this study according to Eq. (6.2)) *i.e.* [N1888][(CF3SO2)3N], [P666–16][(CF3SO2)2N], [P666–16][BF4], [IM1–18]Cl and [N1,1,14,Bz]Cl were excluded.

In order to have a positive trend of the cytotoxicity values, all effective concentrations (EC_{50}) were transferred into the logarithm of the inverse molar concentration log [$1/EC_{50}$]. The robustness and periodicity of the obtained model were checked by comparing the standard deviations of a training and a test set of ILs, which both were randomly set up out of the ILs tested. The training and test set comprised 100 and 96 data points, respectively.

The initial regression analysis showed that all descriptors of the Abraham equation [Eq. (6.1)] can be yielded as follows:

Log [$1/EC_{50}$] [µmol/L], *Leukaemia rat cell line* = $-6.824(0.851) + 0.416(0.229)E_c + 0.333(0.579)S_c + 0.183(0.418)A_c - 2.509(0.841)B_c + 1.960\ (0.156)V_c - 0.839(0.386)\ E_a - 0.145(0.490)S_a - 0.780(0.485)A_a + 0.194(0.178)B_a + 0.147(0.160)V_a$ Eq. (6.5)

R^2=0.764, SD=0.519 log units, F=28.9, N=100

The result showed that all calculated descriptors in Eq. (6.1) can be used to predict the cytotoxicity with a R^2 of 0.764 and a SD of 0.519 log units. To further address ionic interactions, and hence to achieve a more realistic model we added the charge density terms +1 for cations and –1 for anions divided by their volume; $+1/V_c + -1/V_a$ to Eq. (6.1) and performed again the multiple linear regression. The derived equation is the following:

Log [$1/EC_{50}$] [µmol/L], *IPC-81 cell line* = $-9.277(1.264) + 0.436(0.224)E_c + 0.374(0.569)S_c - 0.144(0.429)A_c - 2.229(0.828)B_c + 2.631\ (0.333)V_c + 1.652(0.692)1/V_c - 0.692(0.384)E_a + 0.161(0.485)S_a + 0.553(0.488)A_a - 0.200(0.177)B_a + 0.361(0.254)V_a - 0.106(0.134)1/V_a$

R^2=0.781, SD=0.506 log units, F=25.9, N=100

The result shows that the charge density terms enhanced the predictability of cytotoxicity yielding a R^2 of 0.781 and a SD of 0.506 log units, which means a higher R^2 and a lower SD than obtained for Eq. (6.6).

To identify the most contributing molecular interaction among the six descriptors – E, S, A, B, V, and charge density terms – we attempted to rebuild the model by adding each descriptor step by step. Firstly, we found out that the V of cation and the anion – representing the predominant measure of hydrophobicity as shown above while predicting log k_o values – shows a good correlation with the cytotoxicity [Table 6.3, Eq. (6.7)] (R^2 of 0.575 and SD of 0.667 log units). The combination of hydrogen–bonding basicity (B_c and B_a) with V terms in the next step significantly improves the prediction with a R^2 of 0.692 and a reduced SD of 0.574 log units (Table 6.3, Eq. (6.8)). The next contributing descriptor is the excess molar refraction (E_c and E_a), its introduction helped to reach a slightly better predictivity [Table 6.3, Eq. (6.9), R^2 of 0.745, SD of 0.528 log units]. Finally, by adding the charge density terms to the model equation, the predictability is remarkably improved as shown by a SD of 0.500 log units and a R^2 of 0.776 [Table 6.3, Eq. (6.10)]. This means that the standard deviation is significantly lower and the number of descriptors can be reduced compared to the Abraham equation including all descriptors [Table 6.3, Eq. (6.6)].

For assessing the predictivity and robustness of our model, we calculated the EC_{50} values of a test set consisting of 95 IL data according to Eq. (6.10) in Table 3. The result shows that the predicted values correlate well with the experimentally measured values with a R^2 of 0.786 and a SD of 0.463 log units, which is slightly better than the results obtained for the training set. Therefore we assume the prediction model Eq. (6.10) to be robust and useful. Additionally when correlating with whole dataset, the Eq. (6.10) allows us to predict the toxicity values in R^2 of 0.779. Figure 6.3 shows the correlation between measured and predicted cytotoxicity values of the training set and the test set. In Table 6.4 the measured and predicted cytotoxicity values of ILs are given (training set and test set).

The finally obtained equation [Eq. (6.10)] using four descriptors – i.e. V, B, E, and the charge of cations and anions – shows that increasing the volume of cations and/or anions increases the toxicity. In contrast, increasing the B values the cytotoxicity value is reduced because B reduces the hydrophobicity, as the same trend could be shown in the hydrophobicity prediction above. The increase of E_c and $1/V_c$ causes an increase in the toxicity while the effect of increasing E_a and $-1/V_a$ values are vice versa. The reason is that the E_a and $-1/V_a$ are in general minus, while E_c and $1/V_c$ are opposite direction.

Table 6.3. System parameters (with standard deviation in parentheses) for predicting cytotoxicity to IPC-81 cells, *Vibrio fischeri*, and *Scenedesmus vacuolatus* using the calculated solute descriptors of cation and anion

	Eq.	e_c	e_a	s_c	s_a	b_c	b_a	v_c	v_a	g_c	g_a	c	R^2	SD	F	N
Leukaemia rat cell line	(6.7)							1.927 (0.169)	0.313 (0.122)			–5.994 (0.299)	0.575	0.667	65.7	100
	(6.8)					-2.590 (0.445)	-0.045 (0.066)	2.069 (0.151)	0.423 (0.158)			–6.162 (0.392)	0.691	0.575	53.3	100
	(6.9)	0.403 (0.175)	–0.756 (0.211)			–2.298 (0.427)	0.073 (0.072)	1.910 (0.150)	0.216 (0.156)			–6.638 (0.375)	0.745	0.527	45.5	100
	(6.10)	0.514 (0.170)	–0.528 (0.225)			–1.822 (0.475)	–0.049 (0.093)	2.653 (0.316)	0.555 (0.244)	1.738 (0.607)	–0.184 (0.115)	–9.423 (0.940)	0.776	0.500	45.3	100
Vibrio fischeri	(6.12)							1.798 (0.260)	0.133 (0.181)			–5.300 (0.388)	0.420	0.774	23.9	69
	(6.13)					–2.619 (0.360)	0.115 (0.066)	3.061 (0.236)	0.766 (0.170)			–8.027 (0.476)	0.724	0.542	41.9	69
	(6.14)					–2.227 (0.410)	0.116 (0.076)	3.822 (0.416)	0.778 (0.312)	1.084 (0.485)	–0.005 (0.141)	–9.918 (1.020)	0.744	0.530	30.1	69
Senedesmus	(6.16)							4.925 (0.621)	0.426 (0.278)			–8.654 (0.938)	0.605	1.026	32.5	44
	(6.17)							15.372 (1.707)	0.981 (0.601)	19.232 (3.024)	–0.133 (0.217)	– 38.295 (4.598)	0.811	0.728	41.9	44
	(6.18)					–3.270 (1.007)	–0.203 (0.155)	14.12 (1.613)	1.106 (0.541)	16.856 (2.966)	–0.289 (0.238)	– 34.670 (4.422)	0.857	0.650	37.0	44
	(6.19)			–0.382 (0.676)	0.897 (0.643)	–2.702 (1.172)	–0.600 (0.302)	13.714 (1.755)	1.768 (0.702)	16.101 (3.334)	–0.766 (0.392)	– 34.787 (4.397)	0.868	0.655	28.7	44

Table 6.4. The measured (Exp.) and predicted (Calc.) cytotoxicity values of training set and test set of ionic liquids toward *rat leukaemia cell line*

Training set	Exp.	Calc.	Test set	Exp.	Calc.
[Gu011112][(C2F5)3PF3]	-2.09	-2.01	[IM1-10][PF6]	-1.50	-1.57
[IM1-10][BF4]	-0.77	-1.29	[IM1-10]Cl	-1.34	-1.48
[IM1-10]Br	-0.27	-1.56	[IM1-16]Cl	0.24	0.94
[IM1-14]Cl	0.42	0.08	[IM1-1Ph][[BF4]]	-2.97	-2.71
[IM11CN][(CF3SO2)2N]	-3.90	-3.03	[IM12][(C2F5)3PF3]	-3.47	-2.46
[IM12][(C2F5)2PO2]	-2.83	-2.97	[IM12][[BF4]]	-3.44	-3.69
[IM12][(CF3SO2)2N]	-3.26	-3.43	[IM12][1O2O2OSO3]	-3.85	-3.86
[IM12][1COO]	-4.23	-4.27	[IM12][1SO3]	-3.97	-4.03
[IM12][1OSO3]	-4.20	-3.98	[IM12][4MePhSO3]	-3.81	-4.28
[IM12][2OSO3]	-3.93	-4.01	[IM12][B(CN)4]	-3.50	-3.79
[IM12][8OSO3]	-3.22	-3.98	[IM12][CF3SO3]	-4.09	-3.71
[IM12][CF3COO]	-4.00	-4.08	[IM12][N(CN)2]	-3.82	-3.12
[IM12][HSO4]	-3.99	-3.70	[IM12][SCN]	-4.23	-4.26
[IM12][PF6]	-3.92	-3.97	[IM12O1][(CF3SO2)2N]	-3.25	-3.58
[IM1-2C6F13][PF6]	-1.94	-1.48	[IM12O2]Br	-4.14	-3.67
[IM12O2][(CF3SO2)2N]	-3.18	-3.13	[IM12OH][BF4]	-3.48	-4.12

[IM12OH][(CF3SO2)2N]	-3.76	-3.86	[IM13O1][(CF3SO2)2N]	-3.34	-3.58
[IM13][BF4]	-3.45	-3.52	[IM14][(C2F5)3PF3]	-1.81	-2.05
[IM13O1]Cl	-4.49	-4.04	[IM14][(CF3SO2)2N]	-2.68	-3.01
[IM14][(CF3)2N]	-2.19	-3.21	[IM14][1OSO3]	-3.21	-3.60
[IM14][1O2O2OSO3]	-3.16	-3.44	[IM14][4MePhSO3]	-3.29	-3.87
[IM14][1SO3]	-3.51	-3.62	[IM14][BF4]	-3.11	-3.28
[IM14][8OSO3]	-3.23	-3.57	[IM14][HSO4]	-3.29	-3.28
[IM14][CF3SO3]	-3.02	-3.30	[IM14][PF6]	-3.10	-3.56
[IM14][N(CN)2]	-3.15	-3.64	[IM14][SCN]	-3.42	-3.85
[IM14][SbF6]	-2.26	-3.11	[IM14]Cl	-3.55	-3.48
[IM14]Br	-3.43	-3.56	[IM14-2Me][BF4]	-1.37	-3.08
[IM14]I	-3.48	-3.78	[IM16][(CF3SO2)2N]	-2.24	-2.42
[IM16][(C2F5)3PF3]	-1.53	-1.45	[IM16][PF6]	-2.91	-2.96
[IM16][BF4]	-2.98	-2.68	[IM16-2Me][BF4]	-1.90	-2.49
[IM16]Cl	-2.82	-2.88	[IM17][PF6]	-2.30	-2.63
[IM17][BF4]	-2.58	-2.35	[IM18][(C2F5)3PF3]	-0.61	-0.78
[IM17]Cl	-2.53	-2.55	[IM18][8OSO3]	-1.53	-2.29
[IM18][(CF3SO2)2N]	-1.64	-1.74	[IM18][CF3SO3]	-1.09	-2.26
[IM18][BF4]	-1.59	-2.01	[IM18]Cl	-2.01	-2.20
[IM18][PF6]	-1.96	-2.29	[IM19][PF6]	-1.85	-1.93
[IM19][BF4]	-1.65	-1.65	[IM24][BF4]	-3.26	-3.02
[IM19]Cl	-1.40	-1.84	[IM24][CF3SO3]	-3.43	-3.04
[IM24][CF3COO]	-3.31	-3.34	[Mor11O2][(CF3SO2)2N]	-3.42	-3.47
[Mor11CN][(CF3SO2)2N]	-3.53	-3.50	[Mor12][4MePhSO3]	-3.81	-4.61
[Mor11O2]Cl	-3.52	-3.94	[Mor12O2][(CF3SO2)2N]	-3.69	-3.50
[Mor12O1][(CF3SO2)2N]	-3.81	-3.77	[Mor13O1][(CF3SO2)2N]	-3.77	-3.53
[Mor12OH][(CF3SO2)2N]	-3.19	-4.01	[N11-10-1Ph]Cl	-0.64	-0.07
[Mor13OH][(CF3SO2)2N]	-3.55	-3.90	[N11-12-1Ph]Cl	-0.28	0.70
[N1111][(C2F5)3PF3]	-2.03	-2.74	[N1121COO2][(C2F5)3PF3]	-2.37	-2.45
[N1114][(CF3SO2)2N]	-3.61	-3.38	[N1121COO2]Br	-3.85	-3.75
[N1121CN][(CF3SO2)2N]	-3.87	-3.47	[N1121O2]Cl	-3.59	-3.81
[N1121COO2][(CF3SO2)2N]	-3.53	-3.21	[N1122O2][(CF3SO2)2N]	-3.28	-3.35
[N1121O2][(CF3SO2)2N]	-3.80	-3.35	[N1123OH][(CF3SO2)2N]	-3.83	-3.42
[N1122O1][(CF3SO2)2N]	-3.31	-3.68	[P1i4i4i4[4MePhSO3]	-3.16	-1.93
[N1123O1][(CF3SO2)2N]	-3.54	-3.63	[Pip11CN]Cl	-4.58	-3.71
[N1124][(CF3SO2)2N]	-3.53	-3.16	[Pip12O2][(CF3SO2)2N]	-3.34	-3.07
[N4444]Br	-2.25	-1.17	[Pip12OH][(CF3SO2)2N]	-3.65	-3.66

[P4444]Br	-1.66	-0.58	[Pip13O1][(CF3SO2)2N]	-3.27	-3.29
[Pip11CN][(CF3SO2)2N]	-3.95	-3.25	[Pip13OH][(CF3SO2)2N]	-3.60	-3.71
[Pip12O1][(CF3SO2)2N]	-3.25	-3.37	[Pip14]Br	-4.03	-3.06
[Pip12O2]Br	-4.31	-3.62	[Py1-4NMe2]I	-2.89	-3.83
[Pip12OH]I	-4.58	-4.43	[Py1CN]Cl	-3.79	-3.64
[Pip13O1]Cl	-4.40	-3.75	[Py1O2]Cl	-3.32	-3.69
[Pip14][(CF3SO2)2N]	-3.41	-2.52	[Py2-4NMe2][(CF3SO2)2N]	-2.79	-2.82
[Py0]Cl	-3.77	-3.47	[Py2O1][(CF3SO2)2N]	-3.19	-3.48
[Py1CN][(CF3SO2)2N]	-3.50	-3.18	[Py2O2]Br	-4.24	-3.79
[Py1O2][(CF3SO2)2N]	-3.12	-3.22	[Py2OH]I	-4.16	-4.44
[Py2]Cl	-4.22	-3.79	[Py3O1][(CF3SO2)2N]	-3.38	-3.27
[Py2-4NMe2]Br	-2.90	-3.37	[Py3SO3H][CF3SO3]	-3.90	-3.08
[Py2O2][(CF3SO2)2N]	-3.26	-3.25	[Py4][BF4]	-3.60	-3.20
[Py2OH][(CF3SO2)2N]	-3.79	-3.67	[Py4][PF6]	-3.85	-3.48
[Py3][(CF3SO2)2N]	-3.20	-3.17	[Py4-3Me][BF4]	-3.30	-3.01
[Py3OH][(CF3SO2)2N]	-3.55	-3.71	[Py4-3Me][PF6]	-3.47	-3.29
[Py4][1OSO3]	-3.92	-3.49	[Py4-3Me-4Me][BF4]	-3.02	-2.79
[Py4][CF3SO3]	-3.66	-3.22	[Py4-3Me-5Me][BF4]	-3.26	-2.81
[Py4]Br	-3.90	-3.48	[Py4-4Me][B(CN)4]	-2.88	-3.10
[Py4-3Me][N(CN)2]	-3.46	-3.37	[Py4-4Me]Cl	-3.32	-3.20
[Py4-3Me]Cl	-3.86	-3.20	[Py4-4NMe2]Cl	-1.94	-2.68
[Py4-3Me-4Me]Cl	-3.05	-2.99	[Py5]Br	-3.15	-3.00
[Py4-3Me-5Me]Cl	-3.42	-3.01	[Py6][CF3SO3]	-2.54	-2.64
[Py4-4Me][BF4]	-2.98	-3.01	[Py6-3Me]Cl	-2.40	-2.58
[Py4-4NMe2][(CF3SO2)2N]	-1.82	-2.22	[Py6-4Me]Cl	-2.67	-2.57
[Py5][(CF3SO2)2N]	-2.85	-2.44	[Py6-4NMe2]Cl	-0.94	-2.05
[Py6][(CF3SO2)2N]	-2.87	-2.36	[Py8-3Me]Cl	-1.47	-1.87
[Py6]Cl	-2.80	-2.82	[Py8-4Me]Cl	-1.63	-1.87
[Py6-4Me][BF4]	-2.17	-2.37	[Pyr11COO2][(CF3SO2)2N]	-3.59	-3.13
[Py6-4NMe2][(CF3SO2)2N]	-1.02	-1.59	[Pyr11O2][(CF3SO2)2N]	-3.26	-3.38
[Py8]Cl	-1.27	-2.15	[Pyr12O1[(CF3SO2)2N]	-3.30	-3.64
[Py8-4Me][BF4]	-1.49	-1.67	[Pyr12O2][(CF3SO2)2N]	-3.20	-3.37
[Pyr11COO2][(C2F5)3PF3]	-2.91	-2.17	[Pyr13O1][(CF3SO2)2N]	-3.40	-3.63
[Pyr11COO2]Br	-3.84	-3.68	[Pyr14][(C2F5)3PF3]	-2.41	-1.55
[Pyr11O2]Cl	-3.05	-3.84	[Pyr14][BF4]	-2.90	-2.78
[Pyr12O1][(C2F5)3PF3]	-2.16	-2.68	[Pyr14]Br	-3.77	-3.06
[Pyr12OH][(CF3SO2)2N]	-3.72	-3.91	[Pyr16]Cl	-2.93	-2.95

[Pyr13OH][(CF3SO2)2N]	-3.60	-3.99	[Pyr18]Cl	-2.59	-2.24
[Pyr14][(CF3SO2)2N]	-3.01	-2.52	[Quin8][BF4]	-0.14	-0.79
[Pyr14][N(CN)2]	-4.23	-3.14	[S122][(CF3SO2)2N]	-3.48	-3.41
[Pyr16][(CF3SO2)2N]	-2.56	-2.49	[Xn1111][CF3SO3]	-2.96	-3.19
[Pyr18][BF4]	-1.82	-2.04	[Py6] [PF6]	-2.51	-2.90
[Pyr66][BF4]	-1.23	-1.00			
[Quin8]Br	0.03	-1.07			
[S222][(CF3SO2)2N]	-3.40	-3.31			
[Pip11O2][(CF3SO2)2N]	-3.41	-3.08			

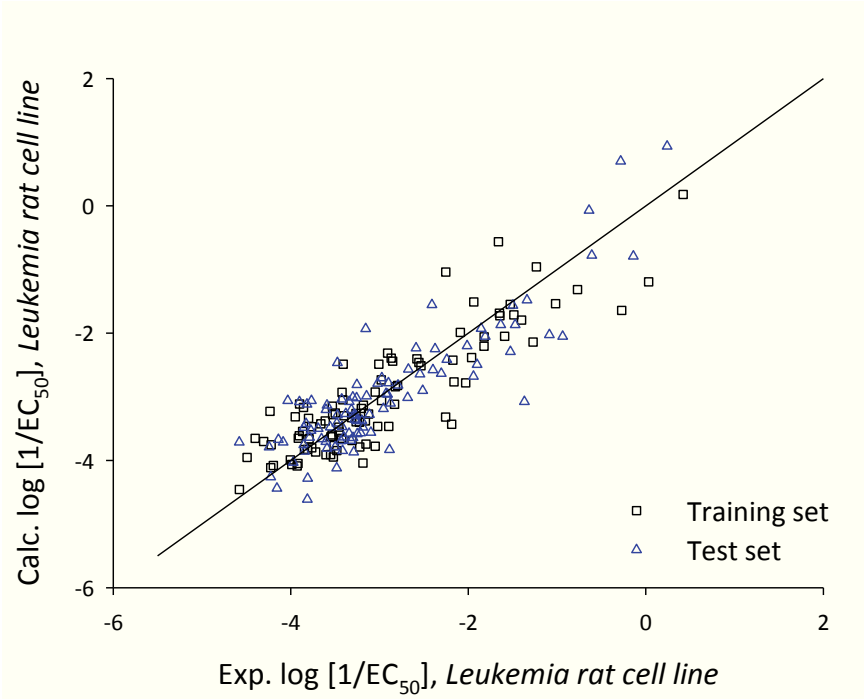

Figure 6.3. The relationship of experimental and predicted log cytotoxicity values (1/toxicity of ILs towards the IPC-81 *rat cell line*) of the training set (square) and the test set (triangle) according to Eq. (6.10)

6.3.3. Prediction of IL toxicity towards the marine bacterium *Vibrio fischeri*

The *Vibrio fischeri* cytotoxicity was also modeled using the calculated LFER descriptors. Here we obtained 105 measured values from the literatures[68, 112, 130, 138, 139, 152] and the UFT Merck Ionic Liquids Database.[69] We could identify two big outliers *i.e.* [IM1–18]Cl and [IM1–16]Cl.

Similar to the model described above for the IPC-81 cytotoxicity, we randomly divided the available IL data into a training set of 69 and a test set of 34 IL structures. Firstly, we performed a multiple linear regression using the training set with all descriptors [Eq. (6.1)] including charge density terms

like in Eq. (6.6). The derived system parameters are the following ones:

Log $(1/EC_{50})$ [µmol/L], *Vibrio fischeri* = –8.741(1.671) + 0.243 (0.505)E_c + 0.497 (0.834)S_c – 0.341(0.401)A_c – 3.139(1.361)B_c + 3.654(0.442)V_c + 1.075(0.520)$1/V_c$ + 1.095(0.564)E_a – 1.576 (0.779)S_a – 0.984(0.637)A_a + 0.371 (0.189)B_a + 0.797(0.340)V_a + 0.005 (0.158) $(-1/V_a)$ Eq. (6.11)

R^2=0.767, SD=0.532 log unit, F=15.4, N=69

The result shows that all descriptors including charge density terms can be used to predict the cytotoxicity (*Vibrio fischeri*) with a R^2 of 0.767 and a SD of 0.532 log units.

Secondly, to investigate which molecular interaction potential is the most contributing factor to the cytotoxicity, we rebuilt the prediction model by step-by-step adding the various descriptors to the model. As expected, the V descriptor has the most contributing correlation with the measured cytotoxicity of the training set [Table 6.3, Eq. (6.12)] with a R^2 of 0.42 and a SD of 0.774. A combination of V with the B descriptor of cations and anions can predict the cytotoxicity values with a SD of 0.542 log units and a R^2 of 0.724 [Table 6.3, Eq. (6.13)]. Adding the charge density terms ($1/V_c$ and $-1/V_a$) to Eq. (6.13) contributes only slightly to decrease the SD value to 0.530 [Table 3, Eq. (6.14)] and increases the statistical coefficient (R^2) to 0.744. The remaining terms – E, S, and A – are not statistically important for the prediction accuracy. Thus, we obtain a linear model composed of V, B, E, and number of charge/V of cations and anions to predict the toxicity of ILs towards marine bacteria. To check the robustness and predictivity of the model described by Eq. (6.14) we used the test set of 34 IL structures. The predicted values of the test set according to Eq. (6.14) can be correlated with measured values with a R^2 of 0.724 and a SD of 0.527 log units, which means lower SD values than that obtained for the training set (Figure 6.4). Thus, the developed model can be also accepted as a sound prediction tool like Eq. (6.14) above. The measured and predicted cytotoxicity values according to Eq. (6.14) are given in Table 6.5.

Eq. (6.14) shows that the V term is the most contributing descriptor to cytotoxicity of ILs. The high hydrogen bonding basicity (B) is the next contributing factor and the charge density term is third important. Increasing the B_c and $-1/V_a$, values the toxicity values decrease, while B_a and $1/V_c$ show the opposite trend.

Table 6.5. The measured (Exp.) and calculated (Calc.) 1/EC50 values of training set and test set of ionic liquids toward *Vibrio fishceri*

Training set	Exp.	Calc.
[IM][1COO] [138]	-3.61	-3.33
[IM][Cap] [138]	-2.29	-2.63
[IM][CF3SO3] [1386]	-3.81	-3.42
[IM01][1COO] [138]	-4.07	-4.00
[IM01][CF3COO] [138]	-3.57	-3.91
[IM01][CF3SO3] [138]	-4.35	-4.10
[IM04][1COO] [138]	-3.32	-3.09
[IM04][Cap] [138]	-2.00	-2.40
[IM04][CF3SO3] [138]	-2.77	-3.18
[IM04][HCOO] [138]	-3.19	-3.26
[IM1-10]Cl	0.23	-0.36
[IM11CN][(CF3SO2)2N]	-3.81	-3.61
[IM12][(2-OPhO)2B]	-2.96	-3.48
[IM12][(C2F5)2PO2]	-3.05	-3.55
[IM12][B(CN)4]	-3.56	-4.07
[IM12][CF3COO]	-4.28	-3.98
[IM12]Cl	-4.34	-4.25
[IM12O1][(CF3SO2)2N]	-2.84	-3.53
[IM12O2][(CF3SO2)2N]	-2.96	-2.86
[IM12OH][(CF3SO2)2N]	-4.08	-4.02
[IM13][(CF3SO2)2N]	-2.77	-3.30
[IM13][BF4]	-3.94	-4.04
[IM13OH][(CF3SO2)2N]	-3.89	-3.05
[IM14][(CF3)2N]	-3.46	-3.39
[IM14][4MePhSO3]	-3.53	-2.73
[IM14][8OSO3]	-1.82	-2.46
[IM14][CF3SO3]	-3.60	-3.31
[IM14][N(CN)2] [113]	-3.67	-3.40
[IM14]Br	-3.07	-3.42
[IM14]Cl	-3.47	-3.40
[IM15][BF4]	-3.14	-3.12
[IM16][(2-SO2PhCO)N]	-2.67	-1.91
[IM16][(CF3SO2)2N]	-2.05	-1.89
[IM16][BF4]	-3.18	-2.63
[IM16]Br [113]	-1.42	-2.45
[IM16]Cl	-2.93	-2.43

(*Continuous.*)	Exp.	Calc.
[Py4]Br [113]	-3.40	-3.52
[Py4]Cl	-3.18	-3.49
[Py4-3Me]Br [113]	-2.75	-3.13
[Py4-3Me-5Me][N(CN)2] [113]	-2.38	-2.67
[Py4-4Me][BF4]	-3.02	-3.30
[Py4-4NMe2][(CF3SO2)2N] [7]	-1.85	-1.81
[Py6-4Me]Cl [68]	-1.44	-2.09
[Py6-4Me]Br [130]	-2.06	-2.12
[Py8]Cl	-1.69	-1.49
[Pyr11COO2][(CF3SO2)2N]	-3.23	-2.66
[Pyr13OH][(CF3SO2)2N]	-3.91	-3.75
[Pyr14][(C2F5)3PF3]	-1.70	-2.24
[Pyr14]Cl	-4.65	-3.24
[Pyr16][(CF3SO2)2N]	-2.40	-1.74
[S222][(CF3SO2)2N]	-3.26	-3.48
[TMG][1COO] [139]	-3.17	-3.97
[TMG][CF3SO3] [139]	-3.52	-4.06

Test set	Exp.	Calc.
[IM][CF3COO] [139]	-4.07	-3.23
[IM01][Cap] [139]	-2.13	-3.31
[IM01][HCOO] [139]	-2.83	-4.17
[IM04][CF3COO] [139]	-3.28	-3.00
[IM1-10][BF4]	0.18	-0.57
[IM11O2][(CF3SO2)2N]	-3.00	-3.23
[IM12][2OSO3]	-4.28	-4.02
[IM12][SCN]	-4.15	-4.40
[IM12O1]Cl	-4.18	-4.07
[IM12OH]I	-3.89	-4.60
[IM13O1][(CF3SO2)2N]	-3.24	-3.35
[IM14][(CF3SO2)2N]	-2.47	-2.86
[IM14][BF4]	-3.55	-3.60
[IM14][PF6]	-3.51	-3.50
[IM14]I	-3.59	-3.44
[IM16][(C2F5)3PF3	-2.65	-1.42
[IM16][PF6] [152]	-2.17	-2.53
[IM16-2Me]Cl [138]	-1.74	-2.15

[IM17][BF4]	-2.44	-2.14	[IM18][BF4]	-1.40	-1.59
[IM18][(CF3SO2)2N]	-0.83	-0.85	[IM18]Cl	-1.05	-1.39
[IM18][PF6] [115, 152]	-0.82	-1.49	[IM26][BF4]	-2.15	-2.12
[IM18]Br	-0.63	-1.42	[Melamine][CF3SO3]	-2.45	-2.25
[IM19][BF4]	-0.72	-1.09	[N0,1,1,2OH][1COO]	-4.29	-3.80
[IM24][BF4]	-2.80	-3.13	[N1122O1][(CF3SO2)2N]	-3.35	-3.37
[Melamine][1COO] [139]	-2.39	-2.17	[Pip14][(CF3SO2)2N]	-2.57	-2.37
[Melamine][CF3COO] [139]	-2.24	-2.07	[Py4][N(CN)2] [113]	-3.31	-3.50
[Mor11O2][(CF3SO2)2N]	-3.38	-3.12	[Py4-3Me][N(CN)2] [113]	-2.66	-3.10
[Mor14][(CF3SO2)2N]	-2.48	-2.87	[Py4-3Me-5Me]Br[113]	-2.69	-2.70
[N1124][(CF3SO2)2N]	-3.21	-2.84	[Py4-4NMe2]Cl	-2.55	-2.35
[N1121COO2][(CF3SO2)2N]	-3.32	-2.81	[Py6-4NMe2][(CF3SO2)2N]	-1.38	-0.81
[N1124][(CF3SO2)2N]	-3.23	-2.84	[Pyr12O2][(CF3SO2)2N]	-2.97	-2.95
[N2226]Br	-2.46	-1.61	[Pyr14][(CF3SO2)2N]	-2.55	-2.70
[Pip14]Br	-4.32	-2.93	[Pyr16]Cl	-3.00	-2.28
[Py3OH][(CF3SO2)2N]	-4.01	-3.74	[TMG][Cap] [139]	-2.29	-3.28
			Outliers		
			[IM1–18]Cl	-1.26	-3.16
			[IM1–16]Cl	-0.23	-2.13

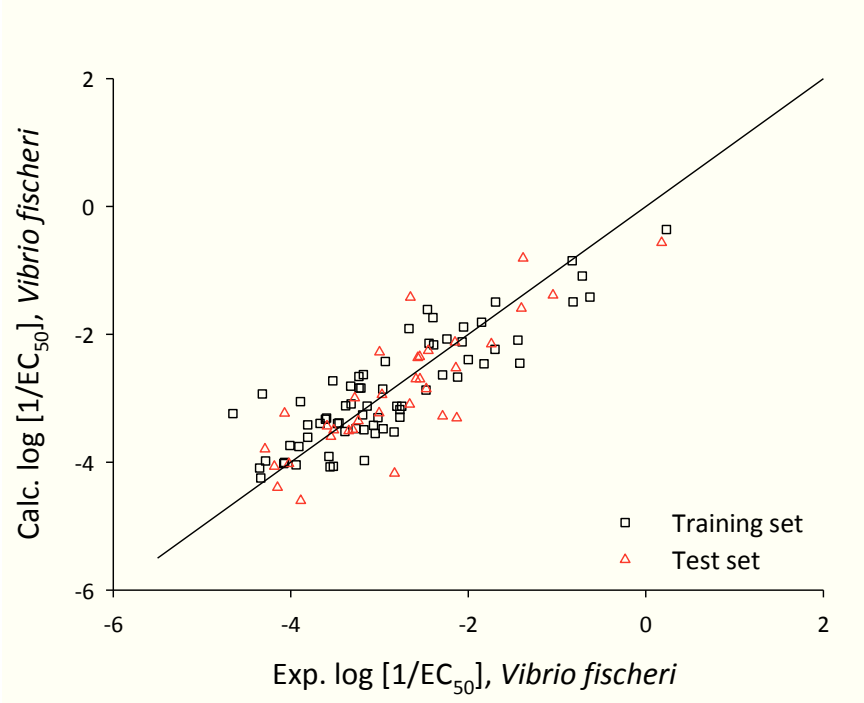

Figure 6.4. The relationship of experimental and predicted log cytotoxicity values ($1/EC_{50}$ of ionic liquids toward *Vibrio ficheri*) of training set (square) and test set (triangle) according to Eq. (6.14)

6. 3.4. Prediction of IL toxicity towards the limnic green alga *Scenedesmus vacuolatus*

The experimental toxicity data available for *Scenedesmus vacuolatus* was analyzed in a similar manner as described above. But here the data set was not divided into a training set and a test set because the number of data (44) is not high enough for being separated. Here we found out the four outliers i.e. [IM1–14]Cl, [N4444][F4SO3], [Py6][(CF2SO3)2N], and [Pyr16][(CF3SO2)2N]. After excluding the outliers, we performed a multiple linear regression analysis using all descriptors and we estimated the following system parameters:

$$\text{Log } (1/EC_{50}) \text{ [µmol/L], } \textit{Scenedesmus} = -34.965\ (4.644) - 0.326\ (0.543)E_c - 0.857(1.079)S_c + 0.459(0.588)A_c - 2.552(1.883)B_c + 13.764(1.875)V_c + 15.696(3.508)1/V_a - 0.374(0.639)E_a + 1.126(1.353)S_a - 0.593(1.382)A_a - 0.333(0.834)B_a + 1.801(0.816)V_a - 0.782(0.553)(-1/V_a) \quad \text{Eq. (6.15)}$$

$$R^2=0.879,\ SD=0.654 \text{ log unit},\ F=18.7,\ N=44$$

The result shows that all descriptors including charge density terms can be used to predict the cytotoxicity of ILs towards *Scenedesmus vacuolatus* with a R^2 of 0.879 and a SD of 0.654 log units.
Next, we analyzed the most contributing molecular interaction potentials of the IL ions to cytotoxicity. The results show that V terms – not surprisingly – highly correlate to the measured cytotoxicity of ILs towards *Scenedesmus vacuolatus* with a R^2 of 0.605 and a SD of 1.026 log units [Table 6.3, Eq. (6.16)]. The charge density terms helped to enhance the accuracy of the model by reducing the SD to 0.728 log units while R^2 increased to 0.811 [Table 6.3, Eq. (6.17)]. By adding hydrogen bonding donor and acceptor terms to the model the prediction accuracy could further be improved to a SD of 0.650 log units and R^2 could be increased to 0.857 [Table 6.3, Eq. (6.18)]. The additional S term enhanced only slightly the predictivity yielding a R^2 of 0.868 and a SD of 0.643 log units [Table 6.3, Eq. (6.19)]. The Eq. (6.19) shows comparable accuracy to Eq. (6.15) but consists of less parameter than Eq. (6.15) using all parameters. The predicted values according to Eq. (6.19) are correlated to the measured values of toxicity in Figure 6.5 and results are tabulated in Table 6.6.
As shown in Eq. (6.19) with increasing the V terms the toxicity increases, while an increase in the B terms reduces the toxicity. Increasing the S value of cations and the charge density of anions toxicity decreases the toxicity while the S descriptor of the anion and the charge density of anions show an opposite trend.

Table 6.6. The measured (Exp.) and calculated (Calc.) $1/EC_{50}$ values of training set and test set of ionic liquids toward *Scenedesmus vacuolatus*

Ionic liquids	Exp.	Calc.	Ionic liquids	Exp.	Calc.
[IM1-10]Cl	3.57	4.34	[IM16][PF6]	-0.34	-0.6
[IM1-14]Cl		10.9	[IM16](CF3SO2)2N]	-0.04	-0.2
[IM11CN]Cl	-4.01	-2.97	[IM16][(C2F5)3PF3]	0.37	0.47
[IM11CN][(CF3SO2)2N]	-2.07	-2.22	[IM18]Cl	2.76	1.53
[IM11O2]Cl	-2.8	-2.99	[IM18][BF4]	2.24	1.99
[IM11O2](CF3SO2)2N]	-1.93	-2.24	[Mor11O2][(CF3SO2)2N]	-2.34	-2.23
[IM12]Cl	-2.78	-2.59	[Mor14][(CF3SO2)2N]	-2	-1.83
[IM12][(2-OPhO)2B]	-1.42	-1.04	[N1121COO2]Br	-2.63	-2.82
[IM12][Cl4SO3]	-2.98	-2.4	[N1121COO2][(CF3SO2)2N]	-2.18	-1.79
[IM12][F4SO3]	-1.59	-2.62	[N1124][(CF3SO2)2N]	-1.79	-1.75
[IM12O1]Cl	-3.26	-3.43	[N4444][F4SO3]		7.72
[IM12O1][(CF3SO2)2N]	-1.98	-2.68	[Pip13O1][(CF3SO2)2N]	-1.87	-1.33
[IM12O2]Br	-2.52	-2.88	[Pip14]Br	-3.28	-2.03
[IM12O2][(CF3SO2)2N]	-1.88	-1.84	[Pip14][(CF3SO2)2N]	-2.09	-1
[IM12OH][(CF3SO2)2N]	-2.15	-2.87	[Py4]Cl	-2.59	-2.71
[IM13O1][(CF3SO2)2N]	-2.06	-2.52	[Py4-4NMe2]Cl	0.27	-0.67
[IM13OH][(CF3SO2)2N]	-1.98	-2.09	[Py4-4NMe2][(CF3SO2)2N]	0.43	0.08
[IM14]Cl	-2.25	-2.55	[Py6][(CF3SO2)2N]		-0.46
[IM14][BF4]	-2.13	-2.09	[Pyr11COO2]Br	-3.16	-2.53
[IM14][(CF3SO2)2N]	-1.8	-1.8	[Pyr12O1][(CF3SO2)2N]	-2.03	-2.53
[IM14][Cl4SO3]	-2.39	-2.35	[Pyr14]Cl	-3.39	-2.32
[IM14][(CF3)2N]	-2.83	-2.58	[Pyr14][(CF3SO2)2N]	-2.53	-1.57
[IM14][8OSO3]	-1.72	-1.73	[Pyr16][(CF3SO2)2N]		0.35
[IM16]Cl	-0.08	-0.95	[S222][(CF3SO2)2N]	-1.97	-2.29

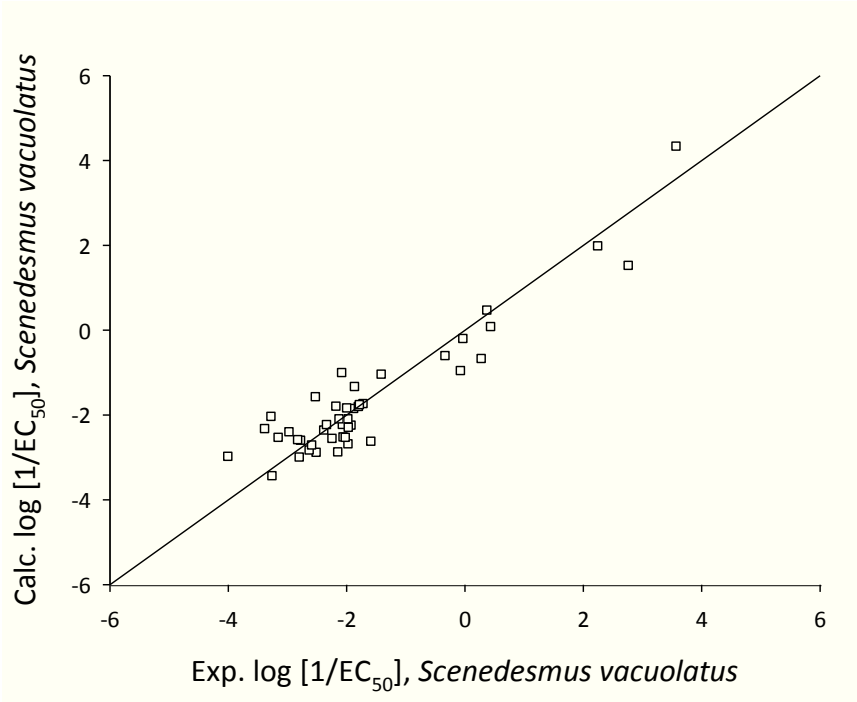

Figure 6.5. The relationship of experimental and predicted log ($1/EC_{50}$ to *Scenedesmus vacuolatus*) values of ionic liquids according to Eq. (6.19)

On the whole, it can be stated that the ion volume is the most important factor to predict cationic hydrophobicity and cytotoxicity of ILs. It is positively contributing to hydrophobicity and hence to increase the cytotoxicity while in general the B terms are negatively contributing to hydrophobicity and thus to reduce the cytotoxicity of an IL. This may be explained by the fact that biomembranes show considerable hydrogen bonding basicity while they posses less hydrogen bonding acidity than water as reported by Gunatilleka and Poole.[153] Similarly, the solute size and hydrogen bonding basicity of ions have unsurprisingly the same effect to physical and chemical properties i.e. critical micelle concentration, water solubility and log P values of ILs.[59] The increase of hydrophobic effect due to increasing the volume of solute contributes to weigh the concentration of ILs toward octanol phase than water phase, while to decrease water solubility and critical micelle concentration.[59] On the other hand the hydrogen bonding basicity terms (B) show opposite trends than the volume as an increase of the B increases water solubility and the octanol-water partitioning coefficient decreases. Especially an increase in the B term increases the activity coefficients of anions in water. The hydrogen bonding acidity term is of minor importance to predict the cationic hydrophobicity. Also interactions of the excess molar refraction (E) and the dipolarity/polarizability (S) are not important or only weakly contributing to predict the toxicity of ILs. The facts indicate that the lone-pair electron and dipolar-type are not large between ILs and biomemrane of *Leukaemia rat cell line*, *Vibrio fischeri*, *Scenedesmus vacuolatus*.

In our prediction study, several outliers are observed. The strong outliers are typically a type of cations with large volume. It might be explained as cutoff effects - as previous researchers mentioned.[112, 154,155] The one of cutoff effects is due to low-solubility of strong hydrophobic cations; therefore nominal concentration is deviated from real test concentration.[154] And uptake of the large volume at the cutoff threshold above to membrane of the organism is slow downed due to their steric effect[155] or even started to decrease with increasing molecular size.[156,157] Thus in order to improve the predictability of prediction model including the large molecules, it is implicated to add the membrane partitioning effect into the model. Moreover it was observed two other outliers i.e. [(CF3)2N]-, [SbF6]- in prediction study towards *Leukaemia rat cell line*. The anions are rapidly hydrolyzed in water and produce very reactive fluoride ion; therefore its toxic effect increase.[117, 158] In fact, as comparing the measured and predicted values, we can see the predicted values are lowered then measured ones. Additionally it should be noticed that difference of toxicity test and specific toxic mode e.g. narcosis, inhibition of distinct enzyme shouldn't be ignored to understand the outliers.

6.4. Conclusion

I could demonstrate that using descriptors calculated by well-established computational methods *i.e*. COSMO–RS, COSMO, and OBPROP using the Eqs. (2.5)~(2.9) derived based on 470 neutral molecules can be used to develop models that allow for the prediction of IL toxicity in various toxicologically and ecotoxicologically relevant test systems. Firstly, we were able to predict IL cation hydrophobicity using the three descriptors – A, B, and V. Here the V is the key descriptor, B and A are second and third important. The developed prediction models would be helpful to investigate various environmental behaviors of ILs like sorption, water solubility and partitioning coefficients of ions in a much easier, less resource-consuming and faster way. We could also show that the V of IL cations and anions are also the most important descriptors to predict the cytotoxicity values of ILs in all three testing species investigated, i.e. *IPC-81 cells*, *Vibrio fischeri*, and *Scenedesmus vacuolatus*. The B terms of cations and anions combined with the V terms remarkably enhanced the predictability of toxicity in two cases i.e. the *IPC-81 cell line* and the marine bacterium *Vibrio fischeri*. The second contributing factor of toxicity of ILs towards *Scenedesmus vacuolatus* are the charge density terms. In the case of the algae the B terms seem to be of third importance. The excess molar refraction (E) and the dipolarity/polarizability (S) show only a slight contribution to enhance the predictive accuracy of the model in the case of the IPC-81 cells and *Scenedesmus vacuolatus,* respectively.

Although the accuracy of the established prediction models is rather lower than previous prediction studies towards *Vibrio fischeri* by Luis et al.[138, 139] and towards *Leukaemia rat cell line* by Torralla et al.[141,142] and Fetami & Izadiyan,[143] our prediction models can be easily used for anyone to calculate the cytotoxicity values only by inserting the calculated descriptors of ions given in Table 2.2 for cations & 2.3 for anions to the established models i.e. Eqs. (6.10, 6.14, 6.19). Furthermore the calculated descriptors we used in this study can be also used to predict several physical, chemical, and environmental properties of ILs.[59] The opportunity to understand and predict physicochemical properties and the toxicological behavior of ILs with same molecular interaction potentials may be important contribution to fulfill the 4th principle of Green Chemistry “Chemical products should be designed to preserve efficiency of function while reducing toxicity”.

7. Conclusion and outlook

In this study, the molecular interaction potentials (MIPs) of ionic liquid (IL) ions were experimentally (HPLC measurement) and computationally (COSMO-calculations) estimated. The MIPs are E (excess molar refraction), S (dipolarity/polarizability), A (hydrogen bonding acidity), B (hydrogen bonding basicity) and V (McGowan volume) which are forming the Abraham equation [Eq.(2.1)]. And based on the measured and computed MIPs of ions, the physical, chemical and biological properties of ionic liquids (ILs) were predicted.

For the theoretical model, the Abraham equation based on neutral compounds [Eq. (2.1)] was extended to z_cZ_c term to address the charge interaction of ions based on our theoretical background –the z_cZ_c descriptor +1 for monovalent cation. The HPLC methods were demonstrated to be very useful for the experimental determination of IL ions i.e. 30 cations (Chapter 3) and 20 anions (Chapter 4). The HPLC methods are very useful to avoid the ion-pairing effect of salts and to obtain the retention characteristics (log k_o) as given property derived from the molecular interactions between a molecule and HPLC system. However when using the HPLC systems, it should be careful to set the mobile phase conditions and stationary phase (column) for determination of the log k_o of calibration compounds (for determination of system parameters) and those of target compounds at the same time in the same condition, because the HPLC methods might be limited to some of cases e.g. small molecules or large molecules. Indeed in Chapter 3 it was shown that the large molecules with molecular weight > 290 g/mol e.g. $[N1,1,10,Bz]^+$ and $[N1,1,12,Bz]^+$ were limited to measure the retention characteristics in one specific mobile phase used (RP-select B –Methanol 65%) due to long their retention time.

From the obtained MIPs descriptors of 30 cations, it was interpreted the quantification of MIPs of ions according to their structures. However in Chapter 4, it was reported the zZ term should be separated to z_cZ_c for cations and z_aZ_a for anions because the single zZ term is not suited for ionic interactions of cation and anion at the same time. Moreover if fixed the ionic term as ± 1, the difference between the fixed charge value (± 1) and real charge effect of ions were partially expressed to other descriptors i.e. S, A, B. Nevertheless the determined MIPs descriptors in the condition of fixed charge value can be used to predict the retention characteristics in multi-stationary phases (Chapter 4). However the determined descriptors are not able to be used with those determined by Abraham and co-workers based on different theoretical background .[31-34]

Furthermore based on the measured (in Chapter 3) and calculated MIPs descriptors (in Chapter 2), we could set out the evolutionary models to predict the octanol-water partitioning coefficient (Log P), the water solubility, and the critical micelle concentration (CMC) of ILs as well as the anionic activity coefficient and anionic hydrophobicity in pure water and octanol-water respectively. With both, calculated or experimental LFER descriptors of IL ions, the physicochemical parameters were predicted with an error bar of 0.182 to 0.217 for the octanol-water partitioning coefficient and 0.131 to 0.166 logarithmic units for the water solubility. Since experimentally determined solute parameters of anions are not enough as of now, the CMC, anionic activity coefficient at the IL saturated condition in water, and hydrophobicity at the IL equilibrated condition in octanol-water could be predicted using only the calculated descriptors with an R^2 of at least 0.99 as well as error bars below 0.168 logarithmic units.

In Chapter 6, using the calculated MIPs descriptors of cations and anions, we could do modeling for prediction of environmental properties i.e. hydrophobicity of IL cation and cytotoxicities of ILs. And the results showed that the combination of three solute descriptors of cation – A_c, B_c, and V_c – allows us to predict the log k_o in the R^2 of 0.985 and SD of 0.150 log unit. And we could predict the cytotoxicity values of ILs towards *Leukaemia rat cell line* (R^2 of 0.776, SD of 0.500 log units), *Vibrio fishceri* (R^2 of 0.744, SD of 0.530 log units), and *Scenedesmus vacuolatus* (R^2 of 0.868, SD of 0.643 log units). And robustness and predictivity of the two models for *Leukaemia rat cell line* and *Vibrio fishceri* were checked by comparing the calculated SD values of the test set with the training set. The comparison results indicate that the models can be used to predict the cytotoxicity values because the SD values of training set and test set are almost similar.

From the sensitivity analysis of solute descriptors by ordering by importance their relevance to several physical chemical properties, we clarified that the V term is the most important factor in prediction studies. The contributions of the volume are summarized:

- The cationic volume is closely related to the water solubility of ILs. With an increasing cationic volume, the water solubility decreased.
- The cationic volume is proportional to the octanol-water partitioning coefficient value of ILs.
- The anionic volume is a contributing factor to improve the hydrophobicity of anion in octanol-water system.

- The volumes of anion and cation are very important to predict the critical micelle concentrations. They are - as negatively effect - if increasing their volume, the critical micelle concentrations of ILs decreases.
- The volumes of cation and anion mostly contribute to the cytotoxicity of ILs. As increasing the volume of cation and anion the cytotoxicity values decreases.

The hydrogen bonding basicity (B) term is in general secondly important to predict the properties of ILs. The roles of the B descriptor can be summarized:

- The B term of anion is a negative effect to an increase of the hydrophobicity of anion at the IL-equilibrated condition in octanol-water system. Therefore, as increasing the B values of anion, the hydrophobicity of anion decreases.
- The B term of cation is a cofactor to improve the predictability of the octanol-water partitioning coefficient of ILs. As increasing the B term, the partitioning coefficient values of ILs decreases.
- The B of anion has a good agreement of 0.775 to predict anionic activity coefficient at the IL saturated condition in water. The increase of the B of anion leads to a increase of anionic activity coefficient in water.
- The increase of the B of cation leads to increase of water solubility in case of using the calculated solute descriptors. While the case of using measured descriptors, the B of cation is not statistically important.
- The increase of the B of anion leads to a increase of the critical micelle concentration of ILs in water.
- The B terms of cation and anion lead to a decrease of toxicity of ILs toward *Leukaemia rat cell line* and *Scenedesmus vacuolatus*.
- The B of cation leads to low toxicity, while the B of anion leads to high toxicity of ILs toward *Vibrio fischeri*.

And the rest terms i.e. E, S and A terms of cation and anion are slightly important to predict the physical, chemical and biological properties of ILs.

- The A descriptor is mainly contributing to a decrease of the octanol-water partitioning coefficient of ILs and cationic hydrophobicity, while to an increase of the water solubility of ILs. However the A term is not important in the toxicity prediction study.

- The E and S terms are slightly important to predicting cytotoxicity values of ILs towards rat leukaemia cell line IPC-81 and *Scenedesmus vacuolatus* respectively. Surprisingly the E and S descriptors have different contributions each other to all physical and chemical properties of ILs. For example (in case of using the calculated values) as increasing the E, the anionic hydrophobicity and log P values decrease, while water solubility increases, on the other hand as increasing the S values the anionic hydrophobicity and log P values increase, while the water solubility decrease. When using the measured descriptors, the E term leads to an increase of log P values and a decrease of water solubility while the S term leads to a decrease of water solubility and an increase of log P values of ILs.

The sensitivity analysis provides us to understand the main driving forces of IL ion to determine their physical, chemical and environmental properties. Therefore using main driving forces we could simplify the prediction models, especially cytotoxicity prediction studies in Chapter 6. And we expect that the main driving force to several properties can be usefully considered to design IL structure with low toxic and appropriate properties.

The further interesting studies are considered.

The measured and calculated descriptors will be able to use additionally for better understanding the molecular interactions of IL ions in other environments, and allow us to predict the other properties of ILs. We are encouraging the further prediction work for:

- retention characteristics of cation and anion in Ion-Chromatography because it has never studied based on the MIPs of ions.
- sorption properties of ILs to soil and to bacteria which is the one of the environmental behaviors of ILs. This is very important to clarify the sorption mechanisms between IL ions and environmental materials e.g. soil and bacteria. The outcome can be used to remove and recover effectively them by sorption processes.
- values of octanol-water partitioning coefficient of multi-ions e.g. two different ILs in a system. This study will provide to understand ionic complex in octanol-water system. And the results as fundamental knowledge in science are expected to be used for further investigation of the environmental effects and chemical processes of multi-salts.

8. References

1 Chemical Abstract Service. www.cas.org., **2011**

2 D. J. Weder, Umwelt: Bedrohung und Bewahrung Bundeszentrale für politische Bildung, Bonn, **2003**.

3 J. S. Dhrubo, *Pharma Times*, **2006**, *38 (7)*, 35-39.

4 P. T. Anastas, J. C. Warner, Green Chemistry Theory and Practice Oxford University Press: New York, **1998**.

5 P. T. Anastas, J. B. Zimmerman, *Environ*. *Sci*. *Technol*., **2003**, *37(5)*, 94-101.

6 S. Tang, R. Bourne, R. Amith, M. Poliakoff, *Green Chem*., **2008**, *10*, 268-269.

7 P. Wassersscheid, W. Keim, *Angew*. *Chem*. *Int*. *Ed*., **2000**, *39*, 3772-3789.

8 K. E. Gutowski, G. A. Broker, H. D. Willauer, J. G. Huddleston, R. P. Swatloski, J. D. Holbrey, R. D. Rogers, *J*. *Am*. *Chem*. *Soc*., **2003**, *125*, 6632-6633.

9 M. C. Buzzeo, R. G. Evans, R. G. Compton, *ChemPhysChem*, **2004**, *5(8)*, 1106-1120.

10 T. O. Kollie, C. F. Poole, *Chromatographia*, **1992**, *33*, 551-559.

11 S. K. Poole, C. F. Poole, *Analyst*, **1995**, *120*, 289-294.

12 J. L. Anderson, J. Ding, T. Welton, D. W. Armstrong, *J*. *Am*. *Chem*. *Soc*., **2002**, *124*, 14247-14254.

13 L. Crowhurst, P. R. Mawdsley, J. M. Perez-Arlandis, P. A. Salter, T. Welton, *Phys*. *Chem*. *Chem*. *Phys*., **2003**, *5*, 2790-2794.

14 J.-M., Lee, J. M. Prausnitz, *Chem*. *Phys*. *Lett*., **2010**, *492*, 55-59.

15 J.-M., Lee, S. Ruckes, J. M. Prausnitz, *J*. *Phys*. *Chem*. *B*, **2008**, *112*, 1473-1476.

16 N. D. Khupse, A. Kumar, *J*. *Phys*. *Chem*. *B*, **2010**, *114*, 376-381.

17 C. Reichardt, *Green Chem*., **2005**, *7*, 339-351.

18 H. Weingärtner, *Angew*. *Chem*. *Int*. *Ed*. *Engl*., **2008**, *47*, 654-670.

19 C. Jungnickel, J. Łuczak, J. Ranke, J. F. Fernandez, A. Müller, J. Thöming, *Colloids Surf*. *A*, **2008**, *316*, 278-284.

20 A. Fredenslund, R. L. Jones, T. H. Prausnitz, *AIChE J*., **1975**, *21(6)*, 1086–1099.

21 Goss, K.-U., R. P. Schwarzenhach, *Environ*. *Sci*. *Technol*., **2001**, *35 (1)*, 1–9.

22 B. Mennucci, J. Tomasi, *J*. *Chem*. *Phys*., **1997**, *106*, 5151–5158.

23 M. H. Abraham, A. Ibrahim, A.M. Zissimos, *J*. *Chromatogr*. *A*, **2004**, 29–47.

24 M. H. Abraham, J. M. Al-Hussaini, *J*. *Environ*. *Monit*., **2005**, *7*, 295–301.

25 M. H. Abraham, P. L. Grellier, R. A. McGill, *J*. *Chem*. *Soc*. *Perkin Trans*. *2*, **1987**, 797–803.

26 M. H. Abraham, G. S. Whiting, *J. Chromatogr.*, **1991**, *587*, 229–236.

27 M .H. Abraham, *J. Phys. Org. Chem.*, **1993**, *6*, 660–684.

28 M. H. Abraham, H. S. Chadha, G. S. Whiting, R. C. Mitchell, *J. Pharm. Sci.*, **1994**, *83*, 1085–1100.

29 M. H. Abraham, Y. H. Zhao, *J. Org. Chem.*, **2004**, *69*, 4677-4685.

30 Y. Marcus, *Pure Appl. Chem.*, **1986**, *58*, 1721-1736.

31 M. H. Abraham, W. E. Acree Jr., *J. Org. Chem.*, **2010**, *75 (4)*, 1006–1015.

32 M. H. Abraham, W. E. Acree Jr., *J. Org. Chem.*, **2010**, *75 (9)*, 3021–3026.

33 M. H. Abraham, W. E. Acree Jr., *New J. Chem.*, **2010**, *34 (10)*, 2298–2305.

34 M. H. Abraham, W. E. Acree Jr., *Phys. Chem. Chem. Phys.*, **2010**, *12 (40)*, 13182–13188.

35 S. H. Lee, S. B. Lee, *J. Chem. Technol. Biotechnol.*, **2009**, *84*, 202-207.

36 H. C. Tülp, K. U. Goss, R. P. Schwarzenbach, K. Fenner, *Environ. Sci. Technol.*, **2008**, *42*, 2034-2040.

37 P. Stepnowski, W. Mrozik, *J. Sep. Sci.*, **2005**, *28*, 149-154.

38 J. Ranke, A. Müller, U. Bottin-Weber, F. Stock, S. Stolte, J. Arning, R. Störmann, B. Jastorff, *Ecotoxicol. Environ. Safety*, **2007**, *67*, 430-438.

39 J. Ranke, A. Othman, P. Fan, A. Müller, *Int. J. Mol. Sci.*, **2009**, *1037*, 1271-1289.

40 A. Klamt, G. Schüürmann, *J. Chem. Soc., Perkin Trans. 2*, **1993**, 799–805.

41 U. Preiss, Quantum Chemical Studies of Weakly Coordinated Ionic Systems: Predictions of Chemical and Physical Properties. University of Freiburg, Freiburg, Germany, **2010**.

42 a)A. Klamt, Wiley Interdisciplinary Reviews: Computational Molecular Science, **2011**, *1(5)*, 699-709. b) http://en.wikipedia.org/wiki/COSMO_Solvation_Model. c) A. Klamt, F. Eckert, M. Hornig, *J. Comput. Aid. Mol. Des.,* **2001**, *15 (4)*, 355-365

43 A. Schäfer, C. Horn, R. Ahlrichs, *J. Chem. Phys.*, **1992**, *97*, 2571–2577.

44 A.D. Becke, *Phys. Rev. A*, **1988**, *38*, 3098–3100.

45 S. Vosko, L. Wilk, M. Nusair, *Can. J. Phys.*, **1980**, *58*, 1200–1211.

46 J. P. Perdew, *Phys. Rev. B*, **1986**, *33*, 8822–8824.

47 P. Deglmann, F. Furche, R. Ahlrichs, *Chem. Phys. Lett.*, **2002**, *362*, 511–518.

48 P. Deglmann, F. Furche, *J. Chem. Phys.*, **2002**, *117*, 9535–9538.

49 A. Schäfer, C. Huber, R. Ahlrichs, *J. Chem. Phys.*, **1994**, *100*, 5829–5835.

50 Y. H. Zhao, M. H. Abraham, Z. M. Zissimos, *J. Chem. Inf. Comput. Sci.*, **2003**, *43*,

1848-1854.

51 U. Preiss, J. M. Slattery, I. Krossing, *Ind*. *Eng*. *Chem*. *Res*., **2009**, *48*, 2290-2296.

52 A. M. Zissimos, M.H. Abraham, A. Klamt, F. Eckert, J. Wood, *J. Chem*. *Inf*. *Comput*. *Sci*., **2002**, *42*, 1320–1331.

53 a) OBPROP (http://openbabel.sourceforge.net), b) http://openbabel.org/wiki/Main_Page, c) N. M. O'Boyle, M. Banck, C. A. James, C. Morley, T. Vandermeersch, G. R. Hutshison, *J*. *Cheminformatics*, **2011**, *3*, 33.

54 S. A. Wildman, G. M. Crippen, *J*. *Chem*. *Inf*. *Model*., **1999**, *39*, 868-873.

55 a) S. I. Sandler **1999**. Chemical and Engineering Thermodynamics. New York: Wiley, 3rd ed. b) c. Hansch, A. J. Leo, **1979.** Substituent Parameters for Correlation Analysis in Chemistry and Biology. New York: Wiley, c) W. F. van Gunsteren, H. J. C. Berendsen, *Angew. Chem.*, **1990**, *29*, 992–1023. d) J. R. Errington, A. Z. Panagiotopoulos, *J. Phys. Chem. B*, **1999**, *103*, 6314–6322. e) M. G. Martin, J. I. Siepmann, *J. Phys. Chem. B*, **1998**, *102*, 2569–77. f) K. E. Anderson, J. I. Siepmann, **2007**. Molecular simulation approaches to solubility. In Developments and Applications in Solubility, ed. TM Letcher, pp. 171–187. Cambridge: RSC Publishing. g) J. Tomasi, B. Mennucci, R. Cammi, *Chem. Rev.*, **2005**, *105*, 2999–3094.

56 a)http://en.wikipedia.org/wiki/Linear_regression,b)http://www.ltrr.arizona.edu/~dmeko/notes_11.pdf

57 http://www.sagepub.com/upm-data/6419_Chapter_5A_Meyers_I_Proof_3.pdf

58 A. Pinkert, K. N. Marsh, S. Pang, M. D. Staiger, *Chem*. *Rev*., **2009**, *109*, 6712-6728.

59 C.-W. Cho, U. Preiss, J. Christian, S. Stolte, J. Arning, J. Ranke, A. Klamt, I. Krossing, J. Thöming, *J*. *Phy*. *Chem*. *B*, **2011**, *115*, 6040-6050.

60 Y.-J. Zhu, W.-W. Wang, R.-J. Qi, X.-L. Hu, *Angew*. *Chem*., **2004**, *116*, 1434-1438.

61 P. K. Chowdhury, M. Halder, L. Sanders, T. Calhoun, J. L. Anderson, D. W. Armstrong, X. Song, J. W. Petrich, *J*. *Phys*. *Chem*. *B*, **2004**, *108*, 10245-10255.

62 T. Yan, C. J. Burnham, M. G. Del Pópolo, G. A. Voth, *J*. *Phys*. *Chem*. *B*, **2004**, *108*, 11877-11881.

63 S. H. Yalkowsky, S. C. Valvani, *J*. *Pharm*. *Sci*., **1981**, *70*, 1177–117.

64 W. M. Meylan, P. H. Howard, R. S. Boethling, D. Aronson, H. Printup, S. Gouchie, *Environ*. *Toxicol*. *Chem*., **1999**, *18*, 664–672.

65 R. L. Swann, D. A. Laskowski, P. J. Mccall, K. Vanderkuy, H. Dishburger, *J*. *Residue Rev*., **1983**, *85*, 17–28.

66 Y. H. Zhao, M T. D. Cronin, J. C. Dearden, *Quant*. *Struct*.- *Act*. *Relat*., **1998**, *17*, 131–138.

67 Y. H. Zhao, M. H. Abraham, J. Le, A. Hersey, C. N. Luscombe, G. Beck, B. Sherborne, I. Cooper, *Pharm*. *Res*., **2002**, *19*, 1446–1457.

68 J. Ranke, K. Mölter, F. Stock, U. Bottin-Weber, J. Poczobutt, J. Hoffmann, B. Ondruschka, J. Filser, B. Jastorff, *Ecotox*. *Environ*. *Safe*., **2004**, *58(3)*, 396-404.

69 The UFT / Merck Ionic Liquids Biological Effects Database; University of Bremen: Bremen, Germany; available at http://chem. uft.uni-bremen.de/il-eco/ [supported by Zentrum für Umweltforsc hung und nachhaltige Technologien (UFT) and Merck].

70 L. J. Ropel, Diffusion coefficients and 1-octanol-water partitioning coefficient of ionic liquids, **2004,** Notre Dame, Indiana, IN, USA

71 L. Ropel, L. S. Belvéze, S. N. V. Aki, A. Stadtherr, J. F. Brennecke, *Green Chem*., **2005**, *7*, 83–90.

72 J. L. Kaar, A. M. Jesionowski, J. A. Berberich, R. Moulton, A. J. Russell, *J*. *Am*. *Chem*. *Soc*., **2003**, *125*, 4125–4131.

73 S. H. Lee, Biocatalysis in ionic liquids: Influence of physicochemical properties of ionic liquids on enzyme activity and enantioselectivity, **2005**, Pohang University of Science and Technology, Korea

74 L. S. Belvéze, Modeling and Measurement of Thermodynamic Properties of Ionic Liquids, **2004,** University of Notre Dame, Notre Dame, IN, USA.

75 A. Chapeaux, L. D. Simoni, M. A. Stadtherr, J. F. Brennecke, *J*. *Chem*. *Eng*. *Data*, **2007**, *52*, 2462–2467.

76 M. G. Freire, P. J. Carvalho, R. L. Gardas, I. M. Marrucho, L. M. N. B. F. Santos, J. A. P. Coutinho, *J*. *Phys*. *Chem*. *B*, **2008**, *112*, 1604–1610.

77 N. Papaiconomou, N. Yakelis, J. Salminen, R. Bergman, J. M. Prausnitz, *J*. *Chem*. *Eng*. *Data*, **2006**, *51*, 1389–1393.

78 H. Luo, S. Dai, P. V. Bonnesen, *Anal*. *Chem*., **2004**, *76*, 2773–2779.

79 M. G. Freire, C. M. S. S. Neves, P. J. Carvalho, R. L. Gardas, A. M. Fernandes, I.M. Marrucho, L.M. N. B. F. Santos, J. A. P. Coutinho, *J*. *Phys*. *Chem*. *B*, **2007**, *111*, 13082–13089.

80 N. V. Shvedene, S. V. Borovskaya, V. V. Sviridov, E. R. Ismailova, I. V. Pletnev, *Anal*. *Bioanal*. *Chem*., **2005**, *381*, 427–430.

81 J. L. Anthony, E. J. Maginn, J. F. Brennecke, *J*. *Phys*. *Chem*. *B*, **2001**, *105*, 10942–10949.

82 S. Carda-Broch, A. Berthod, D. W. Armstrong, *Anal*. *Bioanal*. *Chem*., **2003**, *375*, 191–199.

83 N. Nishi, T. Kawakami, F. Shigematsu, M. Yamamoto, T. Kakiuchi, *Green Chem*., **2006**, *8*, 349–355.

84 N. Papaiconomou, J. Salminen, J.-M. Lee, J. M. Prausnitz, *J*. *Chem*. *Eng*. *Data*, **2007**, *52*, 833–840.

85 J. Salminen, N. Papaiconomou, R. A. Kumara, J. Lee, J. Kerr, J. Newmana, J. M. Prausnitz, *Fluid Phase Equilib*., **2007**, *261*, 421–426.

86 T. Kakiuchi, N. Tsujioka, S. Kurita, Y. Iwami, *Electrochem. Commun.*, **2003**, *5*, 159-164.

87 U. Preiss, C. Jungnickel, J. Thöming, I. Krossing, J. Luczak, M. Diedenhofen, A. Klamt, *Chem*. *Eur*. *J*. **2009**, *15*, 8880–8885.

88 G. D'Errico, O. Ortona, L. Paduano, V. Vitagliano, *J*. *Colloid Interface Sci*., **2001**, *239*, 264–271.

89 W. Mosquera, *J*. *Colloid Interface Sci*., **1998**, *206*, 66–76.

90 M. Blesic, M. H. Marques, N. V. Plechkova, K. R. Seddon, L. P. N. Rebelo, A. Lopes, *Green Chem*., **2007**, *9*, 481–490.

91 T. M. Perger, M. Bester-Rogac, *J. Colloid Interface Sci.*, **2007**, *313*, 288–295.

92 I. Chakraborty, S. P. Moulik, *J. Phys. Chem. B*, **2007**, *111*, 3658–3664.

93 S. K. Mehta, K. K. Bhasin, R. Chauhan, S. Dham, *Colloids Surf. A*, **2005**, *255*, 153–157.

94 P. Hansson, B. Joensson, C. Stroem, O. Soederman, *J. Phys. Chem. B*, **2000**, *104*, 3496–3506.

95 Y. Hayami, H. Ichikawa, A. Someya, M. Aratono, K. Motomura, *Colloid Polym. Sci.,* **1998**, *276*, 595–600.

96 S. Durand-Vidal, M. Jardat, V. Dahirel, O. Bernard, K. Perrigaud, P. Turq, *J. Phys. Chem. B*, **2006**, *110*, 15542–15547.

97 R. Ueoka, Y. Murakami, *J. Chem. Soc. Perkin Trans. 2*, **1983**, 219–224.

98 I. Goodchild, L. Collier, S. L. Millar, I. Prokeš, J. C. D. Lord, C. P. B. Butts, J. Bowers, J. R. P. Webster, R. K. Heenan, *J. Colloid Interface Sci.*, **2007**, *307*, 455–468.

99 J. Bowers, C. P. Bitts, P. J. Matin, M. C. Vergara-Gurierrez, *Langmuir*, **2004**, *20*, 2191–2198.

100 Z. Miskolczy, K. Sebok-Nagy, L. Biczok, S. Gokturk, *Chem. Phys. Lett.*, **2004**, *400*, 296–300.

101 J. Wang, H. Wang, S. Zhang, H. Zhang, Y. Zhao, *J. Phys. Chem. B,* **2007**, *111*, 6181–6188.

102 Q. Q. Baltazar, J. Chandawalla, K. Sawyer, J. L. Anderson, *Colloids Surf. A,* **2007**, *302*, 150–156.

103 C. Jungnickel, J. Łuczak, J. Ranke, J. F. Fernandez, A. Müller, J. Thöming, *Colloids Surf. A,* **2008**, *316*, 278–284.

104 R. Vanyúr, L. Biczok, Z. Miskolczy, *Colloids Surf. A,* **2007**, *299*, 256–261.

105 O. A. El Seoud, P. A. R. Pires, T. Abdel-Moghny, E. L. Bastos, *J. Colloid Interface Sci.*, **2007**, *313*, 296–304.

106 J. Sirix-Plenet, L. Gaillon, P. Letellier, *Talanta,* **2004**, *63*, 979–986.

107 B. Dong, N. Li, L. Zheng, L. Yu, T. Inoue, *Langmuir*, **2007**, *23*, 4178–4182.

108 T. Inoue, H. Ebina, B. Dong, L. Zheng, *J. Colloid Interface Sci.*, **2007**, *314*, 236–241.

109 S. Thomaier, K. Werner, *J. Mol. Liq.*, **2007**, *130*, 104–107.

110 F. Quina, *J. Phys. Chem.*, **1995**, *99*, 17028–17031.

111 T. Sasaki, M. Hattori, J. Sasaki, K. Nukina, *Bull. Chem. Soc. Jpn.*, **1975**, *48*, 1397–1403.

112 S. Stolte, M. Matzke, J. Arning, A. Böschen, W.-R. Pitner, U. Welz-Biermann, B. Jastorff, *Green Chem.*, **2007**, *9*, 1170-1179.

113 K. M. Docherty, C. F. Kulpa Jr, *Green Chem.*, **2005**, *7*, 185-189.

114 C. Samori, A. Pasteris, P. Galletti, E. Tagliavini, *Environ. Toxicol. Chem.*, **2007**, *26(11)*, 2379-2382.

115 A. Romero, A. Santos, J. Tojo, A. Rodríguez, *J. Hazard. Mater.*, **2008**, *151*, 268-273.

116 C.-W. Cho, T. P. T. Pham, Y.-C. Jeon, K. Vijayaragvahan, W.-S. Choe, Y.-S. Yun, *Chemosphere*, **2007**, *69(6)*, 1003-1007.

117 C.-W. Cho, T. P. T. Pham, Y.-C. Jeon, Y.-S. Yun, *Green Chem*., **2008**, *10*, 67-72.

118 C.-W. Cho, T. P. T. Pham, Y.-C. Jeon, K. Vijayaragvahan, Y.-S. Yun, *Ecotox*. *Environ*. *Safe*., **2008**, *71(1)*, 166-171.

119 A. Latała, P. Stepnowski, M. Nędzi, W. Mrozik, *Aqua*. *Toxicol*., **2005**, *73(1)*, 91-98.

120 K. J. Kulacki, G. A. Lamberti, *Green Chem*., **2008**, *10*, 104-110.

121 T. P. T. Pham, C.-W. Cho, J. Min, Y.-S. Yun, *J*. *Biosci*. *Bioeng*., **2008**, *105(4)*, 425-428.

122 T. P. T. Pham, C.-W. Cho, K. Vijayaghavan, J. Min, Y.-S. Yun, *Environ*. *Toxicol*. *Chem*., **2008**, *27(7)*, 1583-1589.

123 C. Pretti, C. Chiappe, I. Baldetti, S. Brunini, G. Monni, L. Intorre, *Ecotox*. *Environ*. *Safe*., **2009**, *72(4)*, 1170-1176.

124 A. Latała, M. Nędzi, P. Stepnowski, *Green Chem*., **2010**, *12*, 60-64.

125 P. Stepnowski, A. C. Skladanowski, A. Ludwiczak, E. Laczyńska, *Hum*. *Exp*. *Toxicol*., **2004**, *23(11)*, 513-517.

126 X. Wang, C. A. Andre Ohlin, Q. Lu, Z. Fei, J. Hu, P. J. Dyson, *Green Chem*., **2007**, *9*, 1191-1197.

127 R. F. M. Frade, A. Matias, L. C. Branco, C. A. M. Afonso, C. M. M. Duarte, *Green Chem*., **2007**, *9*, 873-877.

128 A. Garcia-Lorenzo, E. Tojo, J. Tojo, M. Teijeira, F. J. Rodriguez-Berrocal, M. P. Gonzalez, V. S. Martinez-Zorzano, *Green Chem*., **2008**, *10*, 508-516.

129 R. J. Bernot, M. A. Brueseke, M. A. Evans-White, G. A. Lamberti, *Environ*. *Toxicol*. *Chem*., **2005**, *24(1)*, 87-92.

130 D. J. Couling, R. J. Bernot, K. M. Docherty, J. K. Dixon, E. J. Maginn, *Green Chem*., **2006**, *8*, 82-90.

131 M. Petkovic, K .R. Seddon, L. P. N. Rebelo, C. S. Pereira, *Chem*. *Soc*. *Rev*., **2011**, *40(3)*, 1383-1403.

132 J. Ranke, S. Stolte, R. Stormann, J. Arning, B. Jastorff, *Chem*. *Rev*., **2007**, *107(6)*, 2183-2206.

133 T. P. T. Pham., C.-W. Cho, Y.-S. Yun, *Water Res*., **2010**, *44(2)*, 352-372.

134 D. B. Zhao, Y.C. Liao, Z.D. Zhang, *Clean-Soil Air Water*, **2007**, *35(1)*, 42-48.

135 R. S. Boethling, E. Sommer, D. DiFiore, *Chem*. *Rev*., **2007**, *107(6)*, 2207-2227.

136 D. Coleman, N. Gathergood, *Chem*. *Soc*. *Rev*., **2010**, *39(2)*, 600-637.

137 S. Stolte, S. Steudte, A. Igartua, P. Stepnowski, *Curr*. *Org*. *Chem*., **2011**, *15(12)*, 1946-1973.

138 P. Luis, I. Ortiz, R. Aldaco, A. Irabien, *Ecotox*. *Environ*. *Safe*., **2007**, *67(3)*, 423-429.

139 P. Luis, A. Garea, A. Irabien, *J*. *Mol*. *Liq*., **2010**, *152*, 28-33.

140 A. García-Lorenzo, E. Tojo, J. Tojo, M. Teijeira, F. J. Rodríguez-Berrocal, M. P. González, V. S. Martinez-Zorzano, *Green Chem*., **2008**, *10*, 508-516.

141 J. S. Torrecilla, J. Garcia, E. Rojo, F. Rodríguez, *J*. *Hazard*. *Mat*., **2009**, *164*, 182-194.

142 J. S. Torrecilla, J. Ralomar, J. Lemus, F. Rodríguez, *Green Chem*., **2010**, *12*, 123-134.

143 M. H. Fatemi, P. Izadiyan, *Chemosphere*, **2011**, *84(5)*, 553-563.

144 M. Alvarez-Guerra, A. Irabien, *Green Chem*., **2011**, *13*, 1507-1516.

145 L. Sprunger, M. Clark, W.E. Acree Jr., M. H. Abraham, *J*. *Chem*. *Inf*. *Model*., **2007**, *47(3)*, 1123-112.

146 L. M. Sprunger, A. Proctor, W. E. Acree Jr., M. H. Abraham, *Fluid Phase Equilibr*., **2008**, *265(1-2)*, 104-111.

147 C.V. Eadsforth, P. Moser, *Chemosphere*, **1983**, *12*, 1459-1475.

148 W. Klein, W. Kördel, M. Weiss, H.J. Poremski, *Chemosphere*, **1988**, *17*, 361-386.

149 OECD guidelines for the test of chemicals No. 117 – Partitioning Coefficient (n-octanol/water), High Performance Liquid Chromatography (HPLC) Method; **2004**.

150 S. Stolte, J. Arning, U. Bottin-Weber, A. Müller, W. R. Pitner, U. Welz-Biermann, B. Jastorff, J. Ranke. *Green Chem*., **2007**, *9*, 760-767.

151 J. Arning, S. Stolte, A. Böschen, F. Stock, W.-R. Pitner, U. Welz-Biermann, B. Jastorff, J. Ranke, *Green Chem*., **2008**, *10*, 47-58.

152 P. Luis, C.A.M. Afonso, I.M. Coelhoso, J. Creso, A. Irabien, Proceedings of the 23rd European symposium on Applied Thermodynamics Congress, ISBN: 2-905267-59-3, **2008**.

153 A. D. Gunatilleka, C. F. Poole, *Anal*. *Commun*., **1999**, *36*, 235-242.

154 H. Konemann, *Toxicology*, **1981**, *19(3)*, 209-221.

155 P. Mayer and F. Reichenberg, *Environ*. *Toxicol*. *Chem*., **2006**, *25(10)*, 2639-2644.

156 F. A. P. C. Gobas, J. M. Lahittete, G. Garofalo, Y. S. Wan, D. A. Mackay, *J*. *Pharm*. *Sci*., **1988**, *77*, 265-272.

157 W. J. Dulfer, H. A. J. Govers, *Environ*. *Sci*. *Technol*., **1995**, *29*, 2548-2554.

158 S. Stolte, J. Arning, U. Bottin-Weber, M. Matzke, F. Stock, K. Thiele, M. Uerdingen, U. Welz-Biermann, B. Jastorff, J. Ranke, *Green Chem*., **2006**, *8*, 621-629.

List of Publications

1. **C.-W. Cho**, S. Stolte, J. Ranke, I. Krossing, J. Thöming. Determination of solute descriptors of ionic liquid anions using multiple functionalized systems. ***In preparation***

2. **C.-W. Cho**, C. Jungnickel, S. Stolte, U. Preiss, J. Arning, J. Ranke, I. Krossing, J. Thöming. Experimental determination of LFER parameters of 30 cations of ionic liquids. ***Submitted to ChemPhysChem.***

3. **C.-W. Cho**, U. Preiss, C. Jungnickel, S. Stolte, J. Arning, J. Ranke, A. Klamt, I. Krossing, J. Thöming. Ionic Liquids: Predictions of physicochemical properties with experimental and/or DFT-calculated LFER parameters to understand molecular interactions in solution. ***Journal of Physical Chemistry B*** 115(19), 6040-6050, (APR. 2011).

4. **C.–W. Cho**, J. Ranke, J. Thöming, J. Arning, U. Preiss, C. Jungnickel, M. Diedenhofen, A. Klamt, I. Krossing, S. Stolte, *In silico* modeling for predicting cationic hydrophobicity and cytotoxicity of ionic liquids towards rat leukaemia cell line, *Vibrio fisheri* and *Scenedesmus vacuolatus* based on molecular interaction potentials of ions. ***Submitted to Green Chemistry.***

5. S. Stolte, T. Schulz, **C.-W. Cho**, J. Arning, T. Strassner, Toxicity, biodegradation and physical properties of tunable ary alkyl ionic liquids (TAAILs). ***In preparation***

6. J. Neumann, **C.-W. Cho**, M. Uerding, S. Steudte, J. Thöming, S. Stolte, Biodegradation of floroorganic and cyano-based ionic liquids anions under aerobic and anaerobic conditions. ***Accepted to Green Chemistry.***

Curriculum vitae

28. Nov. 1980	Born in Chonbuk (Buan), South Korea
1988 ~ 1999	Elementary, middle, and high school in Buan (Baeksan), Chonbuk, Korea
1999 ~ 2005	Chemical Engineering studies (Bachelor) at Chonbuk National University
2000 ~ 2002	Military service
2005 ~ 2007	Bioprocess Engineering studies in the group of Prof. Dr. Yeoung-Sang Yun at the **E**nvironmental **B**iotechnology and **T**echnology **L**aboratory (**EBTL**), Chonbuk National University
2007 ~ 2008	Post-master training at the **EBTL** in the Chonbuk National University
2008 ~ 2011	PhD student in the group of Prof. Dr.-Ing. Jorg Thöming at the Centre for Environmental Research and Technology (**UFT**), University of Bremen.
2009 ~ 2010	Visiting student in the group of Prof. Dr. rer. nat Ingo Krossing at the Institut für Anorganische und Analytische Chemie, University of Freiburg

Erklärung

Hermit erkläre ich, Chul-Woong Cho, geboren am 28.11.1980 in Chonbuk (Buan) in Republic of Korea, dass ich

- die Arbeit ohne unerlaubte fremde Hilfe angefertigt habe,
- keine anderen als die von mir angegebenen Quellen und Hilfsmittel benutzt habe und
- Die den benutzten Werken wörtlich oder inhaltlich entnommenen Stellen als solche kenntlich gemacht habe.

Bremen 16, Nov. 2011 Chul-Woong Cho